UQAC
Université du Québec
à Chicoutimi

An investigation of the sound and thermal insulation of facades' wood assemblies by considering environmental impact aspects

by

Ibrahim Ramzi Jaber

Under the supervision of Sylvain Ménard and the co-supervision of Mohamad Bader Eddin

Thesis presented to the University of Quebec at Chicoutimi with a view to obtaining the degree of Master of Applied Science (M.Sc.A.) in Engineering

October 2026

Jury:

Jean Perron, Ph.D. - Professor in the Department of Applied Sciences, UQAC.

Joonhee Lee, Ph.D.-Associate Professor, Department of Building, Civil and Environmental Engineering, Concordia University

Sylvain Menard, Ph.D., Eng. - Professor, Department of Applied Sciences, UQAC.

Mohamad Bader Eddin, Ph.D. – Researcher, UQAC.

Québec, Canada

© Ibrahim Jaber, 2026

RÉSUMÉ

L'amélioration de la performance des enveloppes de bâtiments constitue un enjeu majeur dans le contexte actuel de la construction durable. Les façades en bois sont de plus en plus utilisées en raison de leur faible empreinte carbone, de leur rapidité de mise en œuvre et de leurs bonnes propriétés thermiques. Toutefois, l'amélioration de l'isolation acoustique de ces systèmes nécessite souvent l'ajout de matériaux ou de couches constructives susceptibles d'influencer simultanément leur performance thermique ainsi que leur impact environnemental. Malgré l'importance de ces trois critères, ils sont généralement étudiés de façon indépendante, ce qui limite la compréhension des compromis nécessaires lors de la conception des façades en bois.

L'objectif principal de ce mémoire est d'étudier les relations entre l'isolation acoustique, la performance thermique et le carbone incorporé des assemblages de façades en bois afin d'identifier les solutions offrant les meilleurs compromis entre ces trois critères. Pour ce faire, une base de données regroupant 382 assemblages de façades, répartis en sept familles, a été constituée à partir de résultats expérimentaux publiés dans la littérature scientifique. La performance thermique de chaque assemblage a ensuite été évaluée par le calcul du coefficient de transmission thermique (U), tandis que le carbone incorporé a été estimé à partir d'une analyse du cycle de vie limitée aux étapes A1–A3. Des analyses de corrélation ainsi qu'une optimisation multicritère fondée sur le concept de Pareto ont ensuite été réalisées afin d'évaluer les interactions entre les trois indicateurs de performance.

Les résultats montrent une corrélation positive entre la performance acoustique et la performance thermique selon les différentes familles d'assemblages, avec des coefficients de détermination (R^2) variant de 0,69 à 0,88. En revanche, aucune corrélation significative n'a été observée entre l'isolation acoustique et le carbone incorporé, ce qui indique qu'il est possible d'améliorer la performance acoustique sans augmentation proportionnelle de l'impact environnemental. L'analyse de Pareto a permis d'identifier 46 assemblages Pareto-optimaux représentant les meilleurs compromis entre les trois critères étudiés. Pour les assemblages dont l'épaisseur totale varie de 287,5 à 477 mm, une augmentation de l'épaisseur d'isolant de 120 à 300 mm améliore simultanément la performance acoustique et thermique, tout en entraînant une augmentation relativement limitée du carbone incorporé. Les résultats sont synthétisés dans un catalogue de sept assemblages représentatifs constituant un outil d'aide à la décision pour la conception de façades en bois performantes et durables.

ABSTRACT

Improving the performance of building envelopes has become a major challenge in the context of sustainable construction. Timber-based facades are increasingly being adopted due to their low embodied carbon, rapid construction, and favorable thermal properties. However, enhancing the acoustic insulation of these systems often requires the addition of materials or construction layers that may simultaneously affect their thermal performance and environmental impact. Despite the importance of these three criteria, they are generally investigated independently, limiting the understanding of the trade-offs involved in the design of timber facade assemblies.

The main objective of this thesis is to investigate the relationships between acoustic insulation, thermal performance, and embodied carbon of timber facade assemblies in order to identify solutions that provide the best compromise among these three criteria. To achieve this objective, a database comprising 382 facade assemblies, classified into seven assembly families, was developed using experimental results reported in the scientific literature. The thermal performance of each assembly was then evaluated by calculating the thermal transmittance (U-value), while the embodied carbon was estimated through a life cycle assessment limited to the A1–A3 product stages. Correlation analyses and a multi-objective optimization based on the Pareto efficiency concept were subsequently performed to evaluate the interactions among the three performance indicators.

The results revealed a positive correlation between acoustic and thermal performance across the different assembly families, with coefficients of determination (R^2) ranging from 0.69 to 0.88. In contrast, no significant correlation was observed between acoustic insulation and embodied carbon, indicating that improvements in acoustic performance can be achieved without a proportional increase in environmental impact. The Pareto analysis identified 46 Pareto-optimal assemblies representing the best trade-offs among the three criteria. For facade assemblies with total thicknesses ranging from 287.5 to 477 mm, increasing the insulation thickness from 120 to 300 mm simultaneously improved acoustic and thermal performance while resulting in only a relatively limited increase in embodied carbon. The findings were synthesized into a catalogue of seven representative facade assemblies, providing a practical decision-support tool for the design of high-performance and sustainable timber facade systems.

TABLE OF CONTENT

RÉSUMÉ ..... **ii**

ABSTRACT ..... **iii**

TABLE OF CONTENT ..... **iv**

LIST OF FIGURES ..... **vi**

LIST OF TABLES ..... **viii**

LIST OF ABREVIATIONS ..... **ix**

ACKNOWLEDGMENT ..... **x**

CHAPTER 1 INTRODUCTION **1**

1.1 PROJECT BACKGROUND 1

1.2 STATEMENT OF THE PROBLEM 2

1.3 AIMS AND OBJECTIVES 3

1.4 METHODOLOGY 4

1.5 PROJECT STAGES 6

1.6 ORIGINALITY OF THE RESEARCH 7

1.7 STRUCTURE OF THE REPORT 8

CHAPTER 2 LITERATURE REVIEW **10**

2.1 THEORETICAL BACKGROUND 10

2.1.1 SOUND INSULATION 10

2.1.2 THERMAL INSULATION 22

2.1.3 THEORY OF HEAT AND SOUND PROPAGATION: ANALOGY 29

2.1.4 ENVIRONMENTAL IMPACT OF BUILDING CONSTRUCTION 34

2.1.5 OPTIMIZATION FRAMEWORKS FOR MULTI-CRITERIA PERFORMANCE ASSESSMENT 38

2.2 RESEARCH BACKGROUND 44

2.2.1 IMPORTANCE OF WOOD CONSTRUCTION IN CANADA AND INTERNATIONALLY 44

2.2.2 ACOUSTICS IN WOOD CONSTRUCTION 47

2.2.3 THERMAL INSULATION IN WOOD CONSTRUCTION 50

2.2.4 THERMAL AND ACOUSTIC INSULATION IN WOOD CONSTRUCTION 53

2.2.5 ENVIRONMENTAL ASPECT 55

CHAPTER 3 ARTICLE: "AN INVESTIGATION OF THE SOUND AND THERMAL INSULATION OF FACADES' WOOD ASSEMBLIES BY CONSIDERING ENVIRONMENTAL IMPACT ASPECTS" ... 58

3.1 ARTICLE PRESENTATION 58
3.2 SCIENTIFIC CONTRIBUTION 58
3.3 RELEVANCE TO THE THESIS OBJECTIVES 59
3.4 CURRENT PUBLICATION STATUS 59
3.5 ARTICLE SUMMARY 60
3.6 FULL ARTICLE 61
3.7 STUDENT CONTRIBUTION 100
CONCLUSION 102
LIST OF REFERENCES 105

LIST OF FIGURES

FIGURE 1. GANTT CHART OF THE MASTER'S RESEARCH PROJECT ACTIVITIES CONDUCTED FROM AUGUST 2024 TO JUNE 2026, INCLUDING ACADEMIC OBLIGATIONS, RESEARCH TASKS, SCIENTIFIC DISSEMINATION, AND WRITING ACTIVITIES. 7
FIGURE 2. THE PROPAGATION OF THE AIRBORNE SOUND. 11
FIGURE 3. THE PROPAGATION OF THE IMPACT SOUND. 11
FIGURE 4. SOUND TRANSFER PATHS: 7: FLANKING-FLANKING, 8: FLANKING DIRECT, 9: DIRECT-FLANKING. 12
FIGURE 5. STANDARDIZED TAPPING MACHINE 16
FIGURE 6. TOTAL HEAT DISTRIBUTION IN TERMS OF DENSITY VARIATION. 23
FIGURE 7. HEAT TRANSFER BY CONDUCTION. 24
FIGURE 8. SCHEMATIC VIEW OF THE GUARDED HOT BOX APPARATUS. 28
FIGURE 9. CONCEPTUAL SCHEMATIC ILLUSTRATING THE EXPECTED INVERSE RELATIONSHIP BETWEEN AIRBORNE SOUND INSULATION RW AND THERMAL CONDUCTIVITY K, DERIVED FROM THEORETICAL SCALING CONSIDERATIONS. 34
FIGURE 10. LIFE CYCLE ASSESSMENT SCHEMATIC. 37
FIGURE 11. COMMON PARETO FRONT GEOMETRIES FOR TWO-OBJECTIVE OPTIMIZATION PROBLEMS, ILLUSTRATING THE FOUR POSSIBLE COMBINATIONS OF MINIMIZATION AND MAXIMIZATION OBJECTIVES: MIN–MIN, MIN–MAX, MAX–MIN, AND MAX–MAX. THE BOLD CURVE IN EACH CASE REPRESENTS THE PARETO-OPTIMAL FRONT, DEFINED AS THE SET OF NON-DOMINATED SOLUTIONS BEYOND WHICH IMPROVEMENT IN ONE OBJECTIVE NECESSARILY ENTAILS A DETERIORATION IN THE OTHER. 43
FIGURE 12. SCHEMATIC REPRESENTATION OF THE GENERAL LAYER CONFIGURATION CONSIDERED IN THE DATASET AND SUMMARIZES THE POSSIBLE COMPONENTS THAT MAY APPEAR ACROSS THE DIFFERENT FAÇADE ASSEMBLIES. 67
FIGURE 13. SCATTER PLOTS OF AIRBORNE SOUND INSULATION (R_W) VERSUS THERMAL TRANSMITTANCE (U_{VALUE}) FOR (**A**) FAMILY 1, (**B**) FAMILY 2, (**C**) FAMILY 3, (**D**) FAMILY 4, (**E**) FAMILY 5, (**F**) FAMILY 6, (**G**) FAMILY 7. EACH DOT REPRESENTS ONE FAÇADE ASSEMBLY (OVERLAPPING ASSEMBLIES APPEAR AS A SINGLE DOT), AND THE SOLID LINE IS THE LINEAR REGRESSION FIT FOR THAT FAMILY; THE CORRESPONDING R^2 IS GIVEN ABOVE EACH PLOT. 81
FIGURE 14. SCATTER PLOTS OF AIRBORNE SOUND INSULATION (RW) VERSUS EMBODIED CARBON (EC) FOR (A) FAMILY 1, (B) FAMILY 2, (C) FAMILY 3, (D) FAMILY 4, (E) FAMILY 5, (F) FAMILY 6, (G) FAMILY 7. EACH DOT REPRESENTS ONE FAÇADE ASSEMBLY (OVERLAPPING ASSEMBLIES APPEAR AS A SINGLE DOT), AND THE SOLID LINE IS THE LINEAR REGRESSION FIT FOR THAT FAMILY; THE CORRESPONDING R^2 IS GIVEN ABOVE EACH PLOT. 85
FIGURE 15. PARETO FRONT ANALYSIS OF FACADE ASSEMBLIES SHOWING THE PARETO FRONT AMONG AIRBORNE SOUND INSULATION, THERMAL TRANSMITTANCE, AND EMBODIED CARBON. EACH POINT REPRESENTS A FACADE. STAR POINTS INDICATE PARETO-OPTIMAL SOLUTIONS, WHILE GRAY POINTS REPRESENT

DOMINATED SOLUTIONS. (A) FOR FAMILY 1 (B) FOR FAMILY 2 (C) FOR FAMILY 3 (D) FOR FAMILY 4 (E) FOR FAMILY 5 (F) FOR FAMILY 6 (G) FOR FAMILY 7. 88
FIGURE 16. SCATTER PLOTS OF PARETO-OPTIMAL ASSEMBLY PERFORMANCE AGAINST TOTAL INSULATION LAYER THICKNESS, SHOWN SEPARATELY FOR EACH FAMILY WITH INDIVIDUAL LINEAR REGRESSION FITS. PLOT (A) REPRESENTS AIRBORNE SOUND INSULATION (R_W), PLOT (B) REPRESENTS THERMAL TRANSMITTANCE (U_{VALUE}), AND PLOT (C) REPRESENTS EMBODIED CARBON (EC). 90
FIGURE 18. REPRESENTATIVE PARETO-OPTIMAL ASSEMBLIES FOR EACH FAMILY, SELECTED BASED ON PROXIMITY TO THE IDEAL POINT IN NORMALIZED OBJECTIVE SPACE. (A) FAMILY 1, (B) FAMILY 2, (C) FAMILY 3, (D) FAMILY 4, (E) FAMILY 5, (F) FAMILY 6, (G) FAMILY 7. 94

LIST OF TABLES

TABLE 1. EQUIVALENT ISO AND ASTM STANDARDS FOR AIRBORNE SOUND TRANSMISSION MEASUREMENT AND RATING 19
TABLE 2. EQUIVALENT ISO AND ASTM STANDARDS FOR IMPACT SOUND TRANSMISSION MEASUREMENT AND RATING 19
TABLE 3. DIFFERENCES BETWEEN THE ASTM AND ISO FOR SINGLE-NUMBER RATING PROCEDURES. 20
TABLE 4. MATERIALS AND PHYSICAL PROPERTIES USED TO CONSTRUCT THE FACADE ASSEMBLY DATASET. 67
TABLE 5. CLASSIFICATION OF TIMBER FACADE ASSEMBLY FAMILIES BASED ON FIXED CONFIGURATION PARAMETERS: CLADDING TYPE, SHEATHING BOARD, INSULATION MATERIAL, AND NUMBER OF INSULATION CAVITIES. 69
TABLE 6. EMBODIED CARBON FACTORS (ECf) USED FOR THE MATERIALS CONSIDERED IN THE FAÇADE ASSEMBLY DATASET. 74
TABLE 7. LINEAR REGRESSION RESULTS BETWEEN ACOUSTIC AND THERMAL PERFORMANCE ACROSS THE ANALYZED FAMILIES. MAX. AND MIN VALUE ARE PRESENTED CORRESPONDING TO EACH FAMILY. 79
TABLE 8. LINEAR REGRESSION RESULTS BETWEEN ACOUSTIC PERFORMANCE AND EMBODIED CARBON ACROSS THE ANALYZED FAMILIES. MAX. AND MIN VALUE ARE PRESENTED CORRESPONDING TO EACH FAMILY. 83
TABLE 9. NUMBER OF PARETO-OPTIMAL FACADE ASSEMBLIES PER FAMILY. 85
TABLE 10. CORRELATION AND PRINCIPAL COMPONENT ANALYSIS OF THE PARETO SOLUTIONS FOR EACH FAÇADE FAMILY 89

LIST OF ABREVIATIONS

A: Cross-sectional area (m^2)

A1–A3: Product stage modules in EN 15804 life cycle assessment

ASTM: ASTM International

CLT: Cross-Laminated Timber

CO_2.eq: Carbon dioxide equivalent

dB: Decibel

EC: Embodied carbon (kg CO_2eq/m^2)

ECF: Embodied carbon factor (kg CO_2eq/kg)

EPD: Environmental Product Declaration

GWP: Global Warming Potential

Hz: Hertz

ICE: Inventory of Carbon and Energy

ISO: International Organization for Standardization

LCA: Life Cycle Assessment

MW: Mineral wool

OSB: Oriented Strand Board

R-value: Thermal resistance ($m^2 \cdot K/W$)

Rw: Weighted airborne sound reduction index (dB)

S: Stud spacing (m)

U-value: Thermal transmittance ($W/m^2 \cdot K$)

λ: Thermal conductivity ($W/m \cdot K$)

ρ: Density (kg/m^3)

ACKNOWLEDGMENT

First of all, I would like to thank my research supervisor, Prof. Sylvain Ménard, for his exceptional support throughout my academic journey and for the many opportunities I was given. His guidance and availability were invaluable, and his advice and insights were consistently essential in shaping the direction and quality of this work. I remain sincerely grateful for his support.

I would also like to express my deep appreciation to my co-supervisor, Dr. Mohamad Bader Eddin, for his strong and committed involvement in this project. His continuous availability, constructive feedback, and insightful recommendations were fundamental in achieving a high-quality final outcome. This support was greatly appreciated.

Special thanks are also extended to Dr. Cheng, Mr. Gagnon, and Mr. Anes for inviting me to participate in laboratory measurements and for helping me gain valuable hands-on experience in acoustic testing. Their openness and willingness to share their expertise significantly enriched my practical understanding of the field.

I would like to acknowledge the financial support of the Natural Sciences and Engineering Research Council of Canada (NSERC) through the Alliance Advantage program, Natural Resources Canada (NRCan), Alberta Innovates, BC Forestry Innovation Investment Ltd. (BC-FII), the Ministère des Ressources naturelles et des Forêts (MRNF), the Ontario Ministry of Northern Development, Mines, Natural Resources and Forestry (NDMNRF), Alberta WoodWORKS!, the National Lumber Grades Authority (NLGA), Nordic Structures, Western Archrib, and Element5. We are also grateful to our research partners, FPInnovations and the National Research Council of Canada (NRC), for their in-kind contributions.

Finally, I would like to thank my family, especially my mother, for their continuous support and encouragement throughout these years. I am also deeply grateful to my close friend Jad Walieddine for his constant presence, support, and encouragement, which played an important role throughout this journey.

CHAPTER 1
INTRODUCTION

1.1 PROJECT BACKGROUND

Wooden construction has regained its popularity as one of the most widely used materials in Canada, largely due to the increase in the Canadian share (37%) of the total certified sustainable forests worldwide. With population growth, using wood in multi-story buildings has become a viable solution [1]. Furthermore, due to the valuable properties of wood, such as weight, cost, sustainability, and environmental consequences, mass timber made of wooden materials is becoming a staple in the industry [2]. One of the implementations of wood in building construction is facades, offering both aesthetic and functional benefits. In its simplest form, a facade acts as a barrier, regulating heat flow and maintaining a desired indoor temperature. Wooden facades contribute to high thermal efficiency performance, leveraging the high thermal properties of wood and creating high-quality indoor environments. Thermal comfort for residents is consistently ranked as the most important aspect of indoor environmental quality by building occupants, surpassing other factors such as visual and air quality [3].

Besides thermal comfort, acoustic insulation is a crucial factor that affects the comfort of residents in buildings. The acoustic factor is a critical issue to handle. It is a powerful force, shaping people's moods, influencing their behavior, and even impacting their health [4]. Sound can be a source of comfort and joy, but has the potential to be a relentless source of noise and harm. In building facades, noise pollution has been linked to various health issues, including stress, anxiety, high blood pressure, heart disease, and even cognitive decline [5]. While Canadian building codes

specify requirements for airborne sound insulation and provide recommendations for impact noise for walls and floors, no specific regulations currently address the acoustic performance of facades [6]. The lack of requirement codes for building facades is due to historically lower levels of external noise exposure, particularly from traffic that was not present before. However, as cities grow, residential and commercial buildings are increasingly being constructed in high-density areas, where combustion engines, including those in diesel buses and vehicles, are a critical issue.

On the other hand, the environmental impact of recent building designs considers minimizing their environmental footprint. In line with Canada's commitment to reduce greenhouse gas (GHG) emissions by 45-50% by 2035 and to achieve net-zero emissions by 2050, the adoption of sustainable materials in construction has become more crucial. Moreover, studies indicate that buildings account for nearly 40% of global carbon emissions due to the inefficient facade designs that exacerbate this issue [7]. Wooden facades, as a renewable resource, could be implemented in order to reduce these GHG emissions, as well as contribute to energy-efficient buildings, by decreasing heating energy consumption and consequently driving down heating costs [8].

1.2 STATEMENT OF THE PROBLEM

While residents increasingly associate indoor comfort with maintaining an optimal thermal environment in their living spaces, thermal comfort usually overshadows other comfort factors, such as acoustics in buildings. Consequently, acoustic indoor comfort has faced severe problems in facade wooden buildings. This is due to facades being primarily designed for purposes such as thermal insulation and fire safety, as well as the inherent properties of wood, particularly its low stiffness and mass. Given these points, relying solely on the wood properties is insufficient to fulfill

the building code requirements in terms of acoustic insulation. Therefore, wood-based structures must be complemented with additional acoustic insulation solutions, such as resilient layers or composite assemblies [9].

Additionally, poorly designed building facades have severe environmental consequences, including excessive energy consumption, higher carbon emissions, and material waste. These impacts are amplified by the common reliance on heavier, carbon-intensive solutions, such as concrete materials to meet acoustic requirements, which adds embodied carbon penalty [10]. As a result, the design choices made to address one performance criterion often worsen another, leaving facade design caught between conflicting requirements.

Research on thermal and acoustic insulation in buildings often treats them as separate aspects. As a result, there is limited understanding of how these two properties interact with each other, making it difficult to optimize both building design and occupant comfort. Therefore, an integrated approach to optimizing both acoustic and thermal performance in wood-based facade systems while minimizing their environmental impact is essential for sustainable and high-performance construction in Canada.

1.3 AIMS AND OBJECTIVES

The research project aims to investigate the trade-offs between sound insulation, thermal performance, and embodied carbon in wood-based facade assemblies through a multi-criteria analysis. Sound reduction index (R_w), thermal transmittance (U_{value}), and embodied carbon (EC) are the main parameters analyzed. The detailed objectives are:

- Compiling a database of timber facade assemblies from published acoustic measurements.
- Calculating the thermal performance of each assembly using Ubakus simulation software in accordance with ISO 6946.
- Assessing the environmental impact of each assembly in terms of embodied carbon (A1–A3 life-cycle stages) using equations consistent with standard LCA methodology.
- Investigating the statistical correlations between the three performance criteria.
- Carrying on a Pareto-based multi-objective optimization to identify non-dominated assemblies representing the best achievable trade-offs.
- Building a catalog of Pareto-optimal assemblies containing their acoustic, thermal, and environmental impact data, to support engineers during project decision-making.

1.4 METHODOLOGY

The present research was carried out through a series of complementary stages designed to investigate the relationships between the acoustic, thermal, and environmental performance of timber facade assemblies. The methodology combined database development, numerical analyses, statistical evaluation, and multi-criteria performance assessment to provide a comprehensive evaluation of facade performance.

The first stage of the research consisted of developing a database of timber facade assemblies using experimental results reported in the scientific literature. Only facade systems for which standardized airborne sound insulation measurements were available

were considered. The information collected included the material composition of each assembly together with its measured acoustic performance, providing a consistent basis for the subsequent analyses.

Following the development of the database, the thermal and environmental performances of each facade assembly were evaluated. The thermal transmittance (U-value) was determined using numerical calculations based on the composition of each facade assembly, while the embodied carbon associated with the constituent materials was estimated using life cycle assessment data available in the literature. These analyses allowed each facade assembly to be characterized according to three complementary performance indicators: airborne sound insulation, thermal transmittance, and embodied carbon.

Once the database was completed, statistical analyses were conducted to investigate the relationships between the three performance indicators and to evaluate the existence of possible correlations between acoustic, thermal, and environmental performance. Finally, a Pareto-based multi-objective analysis was performed to identify facade assemblies offering the best compromises between the considered criteria. The resulting Pareto-optimal solutions were then compiled into a catalogue intended to support designers and engineers in the selection of high-performance timber facade assemblies. A more detailed description of the methodology, including the computational procedures, analytical methods, and performance assessment techniques, is presented in Chapter 3. The timeline of the research activities is provided in the Gantt chart presented in the following section.

1.5 PROJECT STAGES

Figure 1 presents the timeline of the master's research project, structured across four categories: academic obligations, research tasks, scientific dissemination, and writing activities. The early phase (August–December 2024) was dedicated to completing mandatory courses and conducting the literature review, which established the theoretical foundation for the research. The first half of 2025 focused on the construction of the acoustic, thermal, and embodied carbon databases, followed by correlation analysis and the development of the multi-objective analysis framework. Scientific dissemination ran in parallel throughout the project, including two laboratory visits in Winter and Summer 2025, and oral presentations at the Next Generation Wood Construction conferences held in Ottawa (2024) and Edmonton (2025). The final phase (Fall 2025–June 2026) was devoted to the writing of the scientific article and the preparation of the final report, culminating in the submission of the article to the journal *Acoustics* (MDPI) in June 2026. The research is expected to be further disseminated at the INTERNOISE 2026 conference in Adelaide, Australia.

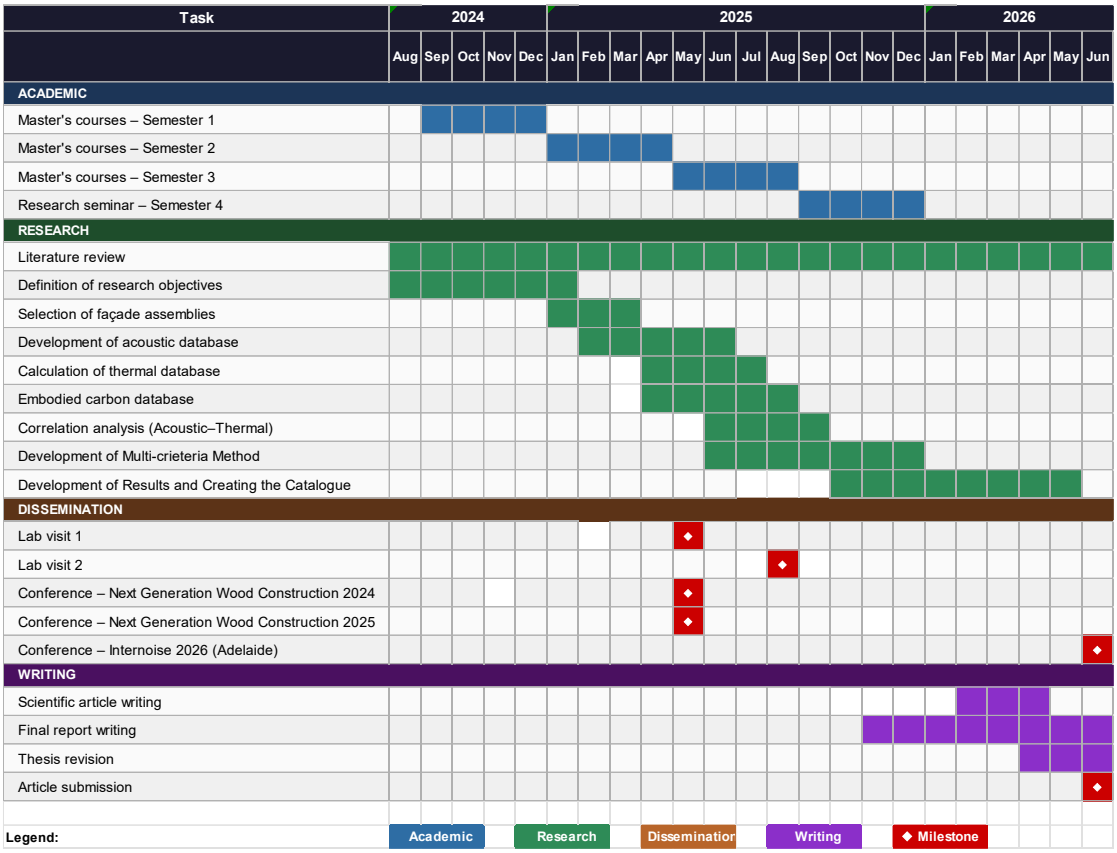


Figure 1. Gantt chart of the master's research project activities conducted from August 2024 to June 2026, including academic obligations, research tasks, scientific dissemination, and writing activities.

1.6 ORIGINALITY OF THE RESEARCH

The originality of this research lies in the integrated evaluation of timber facade assemblies by simultaneously considering airborne sound insulation, thermal performance, and embodied carbon within a unified assessment framework. While previous studies have generally investigated these performance aspects independently, limited research has examined their interactions and the trade-offs that arise when they are considered together especially in timber-based facade designs.

Another original contribution of this work is the application of Pareto-based multi-objective analysis to identify facade assemblies that provide the best compromise between the three performance criteria. Rather than optimizing a single objective, this

approach highlights non-dominated solutions that allow designers and engineers to select assemblies according to specific project priorities without relying on subjective weighting factors.

Finally, the research provides a practical catalogue of Pareto-optimal timber facade assemblies that can support decision-making during the preliminary design stage. This integrated framework contributes to the development of more sustainable and high-performance timber building envelopes while providing a basis for future investigations into multi-criteria facade optimization.

1.7 STRUCTURE OF THE REPORT

To facilitate the reading and understanding of this report, the following paragraphs briefly describe its organization and the logical progression of the research. The first chapters are dedicated to introducing the research context and presenting a comprehensive review of the literature related to timber construction, with particular emphasis on the acoustic, thermal, and environmental performance of timber-based building envelopes. The theoretical concepts, existing methodologies, and research gaps that motivated this study are also discussed (Chapters 1 and 2).

Based on the observations and knowledge acquired through this literature review, a scientific article was developed to investigate the relationship between the acoustic, thermal, and environmental performance of timber facade assemblies. The article presents the methodology adopted in this research, the analyses performed, and the principal findings, while proposing an integrated framework for evaluating and optimizing timber facade assemblies according to multiple performance criteria. The article, together with its scientific contribution and its relationship to the objectives of this master's thesis, is presented in Chapter 3.

Finally, the report concludes with a synthesis of the main findings, highlights the scientific contributions of the research, discusses its limitations, and presents recommendations for future work.

CHAPTER 2
LITERATURE REVIEW

2.1 THEORETICAL BACKGROUND

2.1.1 SOUND INSULATION

Human communication primarily relies on the transmission and reception of sound. Sound itself arises from mechanical vibrations that travel through mediums like air or solid structures as waves. While humans utilize sound for communication, they are also exposed to 'noise', unwanted sounds generated by human activity and equipment [11]. These noises negatively impact well-being, productivity, and health [5]. Given the significant portion of human life spent indoors, optimizing the acoustic environment within buildings constitutes a critical aspect of architectural design. The field of architectural acoustics addresses this by focusing on two key areas: room acoustics and building acoustics. Considering the integral role of building acoustics in mitigating noise transmission, the following section provides a focused overview of its principals, focusing on airborne and impact sound.

2.1.1.1 BUILDING ACOUSTIC

Building acoustics is the branch of acoustics concerned with how sound and vibration propagate through and between building elements, and with the design strategies used to control noise transmission within buildings. Within this field, two types of sound are considered during sound measurements, which are 'airborne sound' and 'impact sound' [12]. Airborne sounds are generated by sources such as speech, audio, or mechanical equipment, and travel as pressure waves through the air, caused by vibrations of a source. Figure 2 shows how airborne sound waves could travel between two adjacent rooms. On the other hand, impact sounds, also known as structure-borne sound**,** occur by direct contact between a source (such as a tapping

machine, footsteps, or a dropped object) and solid surface such as floors or ceilings as illustrated in Figure 3.

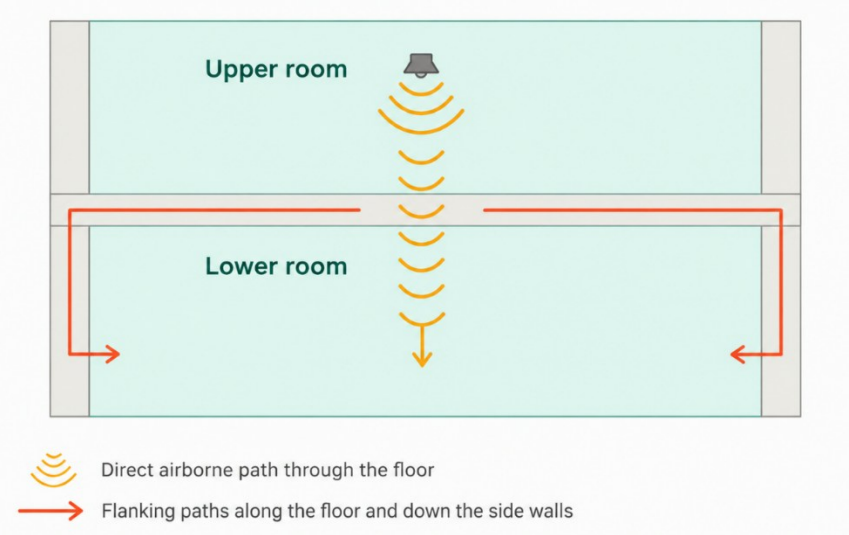


Figure 2. The propagation of the airborne sound.

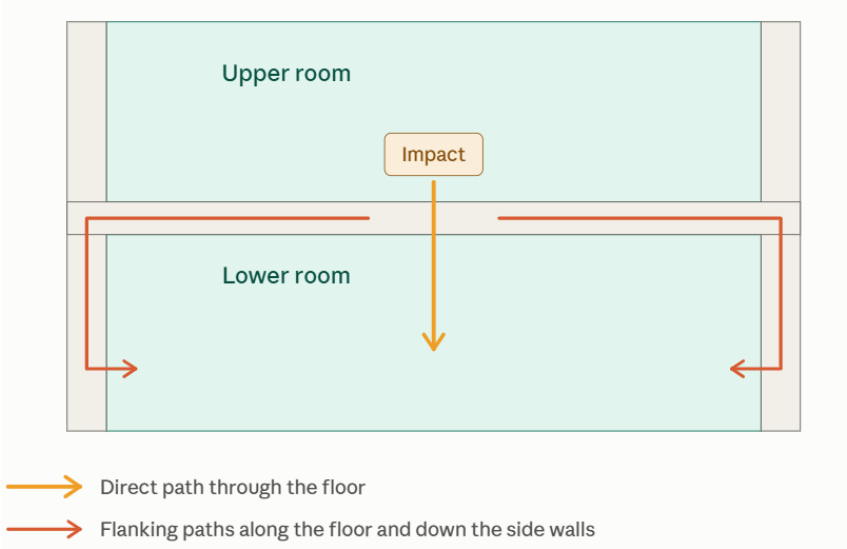


Figure 3. The propagation of the impact sound.

In building acoustics, sound is transmitted from one space to another through multiple pathways, and identifying these pathways is essential for designing effective sound-insulating elements. Two main types of transmission paths are distinguished: the direct (incident) path and the indirect (flanking paths). As shown in Figure 4, the direct

path corresponds to sound transmitted directly through the separating partition between the source and receiving rooms. Flanking paths refer to all other routes through which sound reaches the receiving room, such as adjacent walls, floors, ceilings, or structural junctions [13]. For airborne sound, twelve flanking paths are typically identified between two adjacent rooms, while for impact sound, five paths are considered [14,15]. Although each individual flanking path generally contributes less than the direct path, the combined effect of all flanking paths can result in a substantial increase in overall sound transmission.

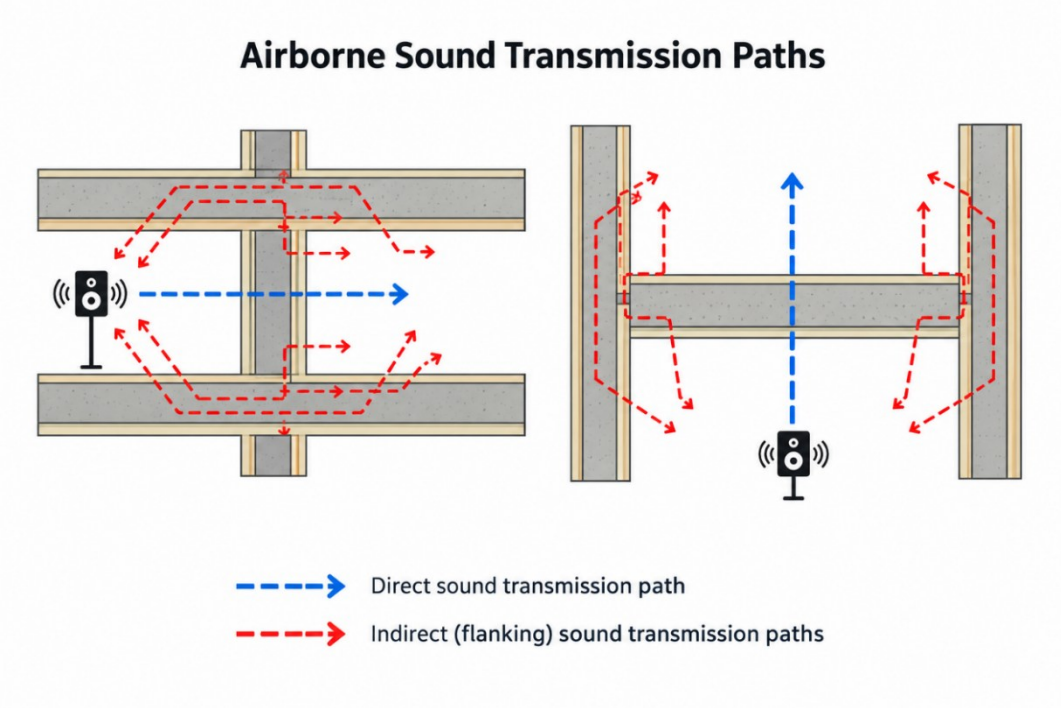


Figure 4. Sound transfer paths: 7: flanking-flanking, 8: flanking direct, 9: direct-flanking.

2.1.1.2 AIRBORNE SOUND MEASUREMENT

The measurement of airborne sound transmission is standardized in ISO 10140-2 [16], which specifies the procedure for evaluating the sound insulation of a partition placed between two rooms. Such measurements are central to assessing the

acoustic performance of walls, floors, and other building elements, and form the basis for the standardized testing of materials and assemblies. Airborne sound measurements are generally classified into two categories: laboratory measurements and field measurements.

2.1.1.2.1 LABORATORY MEASUREMENTS FOR AIRBORNE SOUND INSULATION

Laboratory tests are conducted in two adjacent reverberation rooms separated by the test specimen, with flanking transmission suppressed by structural decoupling between the rooms, in accordance with the ISO 10140-2 [16], and ASTM E90 [17]. The results of the laboratory measurements shall not be applied directly in the field without referring to external factors. However, performing laboratory measurements will guarantee accurate and repeatable results under standardized conditions.

To measure airborne sound transmission through a partition, a speaker is placed in the source room and at least five microphone positions are used in the receiving room. The sound pressure level L_p in each room is calculated by comparing the measured sound pressure p to the reference pressure p_{ref} (20μPa) as follows:

$$Lp = 10\ log\ \frac{p^2}{pref^2} \tag{2.1}$$

The sound reduction index R is defined as the ratio between the sound power incident on the partition P_0 and the sound power transmitted through it P_t:

$$R = 10\ log\ \frac{P_0}{P_t} \tag{2.2}$$

Knowing that sound power $P = I * A_p$, where I represent the intensity, and A_p represents the area of the partition in meter square. Hence, by replacing the latter and

assuming that the sound field on both sides of the partition is diffused, the sound reduction index becomes:

$$R = 10\ log\ \frac{I_0}{I_t} + 10\ log\ \frac{S}{A} \tag{2.3}$$

where I_0 denotes the sound intensity incident on the partition, and I_t denotes the sound intensity transmitted through it. Since the first term represents the difference in sound pressure levels, referring to equation 2.1, R becomes as follows:

$$R = L_{p1} - L_{p2} + 10\ log\ \frac{S}{A} \tag{2.4}$$

ISO has defined that a high value of the reduction index leads to greater sound attenuation. L1 and L2 represent the sound pressure levels of both the source and receiving room respectively, S represents the partition area in square meters, and A represents the absorption area of the receiving room in square meters. It should be mentioned that both ISO and ASTM standards, follow the same methodologies in the measurements as well as in the calculations but differ in terminology as it will be discussed in Section 2.2.1.4; in ISO it refers to sound reduction index R_w, where in ASTM it is referred to as Transmission Loss TL [17].

2.1.1.2.2 FIELD MEASUREMENTS FOR AIRBORNE SOUND INSULATION

Airborne-field measurements involve carrying out sound insulation measurements on real buildings, outside of controlled laboratory settings. As mentioned, the key difference between the laboratory and the field measurements lies in the flanking paths. Conversely, field measurements directly capture the impact of flanking paths, providing a more realistic, but potentially more challenging, assessment of sound insulation.

The main quantity measured has been named as the apparent sound reduction index, referred to as R' and the equation follows the same procedure as equation 2.4, with adding the pressure transmitted by the flanking paths to the receiving sound pressure level L_2:

$$R' = L_{p1} - L_{p2} + 10\ log\ \frac{S}{A} \tag{2.5}$$

As stated before, in the ASTM standard [17], a variation in terminology occurs, where the apparent reduction index here is referred by the apparent transmission loss index ATL. ISO 16283-1 [18] provides another method for measuring sound insulation directly in buildings (field measurements). This method relies on a standardized reverberation time T_0 of 0.5 seconds, which is particularly relevant for assessing dwellings:

$$D_{nT} = D + 10\ log\ \frac{T_{60}}{T_0} \tag{2.6}$$

Where D_{nT} refers to the standardized level difference in dB, D is the level difference between the source and receiving rooms (dB). In practice, T_{60} is determined from a decay over 20 dB (T_{20}) or 30 dB (T_{30}) and extrapolated to 60 dB, since a full 60 dB decay is rarely achievable in field conditions due to background noise [19].

2.1.1.3 IMPACT SOUND MEASUREMENT

Impact sound is the sound generated when a building element is mechanically excited by a source in direct contact with its surface, causing vibrations that are transmitted through the partition and radiated into adjacent spaces. The impact sound waves are usually excited by footsteps, dropped objects, or furniture movement, as shown in Figure 3. However, ISO 10140-3 [20], and ASTM E492 [21], have specified

the impact sound levels measured using a standardized tapping machine as shown in Figure 5, which serves to deliver a continuous, unchanging impact power on the floor structure, leading to more controlled and accurate results. This tapping machine consists of five identical hammers with 500g each; the hammers are arranged in line and separated by 40 cm from each other. Each hammer is freely falling from a height of around 40mm [22]. Moreover, besides the ISO tapping machine, impact sound can also be measured using the ISO rubber ball, which is found to be a suitable source simulating human footfall noise [23].

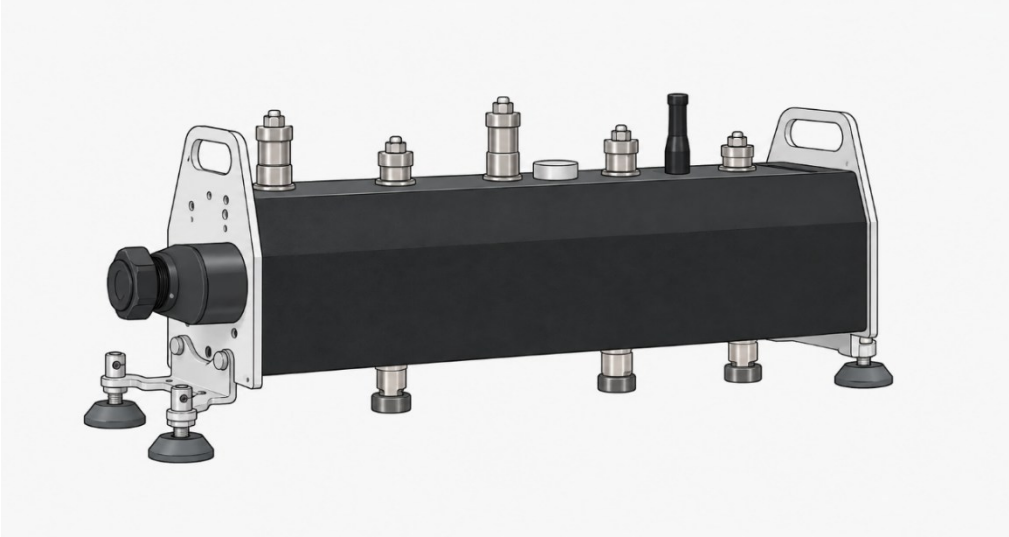


Figure 5. Standardized tapping machine.

2.1.1.3.1 LABORATORY MEASUREMENTS FOR IMPACT SOUND INSULATION

Like the airborne sound measurements procedure, the laboratory test consists of two separated rooms connected by a partition, probably a floor, on which the tapping machine is used to emit the sound on the floor, considering that the flanking paths are suppressed by referring to the ISO 10140-3 [18] and ASTM E492 [21]. The equation

used to quantify the amount of sound transmitted through the ceiling could be expressed as follows:

$$L_n = L_i + 10\ log\ \frac{A1}{A0}\ dB \quad (2.7)$$

Where L_n represents the normalized impact sound level expressed in (dB), L_i is the reference impact sound level, A_1 is the equivalent absorption area in meters squared of the receiving room, and A_0 represents the reference absorption area in meters squared (usually 10 m^2). This is a standardized value used to normalize the L_n measurement across different receiving room sizes and absorption characteristics. A higher L_n value indicates more sound transmission through the partition; therefore, lower L_n values correspond to better impact sound insulation.

2.1.1.3.2 FIELD MEASUREMENTS FOR IMPACT SOUND INSULATION

In field measurements of impact sound waves, the following equation is useful for quantifying the influence of the receiving room's acoustics on the perceived noise level:

$$L'_{nT} = L_i + 10\ log\ \frac{T_{60}}{T_0}\ dB \quad (2.8)$$

Where L'_{nT} represents the standardized impact sound pressure level (dB) measured within the receiving room during an impact sound test, L_i refers to the average impact sound pressure level in the receiving room and T_0 which refers to the reference reverberation time (usually 0.5 seconds) used for normalization, and T_{60} is the time for the sound to decay by 60 dB after the source stops. In practice, T_{60} is obtained from measurements in the receiving room. In building acoustics, a

reverberation time of 0.5 s is commonly used as the reference value for normalizing sound insulation measurements in dwellings.

2.1.1.4 COMPARISON BETWEEN ASTM AND ISO STANDARDS

Building acoustics measurements are covered by two parallel systems of international standards: those published by ASTM International and those developed by the International Organization for Standardization (ISO). The adoption of either standard follows a clear geographic pattern, where ASTM standards are used in North America (the United States and Canada), whereas ISO standards serve as the reference in Europe, Asia, and the majority of other regions worldwide. Given that both standards address the same acoustic phenomena and measurement objectives, a structured comparison between them is relevant, particularly for manufacturers and researchers operating across multiple markets.

The two frameworks differ mainly in terminology and in the procedural details of testing, but their measurement objectives remain equivalent. For airborne sound transmission, the ISO framework relies on ISO 10140-2 in the laboratory measurements, and ISO 16283-1 in the field measurements, while ASTM uses E90 and E336 for the same measurements, respectively. For impact sound transmission, the corresponding standards are ISO 10140-3 (laboratory measurement) and ISO 16283-2 (field measurement), while ASTM uses E492 and E1007, respectively. The single-number ratings used to summarize the measured curves also follow this parallel structure: R_w (ISO 717-1) [24] and STC (ASTM E413) [131] for airborne sound, and $L_{n,w}$ (ISO 717-2) and IIC (ASTM E989) [131] for impact sound. A more complete

mapping of the active ASTM standards and their ISO counterparts is presented in Table *1*, and Table *2* covering airborne and impact sound transmission.

Table 1. Equivalent ISO and ASTM standards for airborne sound transmission measurement and rating

ISO	Year	Title	ASTM
ISO 10140-2	2025	Standard Test Method for Laboratory Measurement of Airborne Sound Transmission Loss of Building Partitions and Elements	ASTM E90
ISO 16283-1	2014	Standard Test Method for Measurement of Airborne Sound Attenuation between Rooms in Buildings	ASTM E336
ISO 717-1	2020	Acoustics - Rating of sound insulation in buildings and of building elements - Part 1: Airborne sound insulation	ASTM E413
ISO 16283-3	2016	Standard Guide for Field Measurements of Airborne Sound Attenuation of Building Facades and Facade Elements	ASTM E966
ISO 717-1	2020	Standard Classification for Rating Outdoor-Indoor Sound Attenuation	ASTM E1332

Table 2. Equivalent ISO and ASTM standards for impact sound transmission measurement and rating

ISO	Year	Title	ASTM
ISO 10140-3	2025	Laboratory measurement of impact sound transmission	ASTM E492
ISO 16283-2	2014	Field measurement of impact sound transmission	ASTM E1007

ISO 717-2	2020	Single-number rating of impact sound insulation	ASTM E989

Although ASTM and ISO standards follow the same general principles for both airborne and impact sound measurements, they differ in several procedural details. For laboratory airborne measurements, the main differences concern the minimum room volume (80 m^3 in ASTM E90 versus 50 m^3 in ISO 10140-5), the specimen area requirements (ISO 10140 specifies approximately 10 m^2 for walls and 10–20 m^2 for floors with a minimum 2.3 m short edge, while ASTM E90 only requires a minimum dimension of 2.4 m).

Furthermore, when sound insulation is referenced in building codes or compared between products, presenting the full frequency-dependent curve is impractical. For this reason, both ISO and ASTM standards reduce the measured curve to a single-number rating, which provides a convenient way to summarize acoustic performance. The procedure is based on a reference curve defined separately for airborne and impact sound, internationally established in ISO 717-1 and ISO 717-2 respectively. The reference curve is shifted in 1 dB steps toward the measured curve until the sum of unfavorable deviations across all one-third-octave bands between 100 and 3150 Hz is as large as possible without exceeding 32 dB. The single-number rating is then read at 500 Hz from the shifted reference curve. The two standards share this general procedure, with several differences summarized in Table 3.

Table 3. Differences between the ASTM and ISO for single-number rating procedures.

Parameter	ASTM	ISO

Rating for airborne measurements	STC (higher is better), unitless	R_w (higher is better), measured in dB
Rating for impact measurements	IIC (higher is better), unitless	$L_{n,w}$ (lower is better), measured in dB
Significant digits	Rounded to the nearest 1	Rounded to the nearest 0.1
Frequency range	125-4000 Hz	100-3150 Hz
Deficiencies	Sum ≤32 and Max deficiencies allowed ≤ 8 dB	Sum ≤32
Spectrum adaptation terms	No	Yes

Despite the differences in testing methodologies and reference curves, a conversion exists between the ISO and ASTM standards, which allows for an approximation in the results. For airborne sound insulation, the sound transmission class (STC) in ASTM standards, and the weighted sound reduction index (R_w) in ISO standards are found to be correlated with R^2 value equal to 0.989, indicating a difference of 1 dB between them [25]:

$$R_w = STC - 1 \tag{2.10}$$

For impact sound insulation, the ASTM Impact Insulation Class (IIC) and the ISO weighted normalized impact sound pressure level (L_n,w) vary inversely. Because the two ratings are derived from different reference curves and frequency ranges, an exact analytical equivalence between them cannot be established. An empirical relationship reported in the literature nonetheless allows a reasonable approximate conversion [25]:

$$IIC = 110 - L_{n,w} \tag{2.11}$$

2.1.2 THERMAL INSULATION

To ensure comfort for the residents and an energy-efficient system for the building, the thermal insulation process must be considered. The ultimate function of an insulating material is to regulate the heat flow and maintain the desired indoor temperature by acting as a barrier between two determined spaces. This plays a critical role in occupant well-being, as extreme temperatures can significantly impact health and productivity. For instance, excessively hot environments can lead to heat stress and discomfort, while inadequately heated spaces can compromise health and hinder concentration.

To determine the quality of a thermal insulation material, one should first know how heat transfers from one side to another. Heat transfer is the process by which heat energy moves from a hot region to a cold region, in this case, the heat should be transferred from a high temperature to a low temperature. This process can occur through three primary mechanisms namely conduction, convection, and radiation.

It should be mentioned that the sum of these three mechanisms gives the total heat transferred and could be shown as follows:

$$\lambda_{tot} = \lambda_{cond} + \lambda_{conv} + \lambda_{rad} \tag{2.12}$$

This is typically stated by referring to the first law of Thermodynamics, which states that 'The energy cannot be created nor destroyed it can only be transferred' [26].

As illustrated in Figure 6, denser materials generally exhibit higher thermal conductivity, signifying a greater capacity to conduct heat. Conversely, radiation becomes a more dominant factor in heat transfer when a material has a low solid content. For conventional insulation materials, gas conduction is considered a relatively

constant value. This constant value is then added to the combined effect of radiation and solid conduction to determine the overall thermal conductivity of the material. By optimizing the properties of the material to minimize the combined effects of radiation and solid conduction, a "sweet spot" can be achieved, resulting in a material with superior insulating capabilities.

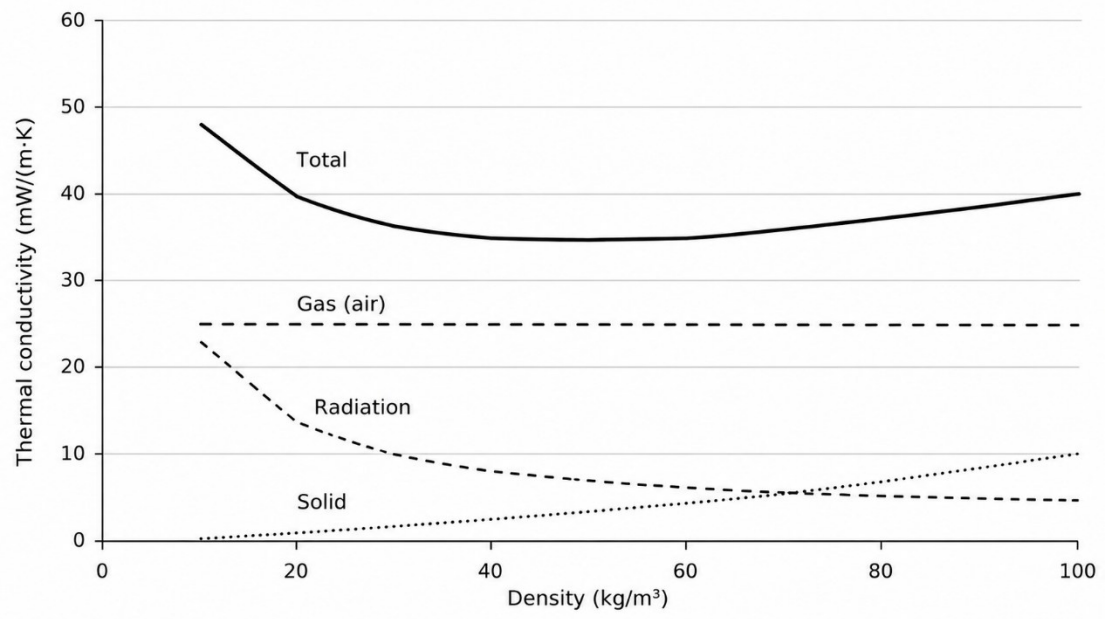


Figure 6. Total heat distribution in terms of density variation.

2.1.2.1 SOLID CONDUCTION

Solid conduction depends on the thermal conductivity of the material, the temperature difference across it, and the geometry of the heat path. This relationship is described by Fourier's law as follows:

$$Q = (K \times A \times \frac{\Delta T}{L}) \tag{2.13}$$

Where Q is the conductive heat flow rate (W), k is the thermal conductivity of the material (W/ (m· K)), A is the cross-sectional area perpendicular to the heat flow (m^2), ΔT is the temperature difference between the two surfaces (Kelvin), and L is the

thickness of the material (m). Equation 2.13 shows that the heat flow is directly proportional to the cross-sectional area available for conduction. As illustrated in Figure 7, heat flows from the hotter surface (T1) to the colder one (T2) across the thickness e, and the rate of conduction is governed by the conductivity k of the material. A material with lower thermal conductivity, or a greater thickness, therefore, reduces the heat flow and provides better thermal insulation.

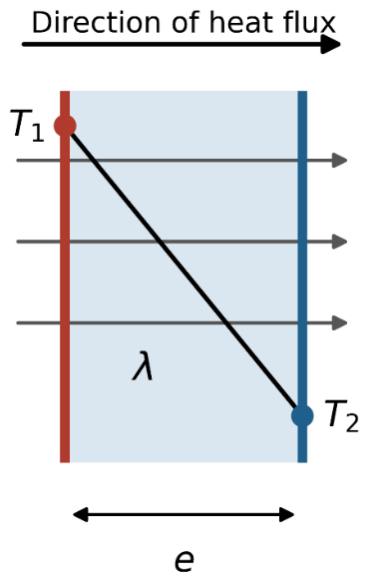


Figure 7. Heat transfer by conduction.

Similar to solid conduction, gas conduction is primarily influenced by the cross-sectional area available for heat transfer through the material. However, gas conduction also depends on the type and movement of the gas itself. Different gases possess varying thermal conductivities (k), signifying their capacity to conduct heat. To minimize heat transfer via gas conduction, employing gases with inherently lower thermal conductivities, such as argon or krypton, is a common strategy utilized in windows and specific insulation materials [27]. This approach reduces gas conduction without changing the geometry of the insulation. In addition, restricting the gas's ability

to move freely within the insulation material further decreases its effective thermal conductivity.

2.1.2.2 CONVECTION IN POROUS MATERIALS

Porous insulation materials can experience two main types of convection: pore cell convection and macro-scale convection. Pore cell convection refers to minor circulatory movements within individual pores due to small temperature differences across their walls. This type of convection is generally negligible. In contrast, macro-scale convection involves the larger-scale circulation of air throughout the entire material, particularly prevalent in materials with open-cell structures. This type of convection can significantly impact heat transfer and should not be disregarded [27].

Convection can be further categorized as natural or forced convection [27]. The Rayleigh number Ra_n and Nusselt number Nu quantify natural convection:

$$Ra_n = \frac{\rho_a \times c_{pa} \times g \times \beta_a \times d \times k \times (T^+ - T^-)}{V \times \lambda_M} \tag{2.14}$$

$$N_U = \frac{q_{with\ convection}}{q_{without\ convection}} \tag{2.15}$$

Natural convection arises from buoyancy forces caused by density variations within the air due to temperature gradients. Conversely, forced convection is driven by externally applied pressure differences, such as those induced by wind or fans. Airflow under forced convection is calculated using:

$$V = A \frac{K}{\mu} \frac{\Delta P}{d} \left(\frac{m^3}{s}\right) \tag{2.16}$$

2.1.2.3 RADIATION

All surfaces, regardless of temperature, emit heat energy in the form of electromagnetic waves, a phenomenon known as thermal radiation. The net rate of heat

transfer by radiation depends on the difference in temperature between two surfaces. A greater temperature difference translates to a higher net radiation heat transfer.

$$\lambda rad = \frac{16n^2\sigma T^3}{3K} \quad (2.17)$$

This equation expresses the relationship between temperature T, refractive index n, Stefan-Boltzmann constant σ, extinction coefficient K, and the rate of heat transfer by radiation (λ_{rad}). Here, T represents the absolute temperature in Kelvin, n reflects the material's ability to bend light, σ is a fundamental physical constant, and K characterizes how much the material absorbs or scatters radiation [27].

2.1.2.4 THERMAL TRANSMITTANCE

In building science there is a difference between the thermal conductivity k of a material, and the thermal transmittance U_{value} [28]. Thermal transmittance is used to assess the thermal performance of the building components, it quantifies the rate of heat through a material or building element per unit area and temperature difference. Thermal conductivity describes a property of a single material independent of thickness, while U_{value} describes the overall heat transfer through a multi-layer building component, taking thicknesses into account. A lower U indicates better insulation, as less heat is transferred through the material.

According to ISO 6946 [28], the thermal transmittance U is calculated as:

$$U_{value} = \frac{1}{R_{Total}} \quad (2.18)$$

Where R_{Total} is the total thermal resistance of the building component (sum of the resistance of its individual layers) in (m^2 k/ W) and could be calculated using the following:

$$R_{Total} = R_{si} + R_1 + R_2 \ldots + R_n + R_{se} \qquad (2.19)$$

Where R_1, R_2, $R_3 \ldots R_n$ are the thermal resistances of individual layers, and R_{si} and R_{se} are the indoor and outdoor surface resistances, respectively, and could be calculated as follows:

$$R = \frac{L}{K} \qquad (2.20)$$

Where L is the thickness of the layer in meters (m) and k is the material's thermal conductivity (W/ m. k).

2.1.2.5 THERMAL METHODOLOGIES AND MODELING TOOLS

Building on the principles of heat transfer described in the previous section, this section presents the experimental and computational tools used to evaluate the thermal performance of building components. Particularly, the calculation of thermal resistance, are validated, and measured using specialized equipment, such as the hot box apparatus described by the ASTM C1363 [29]. As illustrated in Figure 8, the structure of the guarded hot box is made up of two insulated parts, the cold box and the hot box, interconnected by the specimen box. The hot and cold chambers are well insulated from the surrounding temperature and between one chamber and the other. Each chamber contains 9 T-type thermocouples and three heat flow meters, and the test runs until steady-state conditions are achieved [30].

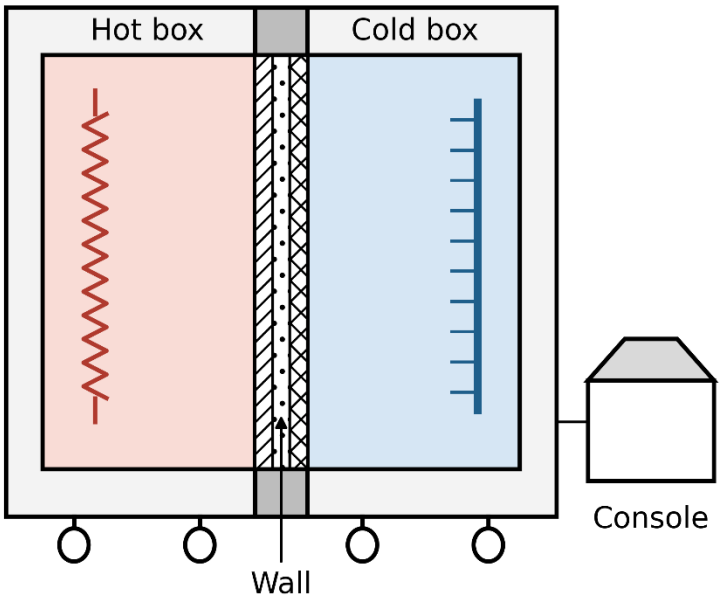


Figure 8. Schematic view of the guarded hot box apparatus.

After reaching a steady state condition in temperature, airspeed, and radiation, in the two sides boxes, the thermal transmittance of the test specimen is calculated using the following:

$$U = \frac{Q_P - Q_2 - Q_3}{A(T_h - T_c)} \tag{2.21}$$

Where $\mathrm{Qp} - \mathrm{Q2} - \mathrm{Q3}$ is the net heat flow through the specimen, after accounting for losses, A is the area of the specimen, and T_h and T_c are the temperatures of the hot and cold sides of the specimen, respectively.

In addition to experimental measurement, several software tools are commonly used to estimate U-values from layer composition, including UBAKUS [31], Energy Plus [32], and COMSOL Multiphysics [32]. These tools apply the analytical principles of ISO 6946 to multi-layer assemblies, providing fast and reliable estimates that are

widely used in design practice. The present study uses UBAKUS for U-value calculation, as detailed in the methodology chapter.

2.1.3 THEORY OF HEAT AND SOUND PROPAGATION: ANALOGY

Heat and sound are two forms of energy that propagate through materials, each governed by its own physical mechanism. Heat is a form of energy transfer that occurs between regions or systems at different temperatures, propagating through molecular interactions, while sound is mechanical energy that travels as pressure waves. Despite these differences, both energy types interact with partitions in similar ways, where part of the energy is dissipated, part is transmitted, and the material's properties influence the propagation. This perspective allows to develop a theoretical framework to describe and compare their behavior. In the following, the governing equations for heat conduction and acoustic wave propagation are presented, followed by characteristic quantities that describe their transmission, dissipation, and the influence of material parameters such as density, thickness, and mass.

Heat is a form of energy that moves from warmer regions to cooler ones whenever a temperature gradient exists. In solid building materials such as timber, this transfer occurs predominantly through thermal conduction, driven by the temperature gradient across the material [33]. The process is inherently gradual, where temperature disturbances introduced at one surface do not instantly reach the opposite surface, but rather spread progressively over time. This behavior is formally described by the one-dimensional transient heat diffusion equation [34]:

$$\frac{\partial T}{\partial t} = \alpha \frac{\partial^2 T}{\partial x^2} \tag{2.22}$$

In this relation, T represents the temperature field (kelvin), t the time (seconds), and α the thermal diffusivity of the material (m^2/s). Thermal diffusivity of the material expresses how quickly a material reacts to thermal changes and is governed by the following equation:

$$\alpha = \frac{k}{\rho C_p} \tag{2.23}$$

Where, k is the thermal conductivity of the material by which it measures how heat flows through the material ($W/m.k$), ρ is the density of material (Kg/m^3), and specific heat capacity C_p which measure the energy required to raise the temperature of a unit mass by one degree ($J/kg.k$). These parameters determine both the speed of thermal penetration and the ability of a material to buffer heat flow. A material with low conductivity and high heat capacity will delay temperature variations, thereby reducing the rate of heat transfer through the assembly and increasing its thermal inertia. In building physics, these behaviors are summarized by the thermal transmittance value (U-value), which decrease with the thickness and increase with conductivity.

On the other hand, sound is also a form of energy, transmitted through materials as pressure waves generated by vibrating sources such as speech, footsteps, or external noise sources. When these vibrations reach a building element, they set its particles into oscillatory motion. This wave motion carries energy through the structure, the resulting elastic deformation propagates through the structure and radiates airborne sound on the opposite side, causing energy to propagate from one side of the structure to the other. Unlike heat, sound does not diffuse gradually, instead, it travels directionally and can reflect, refract, or resonate depending on the characteristics of the element it

encounters. The physical behavior of airborne sound transmission in solids is governed by the one-dimensional acoustic wave equation [35]:

$$\frac{\partial^2 P}{\partial t^2} = c^2 \frac{\partial^2 P}{\partial x^2} \tag{2.24}$$

Where P is the acoustic pressure fluctuations (Pascal), t the time (seconds), and c is the speed of sound in the material (m/s). The value of c depends on both the density and elasticity of the medium, where heavier and stiffer materials transmit sound differently than lightweight or flexible materials. For one-dimensional longitudinal wave propagation in an elastic medium, the wave speed may be approximated by:

$$c = \sqrt{\frac{E}{\rho}} \tag{2.25}$$

Both heat and sound equations relate the temporal variation of energy transport to a second spatial derivative. This term describes how sharply the temperature field or the acoustic pressure field changes within the material. When the spatial curvature is large, heat or sound tends to propagate more rapidly. The main distinction lies in their order of time. Heat conduction is a first-order process, meaning that disturbances are progressively dissipated. However, acoustic propagation is a second-order process, meaning that disturbances oscillate and propagate without decaying immediately. To make both equations directly comparable theoretically and not practically, it is useful to rewrite the acoustic equation in a first-order form with respect to a mechanical energy quantity. Integrating once in time gives:

$$\int_{t_0}^{t} \frac{\partial^2 P}{\partial t^2} dt = c^2 \int_{t_0}^{t} \frac{\partial^2 P}{\partial x^2} dt \tag{2.26}$$

Which gives:

$$\frac{\partial P}{\partial t}(t) - \frac{\partial P}{\partial t}(t_0) = c^2 \int_{t_0}^{t} \frac{\partial^2 P}{\partial x^2} dt \qquad (2.27)$$

Assuming that the analysis is performed after the decay of transient effects, the initial term (t_0) may be neglected. To establish a qualitative mathematical analogy with the heat diffusion equation, it is assumed that, over a characteristic time interval, the spatial curvature of the pressure field varies slowly. Under this simplifying assumption, the time integral may be approximated as

$$\int_{t_0}^{t} \frac{\partial^2 P}{\partial t^2} dt \approx t * \frac{\partial^2 P}{\partial x^2} \qquad (2.28)$$

Resulting the following:

$$\frac{\partial P}{\partial t} = c^2 t \, \frac{\partial^2 P}{\partial x^2} \qquad (2.29)$$

This expression exhibits the same mathematical structure as the one-dimensional heat diffusion equation, in which the thermal diffusivity multiplies the spatial Laplacian. The resulting correspondence is therefore interpreted as a qualitative scaling analogy rather than a physical equivalence between acoustic and thermal transport processes. When the two equations are written in this form, the coefficients governing the rate of spatial energy redistribution can be directly compared. In the heat diffusion equation, this role is played by the thermal diffusivity α whereas in the reduced acoustic formulation it is represented by the term $c^2 t$. Although these quantities arise from different physical mechanisms, they occupy analogous positions in their respective equations. Based on this mathematical analogy, the coefficients governing both equations may be compared through the following scaling relationship:

$$\alpha \propto c^2 t \qquad (2.30)$$

where the symbol $\propto$ denotes a scaling relationship rather than an equality. Replacing each parameter by its previously defined equivalent:

$$\frac{k}{\rho C_p} \propto \frac{E}{\rho}\, t \tag{2.31}$$

This comparison highlights that both transport processes are governed by a balance between a driving property (thermal conductivity or elastic stiffness) and material inertia represented by density. Although these quantities originate from different physical mechanisms, they occupy analogous mathematical positions in their respective governing equations. In practical building acoustics, airborne sound insulation is not evaluated directly through the elastic modulus and density, but rather through standardized performance indicators such as the weighted sound reduction index R_w. Since R_w reflects the combined influence of mass, stiffness, damping, structural configuration, and frequency-dependent behavior, no direct analytical relationship can be established between E and R_w. Nevertheless, the preceding scaling analogy suggests that thermal and acoustic transport may be influenced by common material characteristics. This observation motivates the hypothesis that an empirical relationship may exist between thermal conductivity and airborne sound insulation, which is investigated using the facade database developed in this study. Based on the preceding analogy, the following qualitative trend is hypothesized:

$$k \propto \frac{1}{R_w} \tag{2.32}$$

the proportionality indicates an inverse relationship between thermal conductivity and airborne sound insulation performance. Since higher values of conductivity k correspond to increased thermal transport, while higher values of R_w indicate improved

acoustic insulation, the relation implies that these two quantities vary in opposite directions.

When represented graphically, this inverse proportionality if such an empirical relationship exists, plotting R_w against k would result in a decreasing trend, characterized by a negative slope. In such a representation, assemblies with higher thermal conductivity (worse thermal performance) would tend to exhibit lower airborne sound insulation (worse acoustic performance), whereas assemblies with reduced conductivity would generally correspond to higher R_w values. The validity of this hypothesis is assessed empirically in Chapter 3 through the statistical analysis of the facade database.

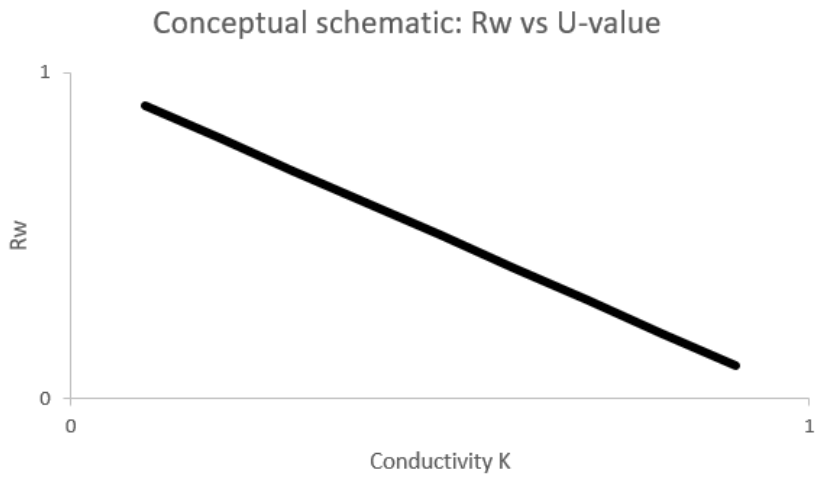


Figure 9. Conceptual schematic illustrating the expected inverse relationship between airborne sound insulation Rw and thermal conductivity k, derived from theoretical scaling considerations.

2.1.4 ENVIRONMENTAL IMPACT OF BUILDING CONSTRUCTION

Building design increasingly extends beyond thermal and acoustic performance to include environmental sustainability. According to the United Nations Environment

Program (UNEP), the building sector is responsible for nearly 40% of global energy consumption, 30% of raw material use, 25% of solid waste, 25% of water use, 12% of land use, and 33% of global greenhouse gas emissions [36]. Within this broader environmental footprint, the embodied carbon emissions (EC) of construction materials have found to be a particularly important indicator, since they illustrate the impact associated with the production of the building envelope itself. The following sections present the theoretical framework used to define and quantify embodied carbon, including the life cycle assessment methodology and the equations applied to estimate the carbon emissions of building materials and assemblies.

2.1.4.1 EMBODIED CARBON EMISSIONS

The carbon emissions in the lifecycle of a building consist of two essential components, namely, operational emissions and embodied emissions. Operational emissions refer to the energy consumed during the building's use phase, such as heating, cooling, and lighting. In contrast, embodied carbon (EC) is defined as all the greenhouse gas emissions generated throughout the building's material lifecycle, including the extraction of raw materials, manufacturing, transportation, construction, maintenance, and end-of-life disposal [37]. Historically, the operational energy use has accounted for the largest share of emissions, which has led designers to focus on reducing energy use during the operation of a building [38]. Consequently, embodied carbon was often overlooked during design and construction.

However, with the increasing use of green building materials such as timber structure, operational emissions have been reduced, and embodied emissions are now seen as the major contributor to total lifecycle emissions. A study conducted on the embodied carbon emissions of recent green building, found that embodied carbon

accounted for 50% or even up to 74% of the building's total carbon footprint depending on the building type, function, climate, and construction method [39]. This shift in environmental burden toward earlier life cycle stages indicates that operational efficiency alone is insufficient, and that sustainable design must increasingly prioritize the minimization of embodied impacts [40].

2.1.4.2 EMBODIED CARBON ANALYSIS

One of the most widely known methods for evaluating the environmental impact of construction materials is Life Cycle Assessment (LCA). LCA is a methodological tool, defined by the ISO 14040 standard [41], that allows the quantification of potential environmental impacts associated with the entire life cycle of a product. As shown in Figure 10, the assessment of the LCA includes studying the entire life cycle of the product, such as the material extraction, manufacturing, transportation to the site, construction and assembly, operation, maintenance, and the end-of-life processes (demolition, recycling, disposal).

One of the branches linked to LCA is the Life Cycle Carbon Emissions Assessment ($LCCO_2A$), which focuses on evaluating the CO_2 emissions as an output over the whole life cycle of a building. Following the framework defined by EN 15978 [42], the whole life embodied carbon emissions of a building are obtained by summing the contributions of each life cycle stage, as expressed in the following:

$$EC_{total} = \sum_{i=1}^{n}\left(Q_i * EF_i{}^{A1-A3}\right) + EC^{A4} + EC^{A5} + EC^{B} + EC^{C} - EC^{D} \quad (2.33)$$

Where EC_{total} is the whole life embodied carbon emissions ($Kg.CO_2$), Q_i is the quantity of material used in mass or volume (kg or m^3), EF^{A1-A3} is the emission factor for product stage ($Kg.CO_2/unit\ Qi$), EF^{A4} and EF^{A5} represent the emissions from

transport to site and construction respectively, EF^{B}, EF^{C} represent the usage and demolition stage of life, and EF^{D}represents the avoided emissions associated with reuse, recycling, or energy recovery beyond the system boundary, in accordance with EN 15978 [42].

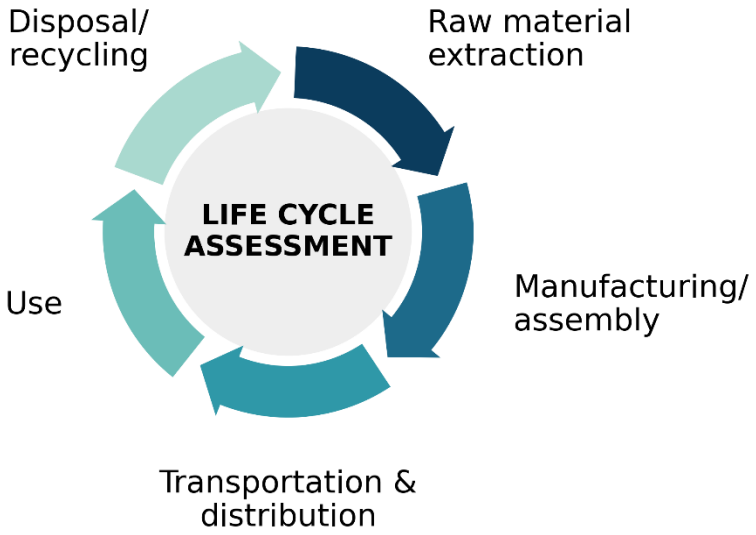


Figure 10. Life cycle assessment schematic.

At the material level, the embodied carbon (EC) of a single material is calculated as:

$$EC = EC_x * \rho_x * V_x \quad (2.34)$$

Where EC_x is the embodied carbon factor of the material ($Kg\ CO_2.eq/Kg$), ρ_x and V_x are the density (kg/m^3) and volume of the material (m^3), respectively.

Beyond the analytical equation above, other methods can be used to quantify the EC emissions, using specialized computational tools such as SimaPro, GestImpact, or OpenLCA [43–46]. These tools serve to facilitate the quantitative evaluation of embodied carbon across different material choices and building assemblies, thereby enabling designers to optimize environmental performance early in the design process.

2.1.5 OPTIMIZATION FRAMEWORKS FOR MULTI-CRITERIA PERFORMANCE ASSESSMENT

2.1.5.1 OPTIMIZATION FRAMEWORKS FOR SINGLE AND MULTI-OBJECTIVE PROBLEMS

Optimization methods are widely used in engineering and applied sciences to support decision making when system performance depends on multiple parameters. Traditionally, optimization problems were formulated in terms of the single-objective method, where a single measure of system performance was optimized to its minimum or maximum [47]. However, in cases where several performance indicators must be considered simultaneously, single-objective optimization is commonly extended through scalarization techniques, such as weighted sums or scoring functions, that combine multiple criteria into a single objective function. While scalarization-based approaches are straightforward to implement, they require the prior definition of weighting factors that reflect the relative importance of each criterion. This often involves a subjective component, where the weights substantially impact the optimal solution [48]. Additionally, since multiple criteria are reduced to a single criterion, the trade-offs between competing factors are hidden, leading to a single optimal solution, considering that various options may perform equally well when prioritized alternatively.

To reduce the impact of these limitations, multi-objective optimization frameworks have been developed to evaluate multiple, potentially conflicting objectives simultaneously without reducing them to a single scalar value. In multi-objective problems, improvement in one objective tends to deteriorate in another, and thus, making the identification and interpretation of trade-offs a central aspect of the

analysis. Rather than producing a unique optimal solution, multi-objective optimization aims to characterize a set of solutions that represent different compromises between objectives.

From a mathematical perspective, an optimization problem is formulated by defining a vector of decision variables:

$$x = \{x_1, x_2, \dots, x_n\} \tag{2.35}$$

Which represents the controllable parameters of the system under study. System performance is quantified through one or more objective functions $f_k(x)$, which express the criteria to be minimized or maximized. In single-objective case, the problem is expressed as:

$$\min_{x \in \Omega} f(x) \tag{2.36}$$

Where Ω denotes the feasible domain of solutions. The feasible domain is defined by a set of inequality and equality constraints, expressed respectively as:

$$g_i(x) \leq 0, i = 1, \dots, m \tag{2.37}$$

$$h_j(x) \leq 0, j = 1, \dots, p \tag{2.38}$$

These constraints represent physical limitations, regulatory requirements, or design rules that restrict the admissible solutions [49]. When multiple performance criteria are considered, the optimization problem is extended to multi-objective formulation, defined as:

$$\min_{x \in \Omega} f(x) = [f_1(x), f_2(x), \dots, f_k(x)] \tag{2.39}$$

where each objective function corresponds to a distinct performance indicator. In such problems, the objectives are often conflicting, and no single solution can simultaneously optimize all criteria [49].

There are two broad categories of multi-objective optimization strategies. In the first category, there are scalarization approaches that extend the concept of single-objective optimization such as Utility Function, Global Criterion, Lexicographic [49]. This type of methods maintains a single-solution outcome but depend strongly on predefined preferences. In the second category or the search approaches, there are generative methods that employ the use of meta-heuristic search algorithms that search for multiple optimal designs within the solution space such as Non-Dominated Sorting Algorithm (NSGA), Particle Swarm Optimization (PSO), and Ant-Colony Optimization (ACO) [49]. This is more effective when generating new designs within a continuous solution space or when new solutions must be generated through systematic variation of design variables.

However, not all optimization problems imply the need to generate new solutions. In instances where a fixed set of solutions is being considered for evaluation with a given dataset of existing options or alternatives, the goal is not to optimize new designs. Rather, the aim revolves around finding and interpreting the best-performing alternatives within a context where the focus changes from optimization as a design generation technique to optimization as an evaluation technique for selecting among known design alternatives that must be compared in a transparent process. This raises the need for the application of Pareto-based methods that enable the formulation of multiple objectives concurrently and the retention of the trade-off between these

objectives. A discussion on the theory and interpretation of Pareto optimality is presented in the next section.

2.1.5.2 PARETO-BASED MULTI-OBJECTIVE OPTIMIZATION AND APPLICATION

Pareto-based multi-objective optimization provides a formal framework for analyzing problems in which several conflicting objectives must be considered simultaneously. Differing from scalarization-based methods, pareto analysis does not require predefined weighting factors and does not reduce the problem to a single objective. Instead, it relies on the concept of dominance to compare solutions across multiple performance criteria. Given a multi-objective minimization problem with objective vector:

$$f(x) = [f_1(x), f_2(x), \dots, f_k(x)] \qquad (2.40)$$

A solution x_1 is said to dominate x_2 if:

$$f_i(x_1) \leq f_i(x_2)\ \forall i\ \in \{1, \dots, k\} \qquad (2.41)$$

And

$$f_j(x_1) \leq f_j(x_2)\ for\ at\ least\ one\ j \quad (2.42)$$

A solution is defined as Pareto-optimal if no other feasible solution dominates it. The set of all Pareto-optimal solutions forms the Pareto front, which represent the boundary of achievable trade-offs among the considered objectives within the feasible solution space. While the Pareto front does not identify a single optimal solution. Rather, it provides a structured representation of competing alternatives, each of which reflects a different compromise between objectives. This characteristic makes Pareto-based

optimization particularly suitable for decision-making problems in which performance criteria cannot be meaningfully ranked a priori.

The shape of a Pareto front carries important information about the nature of the trade-offs between objectives. A smooth and continuous front indicates gradual trade-offs, where incremental improvement in one objective leads to proportional degradation in another. In contrast, discontinuous or clustered fronts may indicate threshold effects, competing mechanisms, or discrete solution characteristics. Convex and non-convex regions further reflect whether trade-offs are balanced or strongly penalized across objectives, with their orientation depending on whether objectives are to be minimized or maximized (Min–Min, Min–Max, Max–Min, Max–Max), as illustrated in Figure 11 [47].

Importantly, Pareto-based optimization is independent of how the solution space is generated. While Pareto fronts are often obtained through iterative search or generative algorithms, the underlying dominance principles apply equally to predefined solution sets. In such cases, Pareto analysis functions as an evaluation and filtering tool, allowing non-dominated solutions to be identified directly from existing data without modification or generation of new alternatives. As a result, Pareto-based optimization serves both as an analytical method for understanding multi-objective trade-offs and as a transparent selection framework for performance assessment. Its ability to retain the full spectrum of efficient solutions while avoiding subjective weighting makes it particularly well suited for comparative studies involving multiple performance indicators.

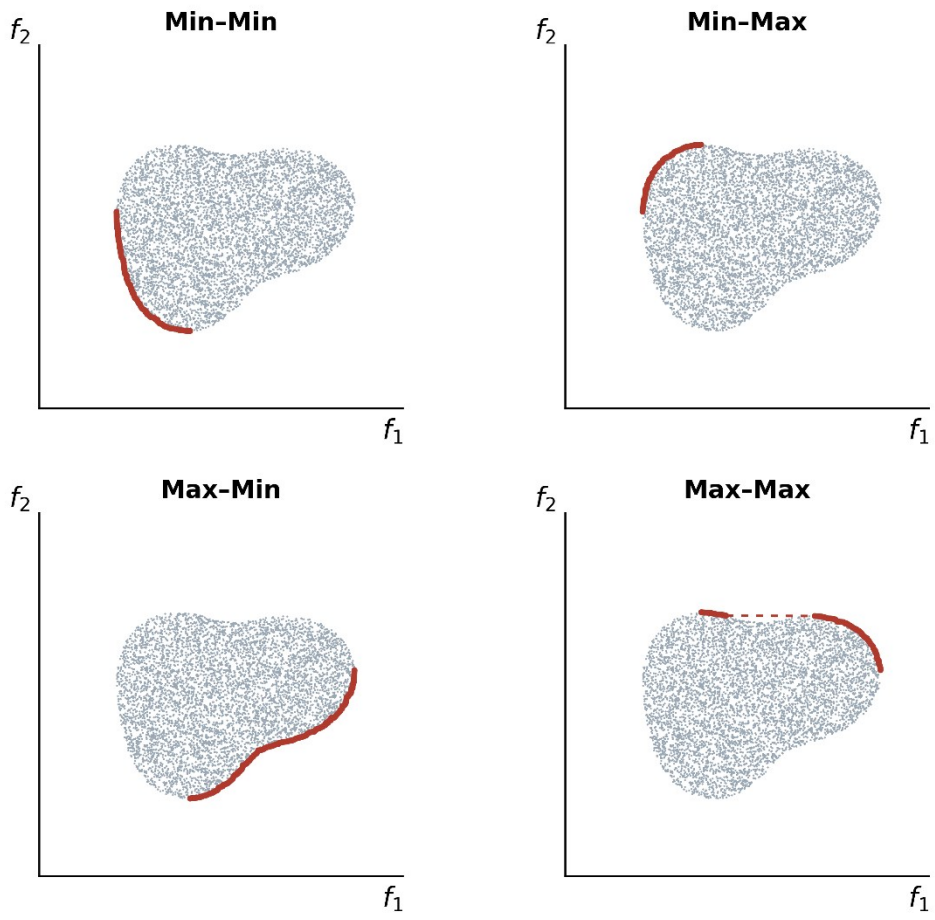


Figure 11. Common Pareto front geometries for two-objective optimization problems, illustrating the four possible combinations of minimization and maximization objectives: Min–Min, Min–Max, Max–Min, and Max–Max. The bold curve in each case represents the Pareto-optimal front, defined as the set of non-dominated solutions beyond which improvement in one objective necessarily entails a deterioration in the other.

Several recent studies in the built environment and engineered wood systems have applied Pareto-based multi-objective optimization methods. For instance, multi-objective genetic algorithms such as NSGA-II have been used to optimize cross-laminated timber composite floor systems with different concrete finishes, generating Pareto fronts that capture trade-offs among structural performance, self-weight, and cost across alternative configurations[50]. Other studies have implemented particle

swarm optimization and related multi-objective techniques for intermediate timber floor systems to balance mechanical performance with environmental and comfort-related criteria across discrete design options [51]. These applications demonstrate how Pareto fronts can reveal trade-offs between conflicting objectives and support transparent evaluation of alternative design sets in engineered wood assemblies. The following section outlines the methodology adopted in this study for constructing and analyzing Pareto solution sets.

2.2 RESEARCH BACKGROUND

2.2.1 IMPORTANCE OF WOOD CONSTRUCTION IN CANADA AND INTERNATIONALLY

Wood construction offers a range of environmental advantages that cover sustainability, low embodied energy, and recycling. It is found that wood has lower greenhouse gas emissions associated with the building materials than other non-renewable materials like steel and concrete [52]. The environmental benefits of wood construction are maximized through the use of sustainably managed forests, coupled with the reuse and repurposing of wood at the end of a building's lifecycle, thereby reducing the demand for alternative materials [3, 13, 14, 15]. Furthermore, wood provides several noteworthy economic advantages [55]. The increase in the popularity of wood construction has led to a rise in the need for jobs, with an estimation that forest products in Canada contribute to over two hundred thousand direct jobs [56]. Wood construction has gained popularity in the past decade, especially in Canada and the United States [57]. It remains a dominant building material in North America, with construction accounting for over half of the wood harvested from its forests [58]. This

is because of several factors, such as aesthetic appeal, structural performance, and cost-effectiveness compared to other materials [14, 20,21].

Mass Timber is an 'Engineering Wood Product' (EWP) widely used in residential and mid-rise construction. Some of the most common types of EWP include cross-laminated Timber (CLT), Glued Laminated Timber (Glulam), Nailed Laminated Timber (NLT), Dowel Laminated Timber (DLT), and their hybrid versions. These panels are wood-based materials that combine wood strands, veneers, or fibers with adhesives to form engineered wood panels or structural components [61]. Compared to Lumber wood, these panels offer several advantages, including improved strength, dimensional stability, and design flexibility. Simple nail and screw connections in these types of wood buildings enable relatively easy deconstruction, increasing the potential for material reuse [61]. Moreover, the EWP panels have a high strength-to-weight ratio, which allows for their use in taller timber structures, including mid-rise buildings, as well as good seismic structural performance [62]. In Canada, the first multi-story CLT building was a six-story building made in 2010, which led to a 12% saving in terms of the total annual cost [63]. The second building was a 13 multistorey called 'Origine' located in Quebec; this building is 40.9 meters tall [64]. Beyond their structural properties, EWP panels can achieve high fire resistance ratings through proper design and construction. The fire resistance of EWP can be evaluated through laboratory tests or calculated using recently developed design methods such as the ASTM E119 standard test methods, which entails three failure/acceptance criteria (Mechanical resistance, integrity, and insulation) [65].

In contemporary wood construction, two main structural approaches dominate building envelope design: light-frame walls and massive timber walls. Light-frame

walls, often referred to as stud walls, consist of repetitive slender timber members (studs and plates) combined with sheathing and insulation layers. This configuration is widely used in North American housing and low- to mid-rise construction due to its material efficiency, ease of prefabrication, and adaptability to various insulation strategies. In contrast, massive timber walls are composed of large prefabricated solid panels, typically made of CLT or Glulam, which serve simultaneously as structural and enclosure elements. These systems provide higher load-bearing capacity and structural rigidity compared to framed walls, making them suitable for mid- and high-rise buildings. The distinction between framed and massive wall assemblies forms a key aspect of this research, as both represent prevalent construction methods in Canada with distinct design principles and performance characteristics.

A direct application of EWP in construction is facades. Facades are essential in building design as they serve multiple functions. Despite their aesthetic appeal, facades serve as protective barriers against external environmental factors such as noise, wind, rain, and moisture penetration, providing a regulating heat transfer for the indoors. Using wood and engineered wood products as facades has been proven to be suitable in construction due to the aesthetic appearance and the durability of the wood with proper use [66]. However, substituting the heavyweight materials like concrete and brick with lighter materials such as the EWP will affect the sound insulation performance of the partition due to the relatively low stiffness and mass of the wood, especially at low frequencies [67].

The next section will examine the acoustic insulation performance of EWP and present the reasons behind their relatively low sound insulation compared to traditional heavyweight materials. It also presents the strategies used to overcome these limitations

through the integration of additional insulation materials, with the aim of improving acoustic indoor comfort.

2.2.2 ACOUSTICS IN WOOD CONSTRUCTION

Acoustic performance is a critical aspect of building design, influencing occupant comfort, productivity, and overall building quality, such as noise levels, speech intelligibility, and privacy [68]. Noise pollution is a major global health concern, ranked as the second most critical pollution type by the World Health Organization [69]. Noise sources can generally be divided into two main types. The first one is airborne sound, which refers to unwanted noise transmitted through the air, such as speech, music, or household activities. The second one is impact sound, which results from the direct contact with elements such as walls, floors, or ceilings, and is typically caused by footsteps or dropped objects [29, 31]. The performance against airborne sound is evaluated using the weighted sound reduction index (R_w) according to ISO 10140 standards [16], or expressed as sound transmission class (STC) following ASTM E90 standards [71], where higher values indicate better insulation. On the other hand, impact sound insulation is measured using the weighted impact sound pressure level (L_w) according to ISO 10140 standards [16], while the equivalent ASTM E492 standard is expressed as the impact insulation class (IIC) [72]. Lower L_w and higher IIC values indicate better performance.

The fundamental acoustic challenge of wood construction stems from the relatively low mass and stiffness of timber compared to conventional heavyweight materials such as concrete or masonry. According to the mass law, sound transmission loss increases with the surface mass of a partition, meaning that lightweight assemblies inherently transmit more sound energy than their heavier counterparts at equivalent

thickness [25]. Furthermore, lightweight panels are susceptible to the coincidence effect, a phenomenon in which the bending wavelength of the panel matches the wavelength of the incident sound at a specific frequency, causing a sharp dip in sound insulation performance [25]. In wood-based assemblies, this coincidence dip tends to occur at frequencies that overlap with common environmental noise sources, particularly traffic and mechanical equipment, which further limits the effectiveness of timber as a standalone acoustic barrier [73].

To overcome these limitations, research has focused on composite assemblies that compensate for wood's inherent acoustic deficiencies through strategic layering, decoupling, and cavity design. In light-frame construction, the National Research Council of Canada (NRC) has demonstrated that the acoustic performance of timber walls varies significantly depending on cladding type, cavity composition, and stud configuration [74]. On a standardized wood-stud wall, low-density claddings such as vinyl or aluminum contributed negligibly to acoustic performance, whereas heavier cladding materials such as brick enhanced insulation by up to 6 dB [74]. Similarly, stud spacing also plays a meaningful role, as increasing the spacing shifts the resonance frequency downward, improving overall facade acoustic performance by 3 to 5 dB. Another improvement strategy involves the use of resilient channels (RCs), which are thin metal spring-like components that decouple the interior wall finish from the structural frame, thereby reducing direct vibration transfer between surfaces. Experimental results on wood-stud facade walls show that resilient channels can increase the overall Rw rating by 3 to 5 dB compared to directly fastened assemblies [74].

In massive timber construction, the acoustic behavior is governed by different mechanisms. CLT and Glulam panels possess higher surface mass than light-frame assemblies, which provides inherently better low-frequency insulation. However, their high stiffness introduces a coincidence effect at relatively low frequencies, which can compromise mid-frequency performance. Research has shown that a 140 mm five-ply CLT panel combined with plasterboard on the interior, a wood panel on the exterior, and an air cavity achieved sound insulation improvements of 5 dB compared with hollow block walls and 8 dB compared with bare CLT panels [75]. Despite these advances, massive timber facades remain less studied than their floor and interior wall counterparts, with relatively few experimental datasets available for design reference [6].

While the research on wood acoustic performance has grown considerably, the majority of studies have focused on interior building elements such as floors and partition walls. Facade acoustics, which involves the transmission of external noise through the building envelope, has received comparatively less attention in the literature [7]. The lack of regulatory requirements for facades is due to historically lower external noise exposure, particularly from traffic. However, as cities grow, residential and commercial buildings are increasingly being constructed in high-density areas, where noise from combustion engines, including diesel vehicles, has become a critical issue [6]. However, acoustic comfort is not the only performance challenge faced by building occupants in timber construction. Thermal comfort is equally critical, and the following section examines how wood-based facade assemblies address heat transfer and energy efficiency.

2.2.3 THERMAL INSULATION IN WOOD CONSTRUCTION

The trend toward high-performance buildings reflects a growing focus on indoor comfort and energy efficiency. Thermal environments can significantly affect human performance both physically and mentally, as thermal comfort notably impacts cognitive function and work performance [76]. Inadequate thermal design, resulting from factors such as building orientation, dimensions, and glazing, can lead to thermal discomfort and higher energy demand [77]. Proper insulation is the key to developing energy-efficient buildings, and by minimizing heat transfer, good insulation creates a comfortable indoor environment while significantly reducing energy consumption for both heating and cooling [18, 43]. In North America, heating, and cooling account for 50-70% of total building energy [79]. This contributes to high electricity demand, a significant portion of which is still generated using fossil fuels like coal, natural gas, and petroleum products [80].

Understanding how insulation materials reduce energy consumption requires examining their thermal behavior. Insulation consists of one or more materials arranged in layers that serve to retard the heat flow rate in different aspects (conduction, convection, and radiation) [81]. Two main factors determine the material's insulation properties: Thermal conductivity (λ) and thermal transmittance (U). Materials with lower thermal conductivity and lower thermal transmittance values effectively resist heat transfer and reduce energy consumption. Several studies have been carried out to determine and investigate the standardized thermal conductivity of different materials under standard laboratory conditions [47, 48, 49]. Materials with a thermal conductivity below 0.1 $W/m.k$ are categorized as effective insulators. Materials with 0.3 to 0.5 $W/m.k$ are considered good insulators, while those above 0.7 $W/m.k$ are only

moderate [85]. Moreover, several factors play a crucial role in affecting the thermal conductivity of a material, namely, density, temperature, moisture content, and porosity [51, 52, 53, 54, 55]. Among these, porosity plays a particularly important role, as higher porosity generally reduces heat transfer by increasing the proportion of air voids within the material. This characteristic is evident in materials such as mineral wool, fiberglass, and natural fibers, which possess high porosities and are commonly used as insulation layers within facade assemblies [56, 57, 58].

Wood provides a relatively low thermal conductivity (0.4 $\mathrm{W/m.k}$), compared to other materials like concrete and stone, which demonstrate significantly higher thermal conductivity (1.7 $\mathrm{W/m.k}$), as well as soil (1.5 $\mathrm{W/m.k}$), making them unsuitable for insulation [94]. This advantage was confirmed by a study demonstrating that mass timber used as a thermal partition improved performance by 24% compared to concrete block walls [95]. Additionally, many studies focusing on the latter have made a comparative study between CLT compositions and concrete. Studies have found that lower thermal transmittance of the CLT wall, and depending on the insulation materials used with it, can exhibit a total energy demand reduction between 0.15 and 0.2 $\mathrm{W/m^2.k}$ compared with the traditional concrete facade [96]. Moreover, using engineered wood product for facades has resulted in a 73% improvement in thermal insulation compared to traditional hollow block wall systems [97]. Besides the low conductivity, the EWP is more stable in facing moisture, seismic, and structural loads, making it more suitable for building construction [62].

The thermal performance of wood facades depends on the type of facade presented, whether being ventilated or unventilated, as each configuration affects how heat is transmitted and absorbed. A ventilated facade is a system consisting of an added

external light cladding on a heavy wall to establish an intermediate ventilation layer [98]. The ventilated facade systems perform better against thermal transmittance. This improvement results from the ventilation cavity, which promotes convective cooling and reduces heat buildup. A comparative analysis between ventilated and unventilated facades was made to test their thermal performance. It was found that the presence of the ventilation layer in the ventilated facade has led to a 44% reduction in total heat transfer into the building, resulting in improved insulation, thermal comfort, and reduced heating energy demand [99].

The unventilated facades are considered less effective in terms of thermal insulation performance due to the presence of thermal bridges. Thermal bridges represent a critical challenge in building insulation as they significantly contribute to heat loss [100]. They are localized areas of higher heat transfer within the building envelope where the continuity of insulation is interrupted. In wood construction, these bridges occur primarily through structural members such as studs, plates, and connection interfaces, which possess higher thermal conductivity than the surrounding insulation. In light-frame facades, the repetitive stud framing forms continuous linear bridges that can increase overall heat loss by 15 to 25%, depending on stud spacing and insulation continuity [101]. Massive timber systems, such as CLT or Glulam panels, also exhibit thermal bridging, though to a lesser extent, mainly through mechanical connections or panel joints. However, research suggests that CLT panels, when installed correctly, can effectively minimize these heat losses by up to 15% compared to traditional light timber structures [102].

Furthermore, many studies have explored the capability of adding internal/ external insulation materials to enhance the characteristic insulation of the timber.

Studies have demonstrated the effectiveness of the External Thermal Insulation Composite systems (ETICS) in improving the thermal performance of timber partitions [67, 68]. Using such materials in building partitions has decreased the heat transfer coefficient by 48.3% after filling them with glass wool [102]. Some of these materials are fiberglass, glass wool, and expanded polystyrene (EPS), which are typically used in walls, floors, and ceilings. These types of insulators are installed between wooden and metallic components, with thermal conductivities of 0.04, 0.045, and 0.7 $\mathrm{W}/m.\mathrm{k}$, respectively [85]. However, factors such as density, thickness, and moisture content can influence the overall thermal performance of these materials. The usage of composite materials in building envelopes has been considered to surpass some of the factors that affect the performance of wood as an insulation material. Integrating wood as a component within composite envelopes has significantly enhanced overall thermal insulation.[105].

Finally, adding thermal insulation materials can also lead to an increase in the sound insulation of structures, as stated by the Mass Law. As additional insulation layers are introduced to improve thermal efficiency, they inevitably affect the acoustic behavior and environmental footprint of the assembly. The following section examines the relationship between thermal and acoustic insulation in wood construction, exploring how these two performance dimensions interact and the extent to which optimizing one influences the other.

2.2.4 THERMAL AND ACOUSTIC INSULATION IN WOOD CONSTRUCTION

Despite the growing body of research on timber building performance, thermal and acoustic insulation have historically been investigated as independent design

objectives, with limited research addressing both properties simultaneously [70, 71, 72, 73]. This imbalance is reflected in the distribution of published work in those fields. One study showed that mechanical and thermal studies accounted for 48% and 41% of the research, respectively, compared with only 11% for acoustic studies [108] The study expanded the review and showed that most of the work is done by European countries (66.7%), in contrast with a decreasing number of studies in North America (16.7%), highlighting a gap that this study aims to address [108]. The reason behind prioritizing thermal insulation over acoustic insulation could be explained by the occupant perception. A survey found that over 80% of respondents prioritized thermal over acoustic insulation in both lightweight and heavyweight timber structures, reflecting a potential bias in design properties rather than a demonstrated correlation between the two [107].

Accordingly, investigations examining both properties simultaneously in wood assemblies remain limited in scope. At the material level, studies on vertical building elements incorporating thermal insulation layers found that adding material improved both thermal and acoustic insulation simultaneously, with the weighted sound reduction index R_w values rising to 46 to 74 dB compared to 28 to 52 dB for bare walls, attributed to the combined effect of added mass and acoustic damping [110]. However, at the assembly level, research on cross-insulated timber (CIT), which replaces the core layer of a five-ply CLT panel with rigid polyurethane insulation material, found that thermal performance improved at the cost of acoustic performance due to the reduction in mass per unit area of the panel [111]. More recently, a study on composite floors of CLT and ribbed CLT-based assemblies reported a strong correlation between total thermal resistance and airborne and impact sound insulation [112]. At facade level,

several design parameters, such as material thickness, plasterboard doubling, and air tightness, have been reported to improve both acoustic and thermal performance simultaneously [113]. Across these studies, however, these results remain qualitative and case specific, with no empirical or numerical model so far proposed to quantify the relationship between thermal and acoustic performance in wood-based facades.

Most of the strategies described above involve adding material to the assembly. The environmental implications of this material use, however, fall outside the scope of the studies discussed so far and require a separate framework. The following section reviews the environmental impact of building materials and the life cycle assessment methods used to quantify it.

2.2.5 ENVIRONMENTAL ASPECT

The building sector currently faces a significant sustainability challenge, as only 5% of newly constructed buildings in 2022 met net-zero emission standards [114]. This falls well short of the objectives set by the International Energy Agency (IEA), which indicates the importance of achieving 100% of net-zero status for new buildings, set for 2030 [114]. As buildings become more energy-efficient, operational emissions are expected to decrease, and embodied carbon is projected to account more than 50% of total life cycle emissions over the first 30 to 50 years of a building's lifecycle [115]. In this context, timber-based systems have emerged as one of the most effective strategies for reducing embodied carbon. Unlike concrete and steel, which involve energy-intensive manufacturing processes, wood products store carbon absorbed during tree growth, making timber both a low-emission material and a carbon sink [116]. The development of engineered wood products such as CLT and Glulam has further extended this advantage to multi-story construction, with comparative studies

reporting GWP reductions of 81–94% and 76–91% relative to concrete and steel respectively [116].

Recent studies have explored the intersection of embodied carbon emissions and acoustic performance in floor timber construction. These investigations have found no direct correlation between higher EC and improved sound insulation in timber floors [117]. This means that acoustic performance can be increased without necessarily increasing the embodied carbon of the assembly. This is supported by laboratory and in situ measurements showing that replacing heavy concrete toppings with a resilient channel and acoustic separation layers can reduce CO_2 emissions by up to 66% with minimal impact on acoustic performance [118]. A study on nine floor assemblies, including wood and concrete composites, found that concrete elements contributed 50% of the total EC, compared with 13% for wood and 12% for acoustic underlayment materials such as gypsum board [83]. Notably, wood composite assemblies incorporating acoustic insulation materials achieved acoustic performance comparable to concrete composite structures while satisfying airborne sound insulation requirements (STC > 50) at significantly lower EC [119].These studies indicate that high acoustic and environmental performance can be simultaneously achieved through optimization analysis, where designers may select the assembly based on the project-specific goals acoustically and ecologically.

Studies have also investigated the relationship between embodied carbon and thermal performance in building assemblies. High-performance thermal insulation materials generally reduce operational energy demand by improving the thermal efficiency of the building envelope. However, in timber construction, where high-carbon structural materials such as concrete are largely absent, insulation materials

often become one of the dominant contributors to the total embodied carbon, especially when high-density materials are used [120]. An analysis of 156 Environmental Product Declarations (EPDs) showed that conventional mineral-based insulation materials, including glass wool and stone wool, can achieve embodied carbon values comparable to or lower than insulation products manufactured from fossil fuel-derived materials [121]. These findings highlight that improving thermal performance does not necessarily require a proportional increase in embodied carbon, provided that appropriate insulation materials are selected. This could be achieved by following the Environmental Product Declarations (EPDs), which are standardized, third party-verified documents that report the environmental impacts of a product based on a product life cycle assessment (LCA) [122].

Overall, the literature demonstrates that thermal, acoustic, and environmental performances are strongly interconnected in timber facade design. Design decisions intended to improve one criterion frequently influence the others, either positively or negatively, making single-objective optimization insufficient for identifying balanced facade solutions. Although previous studies have examined these interactions individually, relatively few have investigated all three performance criteria simultaneously, particularly for timber facade assemblies. This gap motivates the integrated approach adopted in the present study, which evaluates acoustic insulation, thermal performance, and embodied carbon concurrently to identify facade assemblies that provide the most favorable trade-offs.

CHAPTER 3
ARTICLE: “AN INVESTIGATION OF THE SOUND AND THERMAL INSULATION OF FACADES' WOOD ASSEMBLIES BY CONSIDERING ENVIRONMENTAL IMPACT ASPECTS”

3.1 ARTICLE PRESENTATION

This research was presented orally, in person, at two international conferences on timber construction: Next Generation Wood Construction 2024, held in Ottawa, and Next Generation Wood Construction 2025, held in Edmonton. It is also going to be presented at the INTERNOISE Conference 2026, in Adelaide, Australia, an internationally renowned conference in the field of acoustics and noise control.

This article presents the correlation analysis and multi-criteria optimization performed in order to identify the nature of the trade-offs between acoustic, thermal, and embodied carbon performance in timber facade wall assemblies.

382 assemblies were grouped into seven families based on common structural characteristics. Each family was subsequently analyzed individually in order to identify the design parameters that govern the trade-offs among the three performance objectives. This analysis led to the construction of a design catalogue intended to support engineers during the design stage.

3.2 SCIENTIFIC CONTRIBUTION

This research establishes, for the first time for timber facade wall assemblies, a joint analysis of acoustic, thermal, and environmental performance across a database of 382 assemblies. The results show that airborne sound insulation and thermal performance are strongly correlated, while embodied carbon varies independently of both, indicating that the main design trade-off for this type of assembly lies between combined acoustic-thermal performance and embodied carbon.

To the best of our knowledge, no previous work has considered these three objectives simultaneously at the facade assembly level, which has led to designs that prioritize one objective while overlooking the others. This joint analysis fills that gap, offering the construction industry a more balanced basis for facade design.

3.3 RELEVANCE TO THE THESIS OBJECTIVES

The general objective of this thesis is to investigate the trade-offs between sound insulation, thermal performance, and embodied carbon in timber facade assemblies through a multi-criteria analysis. This article directly addresses this objective and constitutes the core contribution of the thesis, as it integrates all six detailed objectives within a single study as illustrated in section 1.3.

The database of 382 assemblies compiled from published acoustic measurements, the thermal transmittance calculations performed using Ubakus in accordance with ISO 6946, and the embodied carbon assessment based on the A1–A3 life-cycle stages together form the dataset on which the entire analysis relies. The statistical correlations investigated between the three performance criteria, along with the Pareto-based multi-objective optimization applied to identify non-dominated assemblies, directly fulfill the corresponding objectives of the thesis. Finally, the design catalogue presented in the article, gathering the acoustic, thermal, and environmental data of the Pareto-optimal assemblies, corresponds to the final detailed objective of supporting engineers during project decision-making.

3.4 CURRENT PUBLICATION STATUS

The work presented in this chapter was first presented at Next Generation Wood Construction 2024 and 2025. It was then revised and expanded during the preparation of this thesis and submitted to the journal Acoustics (MDPI), where it has been

published as: [full citation: Jaber, I., Ménard, S., & Bader Eddin, M. (2026, September). A Study of the Sound and Thermal Insulation of Wood Façade Assemblies by Considering Environmental Impact Aspects. In *Acoustics* (Vol. 8, No. 4, p. 66). MDPI.]. The version reproduced in Section 3.6 is the published article.

3.5 ARTICLE SUMMARY

Les assemblages de façade en bois sont de plus en plus utilisés dans la construction résidentielle, notamment en raison de la préfabrication, de la rapidité de construction et de leur faible empreinte environnementale. Toutefois, l'obtention d'une performance acoustique adéquate dans les assemblages légers nécessite l'ajout de matériaux supplémentaires, ce qui affecte à la fois la performance thermique et les émissions de carbone incorporé. Cette étude examine les compromis entre l'isolation acoustique aux bruits aériens (R_w), la transmittance thermique (U_{value}) et le carbone incorporé des assemblages de facade en bois. Un total de 382 assemblages, répartis en sept familles, a été compilé à partir de la littérature. Des analyses de corrélation et d'optimisation multicritère basée sur le concept de Pareto ont été appliquées afin d'évaluer les relations entre les trois indicateurs de performance. Les résultats montrent une corrélation positive entre la performance acoustique et thermique à travers les familles, avec des valeurs de R^2 variant de 0,69 à 0,88. En revanche, aucune corrélation n'a été observée entre l'isolation acoustique et le carbone incorporé, indiquant que des améliorations acoustiques peuvent être obtenues sans augmentation proportionnelle de l'impact environnemental. L'analyse de Pareto a permis d'identifier 46 assemblages Pareto-optimaux représentant les meilleurs compromis atteignables entre les trois critères. Pour des assemblages de facade dont l'épaisseur totale varie de 287,5 à 477 mm, une augmentation de l'épaisseur d'isolant de 120 à 300 mm, par incréments de 40

mm, améliore la performance acoustique et thermique de 1 dB et de 0,02 à 0,04 W/m²K respectivement, pour un coût en carbone incorporé de 2 à 3 kg CO_2 eq/m². Un catalogue de sept assemblages représentatifs est inclus dans l'article à titre de référence pratique pour la conception.

3.6 FULL ARTICLE

A study of the sound and thermal insulation of wood facade assemblies by considering environmental impact aspects

Ibrahim Jaber [1], Sylvain Ménard [1] and Mohamad Bader Eddin [1]

[1] Department of Applied Sciences, University of Québec at Chicoutimi, Saguenay, QC G7H2B1, Canada; sylvain_menard@uqac.ca.

ABSTRACT: Timber façade assemblies are increasingly used in residential construction for reasons including prefabrication, construction speed, and lower environmental footprint. However, adequate acoustic performance in lightweight assemblies requires additional materials, which affect both thermal performance and embodied carbon emissions. This study investigates the trade-offs between airborne sound insulation (R_w), thermal transmittance (U_{value}), and embodied carbon in timber façade assemblies. 382 assemblies, organized into seven families, were compiled from the literature. Correlation and Pareto-based multi-objective analyses were applied to evaluate the relationships among the three-performance metrics. The findings indicate a positive correlation between acoustic and thermal performance across families, with R^2 values ranging from 0.69 to 0.88. Nevertheless, no correlation was found between acoustic insulation and embodied carbon, indicating that acoustic improvements can be achieved without proportional increases in environmental impact. Pareto analysis identified 45 Pareto-optimal assemblies representing the best achievable trade-offs

between the three criteria. For façade assemblies with overall thickness ranging from 287.5 to 477 mm, increasing insulation thickness from 120 to 300 mm in 40 mm increments improves acoustic and thermal performance by 1 dB and 0.02–0.04 W/m^2 K, respectively, at an embodied carbon cost of 2–3 kg CO_2 eq/m^2. A catalogue of seven representative assemblies is included in the article as a practical design reference.

Keywords: Wood-based facades; Building acoustic; thermal performance; embodied carbon; Pareto analysis.

INTRODUCTION

In North America, mass timber construction has emerged as one of the fastest growing segments of the building industry, with an annual production rising from 158,000 m³ in 2019 to 268,000 m³ in 2024 [123]. This growth has intensified interest in construction materials that can reduce environmental impacts, including engineered wood products (EWP). One important application of EWPs in building construction is facade systems. As part of the building envelope, facades act as the primary barrier separating indoor spaces from the external environment. Among the different aspects of building performance, facade systems contribute to maintaining adequate indoor environmental quality, particularly thermal and acoustic comfort for building occupants.

Acoustic comfort is a critical aspect of building design, and results from adequate control of noise levels, privacy, and speech intelligibility, which in turn directly affect occupant productivity and well-being [68]. Noise pollution is a major global health concern, ranked as the second most critical environmental health risk after air pollution, according to the World Health Organization [124]. The performance of

airborne sound insulation is evaluated according to ISO 10140-2 or ASTM E90, which define the laboratory measurement procedure for building elements by determining the sound transmission loss across a range of frequencies [125,126]. The sound insulation results obtained across the different frequency bands are then reduced to a single number rating using a standardized reference curve, which is expressed as weighted sound reduction index (R_w, dB) per ISO 717-1 or sound reduction index (STC, unitless) per ASTM E413 [24,127]. In both cases, higher values indicate better airborne sound insulation [24,125–127]. Canadian building codes specify requirements and recommendations for airborne and impact sound insulation for interior partitions, while no specific regulations currently address the acoustic performance of facades [128]. The lack of regulatory requirements for facades is due to historically lower external noise exposure, particularly from traffic. However, as cities grow, residential and commercial buildings are increasingly being constructed in high-density areas, where noise from combustion engines, including diesel vehicles, has become a critical issue [129]. In wood-based constructions, sound insulation presents unique challenges due to the relatively low mass and stiffness of the material. This makes bare wood a poor insulator against airborne sounds compared to heavyweight materials such as concrete for the same thickness [25]. Consequently, timber structures must be complemented with additional acoustic insulation solutions to achieve adequate airborne sound insulation, which can also raise the overall environmental footprint and influence the thermal performance of the facade structure [69].

Wooden facades contribute to high thermal efficiency by leveraging the low thermal conductivity of timber, thereby creating high-quality indoor environments. Thermal comfort for residents is consistently ranked as the most important aspect of

indoor environmental quality by building occupants, surpassing other factors such as visual and air quality [130]. In North America, heating and cooling account for 50-70% of total building energy consumption, contributing to high energy demand, a significant portion of which is still generated using fossil fuels such as coal, natural gas, and petroleum products [79]. Wood provides a relatively low thermal conductivity ranging from 0.12 to 0.24 W/ (m· k), depending on the timber products [131]. In contrast, conventional construction materials such as concrete (0.4-0.57 W/ (m· k)) and traditional brick (0.62-0.84 W/ (m· k)) present much higher thermal conductivity values, making them less effective as thermal insulating materials [131]. Implementing the EWPs in facades as a thermal partition can improve performance by 24% compared to concrete block walls [95,97].

High thermal efficiency in facades contributes to reduced operational energy consumption for heating and cooling, while the use of EWPs offers lower embodied carbon compared to conventional materials, together contributing to a lower environmental impact of the facade structure. However, the addition of insulation layers and composite materials to improve thermal and acoustic performance inevitably increases the embodied carbon associated with material production and manufacturing [117,132]. Whether these performance gains justify the associated embodied carbon penalty remains insufficiently quantified in the literature, particularly at the facade assembly level.

It is often assumed that optimizing thermal insulation guarantees adequate acoustic performance [106,107,133]. However, this assumption has not been systematically verified, particularly at the facade assembly level [109]. A survey indicated that over 80% of respondents prioritized thermal insulation over acoustic

insulation in both lightweight and heavyweight timber structures, suggesting a potential bias in design priorities rather than a demonstrated correlation between the two [107]. While both properties rely on mass or porous insulation materials, they are still governed by different physical mechanisms. Acoustic insulation depends largely on the damping and elasticity of materials, whereas thermal insulation is controlled by thermal conductivity and resistance [25,93,110,134]. Consequently, and given the limited integrated facade-level studies, these limitations highlight the need for a comprehensive multi-objective assessment of facade systems, where acoustic, thermal, and environmental performances are evaluated simultaneously rather than independently.

Multi-objective assessment frameworks have been increasingly applied in the built environment to evaluate competing design objectives. Among the available techniques, Pareto analysis enables the systematic identification of trade-offs among conflicting performance criteria by identifying solutions for which no other solution provides an improvement in one objective without deterioration in at least one of the others [49]. This gives the designer the flexibility to choose from a set of balanced solutions without having to assign importance to each objective beforehand, supporting the decision-making process rather than dictating its outcome. In architectural acoustic design, Pareto analysis has been applied to identify optimal timber configurations that balance structural and acoustic performance, reducing the design space while preserving a range of viable solutions for the designer to choose from [135]. Similarly, in building envelope design, Pareto analysis has been employed to evaluate the trade-offs between thermal performance and embodied carbon of wall assemblies, enabling designers to assess alternative material configurations through the resulting set of

optimal trade-off solutions, known as Pareto front [136,137]. It has also been used to investigate insulation design alternatives, where analysis of the Pareto front quantified the compromise between improved thermal performance and increased embodied energy [136,137]. However, no previous study has applied the Pareto dominance principle to an experimentally derived database of timber façade assemblies while simultaneously considering airborne sound insulation, thermal transmittance, and embodied carbon.

This research aims to investigate the relationships among airborne sound insulation, thermal transmittance, and embodied carbon in timber façade assemblies through a multi-criteria design approach, and to identify the trade-offs and optimal design solutions among these performance criteria. A dataset of 382 timber façade assemblies was collected from the literature and organized into seven families, as detailed in Section 2.1. Thermal and embodied carbon performances were calculated, and Pareto analysis was applied to identify the trade-offs among materials, providing an optimized catalogue of façade solutions.

MATERIALS AND METHODS

FACADE ASSEMBLIES

The facade assemblies analyzed in this study were compiled from several published experimental databases containing laboratory acoustic test results [138–140]. The dataset consists of laboratory experimental tests conducted on façade wall assemblies, focusing on opaque elements without any openings such as windows, doors, or other flanking paths in order to eliminate their influence on the acoustic and thermal analyses. For each façade assembly, the reported layer sequence, material type, layer thickness, acoustic rating, and construction details were extracted from the respective reports. The

thermal transmittance (U_{value}, $W/m^2 \cdot k$), which quantifies the rate of heat transfer through the façade, and embodied carbon (EC, kg CO_2 eq/m^2), which represents the greenhouse gas emissions associated with material production and transportation, were subsequently calculated based on the reported layer composition. These calculated values were then compared with the reported acoustic insulation ratings during the analysis.

The general configuration of the facade assemblies considered in this study is illustrated in **Figure 12**. It shows possible layers and components that may appear across the dataset. Furthermore, the physical characteristics of the materials used in these assemblies, including thickness and density, are listed in **Table 4**. Recording each assembly in a consistent exterior-to-interior layer format, allowed direct comparison across assemblies despite differences in source and configuration, supporting subsequent computational analysis [139]. The assemblies vary in both the number and sequence of layers, and may include features such as resilient channel, wider stud spacing, double gypsum board layers, or structural layers composed of different materials, such as OSB and fiberboard. These variations reflect the diversity of facade construction techniques used in timber building systems.

T

Figure 12. Schematic representation of the general layer configuration considered in the dataset and summarizes the possible components that may appear across the different façade assemblies.

Table 4. Materials and physical properties used to construct the facade assembly dataset.

Material (placement)	**Thickness (mm)**	**Density (Kg/m³)**
Wood Cladding (Cladding)	24	450

Plaster (Cladding)	4/7	2000
Wood wool composite board (Sheathing)	50	370
Wood fiber board (Sheathing)	60/100	180
Polystyrene (Sheathing)	60/100	170
OSB (structure)	12/15/18	600
Fiberboard (structure)	15/18	700
Planking spruce wood (structure)	24	450
Particle board (structure)	12/15	700
Mineral wool (Insulation)	120/160/200/240/300	16/30/33/50
Cellulose fiber (Insulation)	120/160/200/240/300	55
Wood fiber (Insulation)	120/160/200/240/300	45
Resilient channel (decoupling)	0.5	7850
Gypsum board (finish)	12.5/15	1000

The façade assemblies considered in this study were selected from the available literature based on two requirements. The first is the complete construction and material data needed to calculate the thermal transmittance and embodied carbon. The second is the availability of the reported acoustic test results needed to compare the calculated values against the measured acoustic performance. Assemblies that lacked this information or did not fit into a group of similar assemblies to form a family were not included. The analysis was performed using a dataset of 382 façade assemblies**,** organized into seven families based on their fundamental construction characteristics. The classification was based on the cladding system, sheathing type, insulation material

type (distinguishing bio-based materials such as cellulose, wood fiber, or sheep wool from non-bio-based insulation materials such as mineral wool), and the number of insulation layers, as summarized in Table 5. The purpose of this classification was to group façade assemblies sharing the same construction concept, ensuring that analysis was performed only among assemblies with comparable structural characteristics. This approach avoided comparing façade systems with different design concepts, for which performance differences may arise from the construction concept itself rather than from design variations within the same concept. Table 5 therefore reflects the seven families that met these screening criteria and summarizes the defining characteristics of each façade family. Families 1 and 2 have no external sheathing layer, while Families 3 and 4 incorporate wood wool composite boards and Families 5, 6, and 7 use wood fiber boards. All families use mineral wool except for Family 6, which uses a bio-based insulation material. Families 2 and 7 feature a single insulation layer, whereas the rest use double insulation layers. It should be noted that, within each family, façade assemblies preserve the defining construction characteristics of that family while differing in their detailed design configurations.

Table 5. Classification of timber facade assembly families based on fixed configuration parameters: cladding type, sheathing board, insulation material, and number of insulation cavities.

Family ID	Number of assemblies	Cladding type	Sheathing board	Insulation material	Insulation layers
1	52	Wood Cladding	None	Mineral wool	2

2	38	Wood Cladding	None	Mineral wool	1
3	20	Wood Cladding	Wood Wool composite boards	Mineral wool	2
4	40	Plastered wall	Wood Wool composite boards	Mineral wool	2
5	141	Plastered wall	Wood fiber boards	Mineral wool	2
6	35	Plastered wall	Wood fiber boards	Biomaterials	2
7	56	Plastered wall	Wood fiber boards	Mineral wool	1

ACOUSTIC INSULATION DATA

The acoustic curves obtained from the different data sources were measured according to ASTM and ISO standards, and reported as Sound Transmission Class (STC, unitless) and the weighted sound reduction index (R_w, dB), respectively [141]. The data were obtained from multiple laboratories and third-party test reports conducted in accordance with ASTM E90 and ISO 10140-2 standards [125,126].

However, to ensure uniformity across the database, assemblies with a reported R_w value retained their original value. For assemblies reported using STC, only cases for which the complete transmission-loss values over the 1/3-octave frequency bands were available were retained. These transmission-loss curves were used to recalculate R_w according to the ISO 717-1 procedure, by vertically shifting the reference curve

until the total unfavorable deviation reached 32 dB [141]. The resulting R_w values were then used as the common acoustic metric for all assemblies. Assemblies without sufficient acoustic data for this harmonization or with results identified as outliers were excluded.

Uncertainties associated with the acoustic data cannot be completely eliminated because the results originate from different laboratories and test reports and may be affected by factors that cannot be fully controlled in a literature-based dataset, such as differences in test facilities, measurement conditions, specimen preparation, and workmanship. Nevertheless, several criteria were applied to limit the variability and improve comparability across the different sources. Although ASTM E90 and ISO 10140-2 differ in specific test requirements, both are based on standardized laboratory measurements of airborne sound transmission [24]. Only laboratory measurements were considered, thereby limiting variability associated with field conditions such as flanking transmission and the influence of openings. All assemblies represent single-story residential wall configurations, which limits variability associated with differences in building application [142]. In addition, assemblies were compared only within families sharing the same fundamental construction concept (Section 2.1). Together with the harmonization of the acoustic results to a common R_w metric, these criteria were used to reduce variability arising from differences among the source datasets and test conditions.

THERMAL ANALYSIS

The thermal performance simulation of each façade assembly was determined using the UBAKUS simulation software [143], which follows standard steady-state heat transfer principles as defined in building insulation codes. In this study, the thermal

performance of each façade assembly was assessed using the thermal transmittance (U_{value}, W/m²K), which represents the rate of heat transfer through the façade assembly under steady-state conditions. The simulations were carried out assuming indoor and outdoor temperatures of 20 °C and −20 °C, respectively, representing typical Canadian winter design conditions [144]. Transient effects were neglected to maintain uniform comparison among assemblies. The timber stud and insulation were modeled as separate fractions within an inhomogeneous layer, allowing UBAKUS to apply the Combined Method of ISO 6946 [145]. This method accounts for the parallel heat flow paths through the insulation and the timber studs, thereby incorporating the effect of repeating thermal bridges into the calculated thermal transmittance.

EMBODIED CARBON EMISSIONS ANALYSIS

The environmental performance of each facade assembly was calculated in terms of embodied carbon (EC) with a unit of comparison of Kg CO_2 eq./m². The EC values represent the carbon emissions associated with the materials used in the assembly and cover only the A1–A3 life cycle stages (raw material extraction, transport, and manufacturing). The calculations were performed using equations consistent with standard Life Cycle Analysis (LCA) methodology [146]. The total embodied carbon of each facade assembly was calculated as the sum of the contributions of its continuous and linear components. For continuous surface materials such as insulation panels, boards, or sheathing layers, the following relation was used:

$$EC_C = EC_f * \rho * t \qquad (2.43)$$

Where:

EC_c: Embodied carbon emissions of a continuous material ($Kg.CO_2/m^2$),

EC_f: Embodied carbon coefficient of material ($Kg.CO_2/Kg$),

ρ: density of material (Kg/m^3),

t: Thickness of material (m).

For the calculation of linear elements such as timber studs or battens, the corresponding embodied carbon contribution (EC_l, $kg.CO_{2_}eq/m^2$) was calculated by considering the center-to-center spacing between consecutive elements S (m) and cross-sectional area of the element A (m^2):

$$EC_l = EC_f * \rho * \frac{A}{S} \quad (2.44)$$

The total embodied carbon of the assembly was then obtained as:

$$EC = \sum(EC_C + EC_f) \quad (2.45)$$

For each material layer, the embodied carbon factor (EC_f) was derived primarily from the inventory of Carbon and Energy (ICE) V3.0 database [147], environmental product declarations (EPD) sheets, or industry wide EPDs. The embodied carbon factors used for each material are summarized in Table 6. The ICE database provides embodied carbon factors (EC_f) linking material quantities to their associated carbon emissions, based on a cradle-to-gate life cycle assessment (LCA). The potential biogenic carbon storage associated with timber products was not included because its reporting was not consistent across the EPDs and database sources used to construct the dataset. Consequently, the EC indicator used in this study represents gross embodied-carbon emissions associated with material production and transportation within life-cycle stages A1–A3, rather than a net carbon balance including biogenic carbon storage. This scope should be considered when interpreting the results,

particularly when comparing timber-based assemblies with construction systems based on other material types.

Table 6. Embodied carbon factors (EC_f) used for the materials considered in the façade assembly dataset.

Material (placement)	Embodied Carbon Factor (EC_f) (kg CO_2 eq/$m^{2)}$	Source
Wood Cladding (Cladding)	0.263	ICE V3.0 [147]
Plaster (Cladding)	0.164	EPD [148]
Wood wool composite board (Sheathing)	0.380	EPD [148]
Wood fiber board (Sheathing)	0.414	ICE V3.0 [147]
Polystyrene (Sheathing)	3.690	ICE V3.0 [147]
OSB (structure)	0.455	ICE V3.0 [147]
Fiberboard (structure)	0.715	ICE V3.0 [147]
Planking spruce wood (structure)	0.263	ICE V3.0 [147]
Particle board (structure)	0.664	ICE V3.0 [147]
Mineral wool (Insulation)	1.250	ICE V3.0 [147]
Cellulose fiber (Insulation)	0.100	EPD [149]
Wood fiber (Insulation)	0.490	EPD [149]
Resilient channel (decoupling)	2.620	ICE V3.0 [147]
Gypsum board (finish)	0.304	EPD [150]

MULTI-OBJECTIVE CRITERIA SETUP

To identify the façade assemblies that represent the trade-offs among airborne sound insulation (R_w), thermal transmittance (U_{value}), and embodied carbon (EC), a Pareto-based multi-objective analysis was conducted. Unlike single objective analyses, which serve for the searching of a single optimum solution, Pareto analysis simultaneously

evaluates multiple objectives and identifies solutions for which no objective can be further improved without compromising at least one of the others [49,151,152]. Consequently, it enables the exploration of trade-offs among acoustic, thermal, and environmental performance without requiring predefined weighting factors that assign subjective importance to one criterion over another [49,151]. In Pareto analysis, solutions are compared based on the concept of dominance. A solution is considered non-dominated when no other feasible solution performs at least as well in all objectives and strictly better in at least one objective [49,152].

To apply the Pareto-based analysis, the considered performances are expressed as objective functions within a unified mathematical formulation. Based on the general vector formulation used for multi-objective problems [49], the three performance objectives considered in this study were defined as:

$$f_{1,i} = -R_{w,i} \qquad f_{2,i} = U_{value,i} \qquad f_{3,i} = EC_i, \tag{2.46}$$

Where i represents an individual facade assembly configuration characterized by its material composition and layer thicknesses. $R_{w,i}$, $U_{value,i}$, and EC_i represent the acoustic, thermal, and environmental performance indicators of assembly i, respectively. While lower U_{value} and EC indicate better performance, higher R_w indicates better acoustic insulation. Since Pareto analysis is commonly formulated as a minimization problem, the acoustic insulation objective was transformed by multiplying R_w by -1. This transformation ensures that assemblies with superior acoustic insulation correspond to lower objective values, preserving the physical preference ranking within the minimization framework. The resulting objective vector is therefore expressed as [49]:

$$minimize\ F(x) = [f_{1,i},\ f_{2,i},\ f_{3,i}] = [-R_{w,i}, U_{value,i}, EC_i\ ], \qquad (2.47)$$

It should be noted that this analysis is data-driven rather than generative; the Pareto analysis identifies non-dominated configurations from within the existing dataset. Moreover, the Pareto analysis was performed separately for each façade family to ensure that only assemblies sharing the same structural characteristics were compared, as presented in Section 2.1. This approach limits the influence of differences in the façade family itself when evaluating design variables, such as insulation thickness and structural configuration. Within each family, the objective vectors defined in Equation 2.47 are compared to identifies the non-dominated solutions. These non-dominated solutions constitute the Pareto front, which maps the trade-off surface in the three-dimensional objective space. The geometry of the Pareto front varies depending on the number of objectives considered, denoted as 'k', and on the nature of the objective functions, whether minimizing or maximizing [49,153]. For 'k' independent and conflicting objectives, the Pareto front forms a manifold of dimension k-1, one dimension fewer than the number of independent objectives [153]. In the present study, three objectives are considered (R_w, U_{value}, and EC), giving k = 3, which corresponds to a two-dimensional surface in the objective space. However, this theoretical dimensionality assumes that the considered objectives contribute independently to the geometry of the Pareto set. Therefore, an additional analysis was conducted to examine the effective dimensionality of the obtained Pareto solutions.

Principal component analysis (PCA) was applied separately to the Pareto solutions of each façade family. PCA transforms the original variables into a set of principal components, with each component accounting for a portion of the total variance in the data. The percentage of variance explained by each component indicates how much of

the overall variation in the three objective variables is represented by that component [154] . In the present study, PCA was performed using the standardized R_w, U_{value}, and EC values of the non-dominated solutions within each façade family. The proportions of variance explained by the first, second, and third principal components were examined to characterize the variance structure of the observed Pareto sets.

Although all non-dominated solutions represent valid trade-offs among the considered objectives, presenting the complete Pareto set would result in a large number of configurations and limit the interpretability of the results [155]. Therefore, following previous studies that adopted a secondary selection procedure to identify a representative solution from the Pareto front [155–157], one representative façade assembly per family was selected from each Pareto front by calculating the distance between each Pareto solution and a reference point corresponding to the best value of each objective [156,157].

After the Pareto fronts have been identified, the resulting non-dominated solutions were normalized using the min-max normalization method [151,156]. Since the three objective functions considered in this study are expressed using different units and numerical ranges, they cannot be directly combined in the distance calculation, as objectives with larger numerical values would have a greater impact on the computed distance comparing to the rest. The normalization was therefore applied exclusively to the Pareto solutions, transforming each objective into dimensionless values ranging from 0 to 1 [151,156]:

$$X^{norm} = \frac{X - X_{min}}{X_{max} - X_{min}}, \quad (2.48)$$

Where X denotes the value of the considered objective, while X_{min} and X_{max} correspond to the minimum and maximum values within the considered Pareto set, respectively. The reference point was defined using the best normalized value of each objective, corresponding to maximum acoustic insulation and minimum thermal transmittance and embodied carbon. The distance between each normalized Pareto solution and the reference point was then calculated as follows [158]:

$$D_i = \sqrt{\sum_{j=1}^{k} \left({f_{j,i}}^{norm} - {f_j}^{ideal} \right)^2}, \quad (2.49)$$

Where D_i represents the distance of the i^{th} Pareto solution from the ideal point, ${f_{j,i}}^{norm}$ is the normalized value of objective *j* for solution *i*, ${f_j}^{ideal}$ is the ideal value of objective *j,* and k is the number of objectives. The solution with the minimum distance was selected as the representative assembly of the studied façade family.

Pareto analysis was implemented in Python, using libraries such as pandas for dataset management, NumPy for numerical operations, and Matplotlib for visualization. The resulting non-dominated assemblies and representative configurations selected through the ideal-point approach were used to develop the façade catalogue presented in Section 3.3.2.

RESULTS

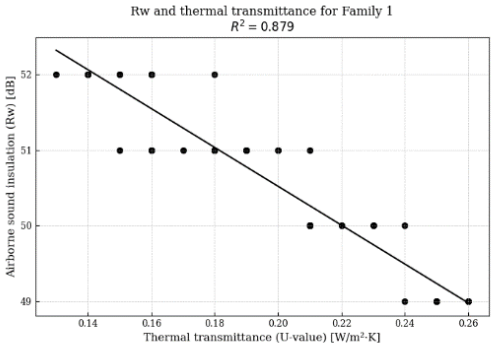
ACOUSTIC AND THERMAL PERFORMANCE CORRELATION

Linear regression analysis was conducted to examine the relationship between airborne sound insulation (R_w) and thermal transmittance (U_{value}) within each of the seven families. **Table *7*** and Figure 13 present the regression results, including the R^2 values and the minimum and maximum R_w and U-value calculated for each family,

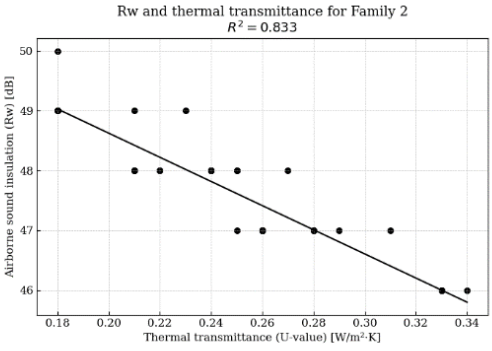
together with the corresponding scatter plots and regression lines. Across all families, a strong correlation is observed between airborne sound insulation (R_w) and thermal transmittance (U_{value}), with R^2 values ranging from 0.69 to 0.88, despite differences in material composition and configuration across families. Figure 13 illustrates this relationship through the scatter plots, with a negative regression slope observed for every family. This negative slope reflects the relationship between R_w and $U_{value,}$ as the first increases, the second decreases, meaning that both acoustic and thermal performance improve together, since a higher R_w and a lower U_{value} each represent better performance.

Table 7. Linear regression results between acoustic and thermal performance across the analyzed families. Max. and Min value are presented corresponding to each family.

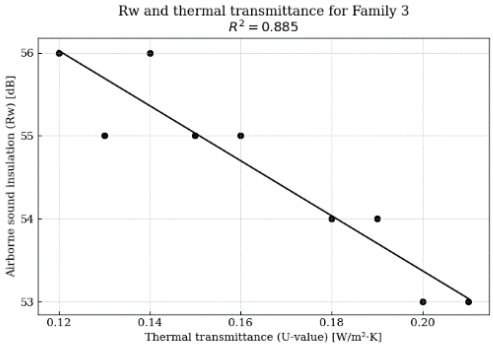
Family	**Number of assemblies**	**R^2**	**Assembly Min R_w value (dB)**	**Assembly Max R_w value (dB)**	**Assembly Min U_{value} (W/m²K)**	**Assembly Max U_{value} (W/m²K)**
1	52	0.86	49	55	0.10	0.26
2	38	0.82	46	50	0.18	0.34
3	20	0.88	53	56	0.12	0.21
4	40	0.85	51	54	0.13	0.24
5	141	0.82	51	57	0.09	0.19
6	35	0.80	52	59	0.10	0.19
7	56	0.69	51	54	0.15	0.21


Rw and thermal transmittance for Family 1
$R^2 = 0.879$
Airborne sound insulation (Rw) [dB]
Thermal transmittance (U-value) [W/m²·K]

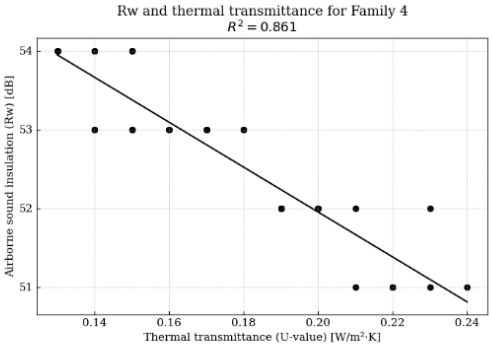
(a)


Rw and thermal transmittance for Family 2
$R^2 = 0.833$
Airborne sound insulation (Rw) [dB]
Thermal transmittance (U-value) [W/m²·K]

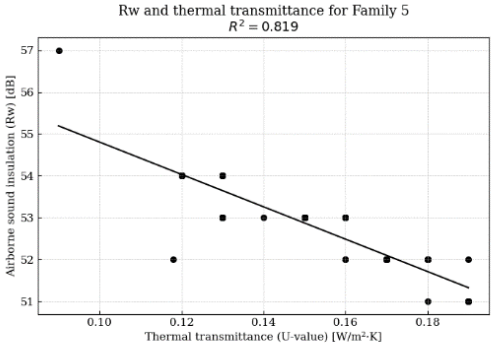
(b)


Rw and thermal transmittance for Family 3
$R^2 = 0.885$
Airborne sound insulation (Rw) [dB]
Thermal transmittance (U-value) [W/m²·K]

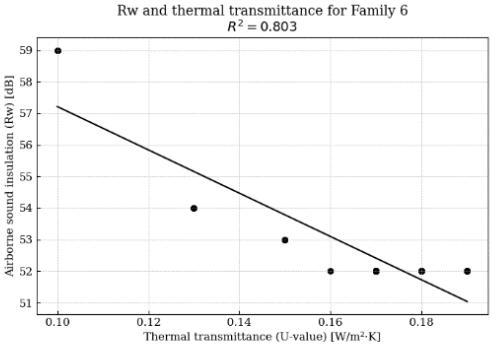
(c)


Rw and thermal transmittance for Family 4
$R^2 = 0.861$
Airborne sound insulation (Rw) [dB]
Thermal transmittance (U-value) [W/m²·K]

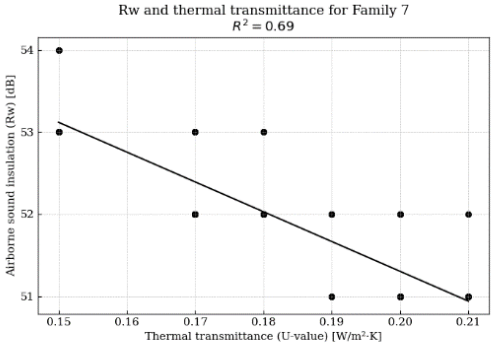
(d)


Rw and thermal transmittance for Family 5
$R^2 = 0.819$
Airborne sound insulation (Rw) [dB]
Thermal transmittance (U-value) [W/m²·K]

(e)


Rw and thermal transmittance for Family 6
$R^2 = 0.803$
Airborne sound insulation (Rw) [dB]
Thermal transmittance (U-value) [W/m²·K]

(f)


Rw and thermal transmittance for Family 7
$R^2 = 0.69$
Airborne sound insulation (Rw) [dB]
Thermal transmittance (U-value) [W/m²·K]

(g)

Figure 13. Scatter plots of airborne sound insulation (R_w) versus thermal transmittance (U_{value}) for (**a**) Family 1, (**b**) Family 2, (**c**) Family 3, (**d**) Family 4, (**e**) Family 5, (**f**) Family 6, (**g**) Family 7. Each dot represents one façade assembly (overlapping assemblies appear as a single dot), and the solid line is the linear regression fit for that family; the corresponding R^2 is given above each plot.

Higher sheathing density was associated with improved R_w and U_{value} ranges. As shown in Table 4, Families 1 and 2, characterized by the absence of an external sheathing layer, exhibit lower R_w ranges of 46–55 dB, while their U_{value} reaches 0.34 W/m^2 K. In contrast, families incorporating wood wool composite boards (Families 3 and 4) and wood fiber boards (Families 5, 6, and 7) achieve higher acoustic performance ranges of 51–56 and 51–59 dB, while maintaining lower maximum U_{value} of 0.24 and 0.21 W/m^2 K, respectively. This pattern is consistent with the mass law, where sound insulation increases with greater surface mass [12]. Consequently, denser wood-based sheathing was associated with improved acoustic and thermal performance within the analyzed families.

The acoustic-thermal correlation is further modulated by the number of insulation layers. Families with two insulation layers (Families 1, 3, 4, 5, and 6) show a higher R^2 of 0.85 compared to 0.75 for single-cavity families, indicating a stronger linear relationship between acoustic and thermal performance. This can be explained by the greater total insulation thickness in these assemblies. Increasing the insulation thickness lowers the U_{value} of the assembly by raising its thermal resistance [159], and it generally also improves airborne sound insulation through increased sound absorption within the cavities [12]. Because both performance indicators tend to improve together with the amount of insulation, the relationship between R_w and U_{value} is more strongly linear in the two-layer families.

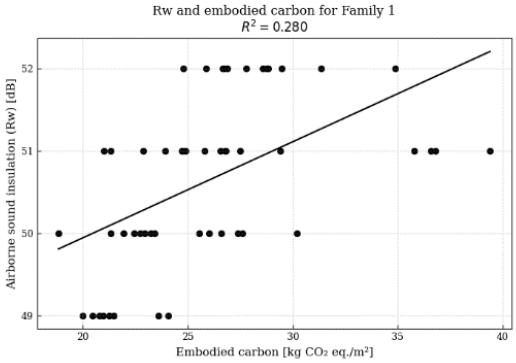
ACOUSTIC AND EMBODIED CARBON CORRELATION

The relationship between airborne sound insulation (R_w) and embodied carbon (EC) was examined across all families using linear regression analysis. **Table 8** summarizes the correlation results (R^2), along with the minimum and maximum EC recorded for each family. The correlation results indicate that acoustic insulation and embodied carbon are independent across the analyzed families, with R^2 values ranging from 0 to 0.361. The scatter plots in Figure 13 further illustrate this independence through two recurring patterns. First, assemblies sharing identical R_w values are distributed across a wide EC range within each family, indicating that the same level of acoustic performance can be achieved at different environmental costs. Family 7 (Figure 13 g), for example, shows that across an EC range of 18.4–34.5 kg CO_2 eq/m^2, all assemblies maintain a constant R_w value of 52 dB regardless of their embodied carbon. This behavior can be attributed to the wide variation in configurations within the family, arising from different combinations of structural layer materials that yield equivalent acoustic performance across a broad range of embodied carbon values. This indicates that variations in embodied carbon do not translate into improved acoustic performance. Second, the maximum R_w value within each family is not achieved at the highest EC value. Family 6 (Figure 13 e), for example, illustrates this pattern, where the maximum R_w of 59 dB was achieved at an EC value of 34 kg CO_2 eq/m^2, while assemblies with the highest EC value of 44 kg CO_2 eq/m^2 do not correlate with the highest acoustic performance. The reason behind the absence of this correlation is attributed to several interacting design parameters. First, the use of a 300 mm-thick bio-based insulation layer simultaneously minimizes embodied carbon emissions and enhances sound attenuation through its increased thickness [12]. Second, the

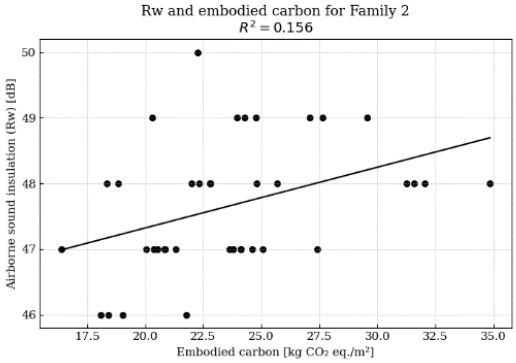
implementation of an I-beam stud system with wider spacing (625 mm) compared to conventional stud configurations (400 mm) reduces acoustic bridging by minimizing the volume fraction of solid timber elements and maximizing the proportion of low-embodied carbon fill material. Third, the incorporation of a resilient channel decoupling system has been shown to improve the airborne sound insulation with a comparatively small impact on embodied carbon [117]. Consequently, enhanced airborne sound insulation can be achieved through appropriate material and configuration selection without necessarily increasing the environmental footprint.

Table 8. Linear regression results between acoustic performance and embodied carbon across the analyzed families. Max. and Min value are presented corresponding to each family.

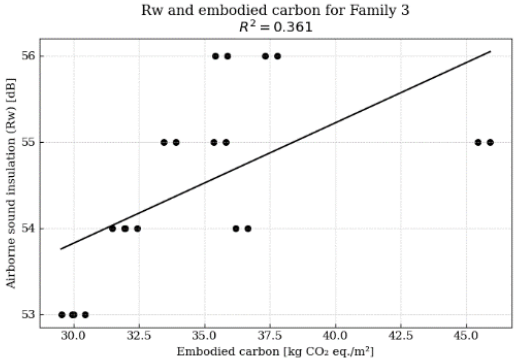
Family	Number of assemblies	R^2	Assembly Min R_w value (dB)	Assembly Max R_w value (dB)	Assembly Min EC value (kg CO_2 eq/m²)	Assembly Max EC value (kg CO_2 eq/m²)
1	52	0.280	49	55	18.8	39.3
2	38	0.156	46	50	16.3	34.8
3	20	0.361	53	56	29.5	45.9
4	40	0.260	51	54	24.4	44.9
5	141	0.175	51	57	31.5	53.9
6	35	0.002	52	59	30.5	43.2
7	56	5.3 e-05	51	54	18.4	34.5


Rw and embodied carbon for Family 1
$R^2 = 0.280$
Airborne sound insulation (Rw) [dB]
Embodied carbon [kg CO₂ eq./m²]

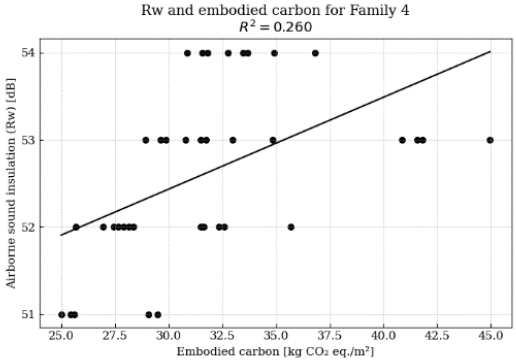
(a)


Rw and embodied carbon for Family 2
$R^2 = 0.156$
Airborne sound insulation (Rw) [dB]
Embodied carbon [kg CO₂ eq./m²]

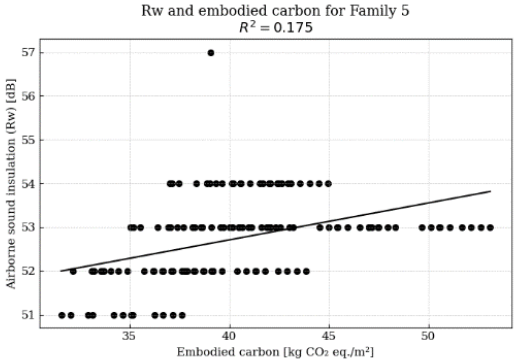
(b)


Rw and embodied carbon for Family 3
$R^2 = 0.361$
Airborne sound insulation (Rw) [dB]
Embodied carbon [kg CO₂ eq./m²]

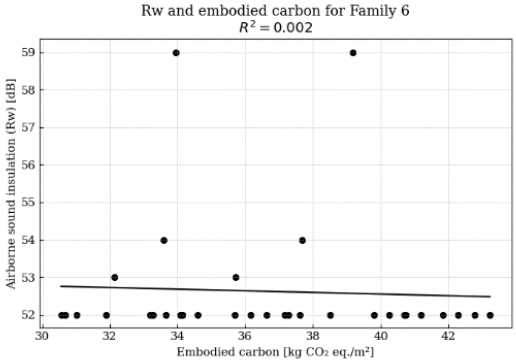
(c)


Rw and embodied carbon for Family 4
$R^2 = 0.260$
Airborne sound insulation (Rw) [dB]
Embodied carbon [kg CO₂ eq./m²]

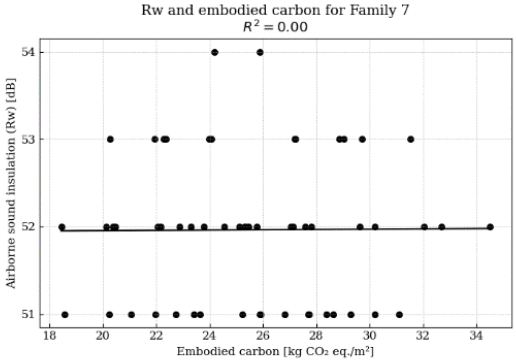
(d)


Rw and embodied carbon for Family 5
$R^2 = 0.175$
Airborne sound insulation (Rw) [dB]
Embodied carbon [kg CO₂ eq./m²]

(e)


Rw and embodied carbon for Family 6
$R^2 = 0.002$
Airborne sound insulation (Rw) [dB]
Embodied carbon [kg CO₂ eq./m²]

(f)


Rw and embodied carbon for Family 7
$R^2 = 0.00$
Airborne sound insulation (Rw) [dB]
Embodied carbon [kg CO₂ eq./m²]

(g)

Figure 14. Scatter plots of airborne sound insulation (Rw) versus embodied carbon (EC) for (a) Family 1, (b) Family 2, (c) Family 3, (d) Family 4, (e) Family 5, (f) Family 6, (g) Family 7. Each dot represents one façade assembly (overlapping assemblies appear as a single dot), and the solid line is the linear regression fit for that family; the corresponding R^2 is given above each plot.

MULTI-OBJECTIVE TRADE-OFF ANALYSIS

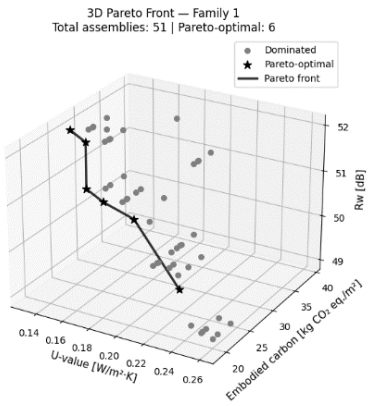
Within each family, a Pareto analysis was independently conducted to identify assemblies that simultaneously maximize airborne sound insulation (R_w) and minimize both thermal transmittance (U_{value}) and embodied carbon (EC). **Table 9** and **Figure 15** present the results for the seven selected families, chosen to represent the range of configurational diversity, yielding a total of 45 non-dominated assemblies, identified as star markers in **Figure 15**.

Table 9. Number of Pareto-optimal facade assemblies per family.

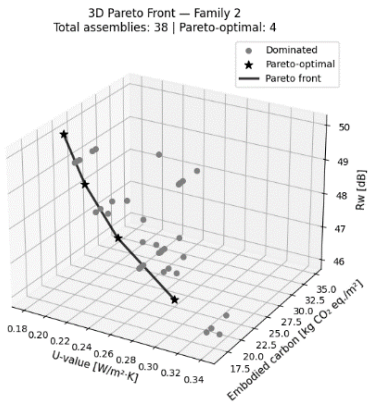
Family	Number of assemblies	Pareto-optimal assembly
1	52	6
2	38	4
3	20	7
4	40	8
5	141	12
6	35	4
7	56	4
Total	382	45

Beyond identifying the representative assemblies, the distribution of the Pareto-optimal solutions provides additional insight into the relationship among the three performance objectives. In multi-objective analysis, k represents the number of objectives studied. When k objectives are mutually independent and conflicting, the Pareto front forms a manifold of dimension k − 1 [160,161]. With three objectives studied ($R_{w,}$ U_{value}, and EC), the Pareto front would theoretically be expected to form a two-dimensional surface. However, as illustrated in **Figure 15**, the non-dominated solutions instead distribute along a one-dimensional curve, indicating that the effective dimensionality of the Pareto front is lower than theoretically expected.

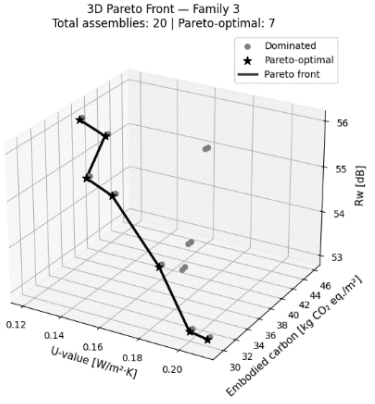
To quantitatively examine this observation, principal component analysis (PCA) was applied to the standardized R_w, U_{value}, and EC values of the Pareto solutions within each façade family. The explained variance obtained from the PCA is presented in Table 10. The first principal component accounts for 90.15–99.46% of the total variance across the seven families, whereas the second component accounts for only 0.54–9.80% and the third component for only 0–0.64%. This indicates that most of the variation among the three objective variables can be represented along a single principal direction, with only a limited part of the variation requiring the second and third principal directions. The consistent dominance of the first principal component provides quantitative support for the approximately one-dimensional distribution observed in Figure 15.


3D Pareto Front — Family 1
Total assemblies: 51 | Pareto-optimal: 6
Dominated
Pareto-optimal
Pareto front
Rw [dB]
U-value [W/m²·K]
Embodied carbon [kg CO₂ eq./m²]

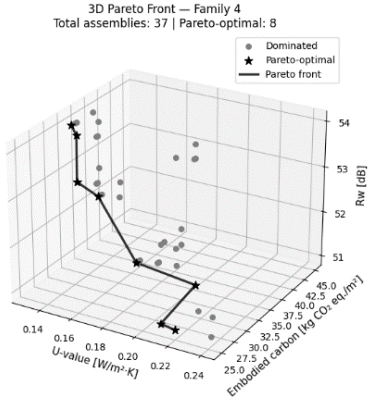
(a)


3D Pareto Front — Family 2
Total assemblies: 38 | Pareto-optimal: 4
Dominated
Pareto-optimal
Pareto front
Rw [dB]
U-value [W/m²·K]
Embodied carbon [kg CO₂ eq./m²]

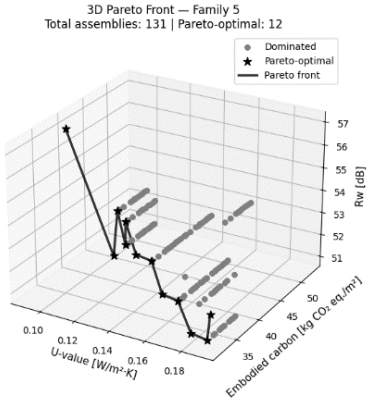
(b)


3D Pareto Front — Family 3
Total assemblies: 20 | Pareto-optimal: 7
Dominated
Pareto-optimal
Pareto front
Rw [dB]
U-value [W/m²·K]
Embodied carbon [kg CO₂ eq./m²]

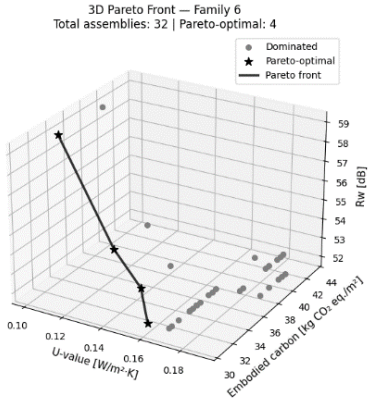
(c)


3D Pareto Front — Family 4
Total assemblies: 37 | Pareto-optimal: 8
Dominated
Pareto-optimal
Pareto front
Rw [dB]
U-value [W/m²·K]
Embodied carbon [kg CO₂ eq./m²]

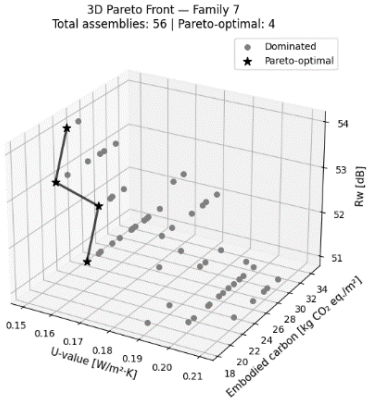
(d)


3D Pareto Front — Family 5
Total assemblies: 131 | Pareto-optimal: 12
Dominated
Pareto-optimal
Pareto front
Rw [dB]
U-value [W/m²·K]
Embodied carbon [kg CO₂ eq./m²]

(e)


3D Pareto Front — Family 6
Total assemblies: 32 | Pareto-optimal: 4
Dominated
Pareto-optimal
Pareto front
Rw [dB]
U-value [W/m²·K]
Embodied carbon [kg CO₂ eq./m²]

(f)


3D Pareto Front — Family 7
Total assemblies: 56 | Pareto-optimal: 4
Dominated
Pareto-optimal
Rw [dB]
U-value [W/m²·K]
Embodied carbon [kg CO₂ eq./m²]

(g)

Figure 15. Pareto front analysis of facade assemblies showing the Pareto front among airborne sound insulation, thermal transmittance, and embodied carbon. Each point represents a facade. Star points indicate Pareto-optimal solutions, while gray points represent dominated solutions. (a) for Family 1 (b) for Family 2 (c) for Family 3 (d) for Family 4 (e) for Family 5 (f) for Family 6 (g) for Family 7.

This reduced-dimensional structure is also examined through the pairwise relationships among the three objectives. Unlike the population-level correlations reported in Sections 3.1 and 3.2, this analysis is restricted to the 45 Pareto-optimal assemblies identified across the seven families and is intended to characterize the trade-off structure that defines the fronts themselves. As illustrated in Table 10, the R^2 values for these Pareto solutions range from 0.500 to 0.976 for the R_w–U_{value} relationship, from 0.562 to 1.000 for R_w–EC, and from 0.806 to 0.981 for U_{value}–EC. These results indicate a strong linear association among the objective variables, although the strength of the association varies across façade families. Such interrelationships help explain why the Pareto solutions do not occupy the full two-dimensional surface that would be expected if the three objectives varied independently. While pairwise relationships describe associations between individual objective pairs, PCA considers the three objectives simultaneously and quantifies the concentration of the variance along the principal directions. The agreement between the curve-like distribution observed in Figure 16, the strong dominance of PC1 across all façade families, and the observed relationships among the objective pairs indicates that the Pareto solutions obtained from the present dataset exhibit a one-dimensional structure in the three-dimensional objective space. This observed structure can therefore be described as a degenerate Pareto front [51,52]. From a practical perspective, these interrelationships suggest that, within the range of assemblies investigated, designers may primarily need to consider the trade-offs among

the acoustic, thermal, and embodied carbon performances rather than treating each objective separately.

Table 10. Correlation and principal component analysis of the Pareto solutions for each façade family.

Family	R^2 (R_w−U_{value})	R^2 (R_w−EC)	R^2 (U_{value}−EC)	PC1 Variance (%)	PC2 Variance (%)	PC3 Variance (%)
1	0.771	0.772	0.981	94.43	5.26	0.31
2	0.976	1.000	0.976	99.46	0.54	0.00
3	0.899	0.925	0.972	97.69	1.89	0.42
4	0.807	0.895	0.943	95.92	3.47	0.62
5	0.690	0.562	0.943	90.15	9.21	0.64
6	0.946	0.623	0.806	92.50	7.31	0.19
7	0.500	0.881	0.824	90.20	9.80	0.00

INFLUENCE OF CONFIGURATION AND MATERIAL SELECTION ON PARETO-OPTIMAL PERFORMANCE

To identify the configuration and material parameters that drive multi-objective performance, the Pareto-optimal assemblies identified across the seven families were analyzed with respect to their insulation layer thicknesses. As presented in Figure 16 a–c, the primary insulation layer thickness was identified as one of the dominant variables governing the performance along the Pareto front. It should be noted that R^2 values were computed separately within each family rather than across the pooled dataset, as each family represents a structurally distinct wall system with its own baseline performance. Both airborne sound and thermal performance improve with increasing thickness, as reflected by the positive slopes in Figure 16a, with R^2 ranging between 0.5 and 1, and the negative slopes in Figure 17b, with R^2 ranging between 0.63 and 1, respectively. These improvements occur at the cost of higher embodied carbon, as illustrated by the positive slopes in Figure 17c (R^2 ranging between 0.53 and 1). Extreme values at both bounds reflect families with a limited number of Pareto-optimal

solutions. Although no correlation between R_w and EC was observed at the population level (Section 3.2), the trade-off becomes visible along the Pareto front within each family; once dominated assemblies are excluded, increasing R_w is achieved primarily through additional insulation thickness, which raises embodied carbon in turn. More specifically, the airborne sound insulation ranges from 47 to 53 dB at 120 mm across the different family configurations, increasing to 55–57 dB at 300 mm. Using energy-based logarithmic averaging of R_w values at each thickness level, this corresponds to an average improvement of 1 dB per 40 mm increment in total insulation thickness. Similarly, the thermal transmittance decreases from 0.22 to 0.24 W/m^2 K at 120 mm to 0.09 W/m^2 K at 300 mm, reflecting an average reduction in a range of 0.02–0.04 W/m^2 K per 40 mm increment. These acoustic and thermal improvements come at the expense of increased embodied carbon, which increases by an average of 2–3 kg CO_2 eq/m^2 per 40 mm increment, though with considerable variation across the families.

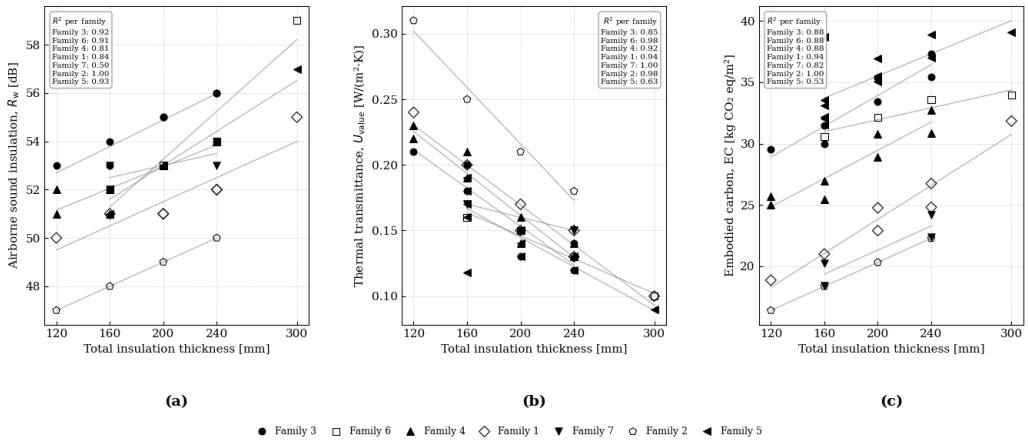


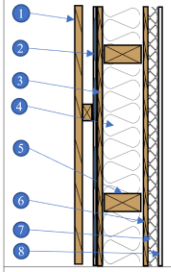
Figure 16. Scatter plots of Pareto-optimal assembly performance against total insulation layer thickness, shown separately for each family with individual linear regression fits. Plot (a) represents airborne sound insulation (R_w), Plot (b) represents thermal transmittance (U_{value}), and Plot (c) represents embodied carbon (EC).

To support practical design applications, Figure 16 presents a representative catalogue of façade assemblies, with one assembly per family. Each representative assembly was selected as the Pareto-optimal solution closest to the ideal point in normalized objective space, where the ideal point is defined as the combination of maximum R_w, minimum U_{value}, and minimum EC. The selected assemblies represent Pareto-optimal configurations identified from the analyzed dataset. Their reported R_w values are based on the standardized laboratory measurements available in the dataset, while the U_{value} and EC values are calculated from the specified material properties, layer thicknesses, and assembly configurations using the procedures described in Sections 2.3 and 2.4. As shown in Figure 18, the selected assemblies share common configuration features, such as using a stud spacing of 625 mm rather than the conventional 400 mm, which reduces the frequency of thermal and acoustic bridges and contributes positively to both acoustic and thermal performance.

At the same time, each assembly is distinguished by the configuration choices that favor a particular objective. For applications prioritizing the lowest embodied carbon emissions, Family 2 (Figure 16b) provides the lowest embodied carbon value in the catalogue (20.3 kg CO_2 eq/m^2). Where the highest acoustic and thermal performance are required, Family 6 (Figure 16f) reaches the maximum R_w of 59 dB and the minimum U_{value} of 0.1 W/m^2 K with the largest insulation thickness of the catalogue (380 mm), combined with a lightweight I-beam system. In addition, mechanical decoupling contributes to airborne sound insulation by reducing vibration transmission between the cladding and the structural frame, while having little effect on thermal transmittance and embodied carbon, as illustrated in Families 3 and 6 (Figure 16c, f). Finally, for applications where overall wall thickness is constrained, Family 7 (Figure

16g) represents the most compact configuration in the catalogue (287.5 mm), yet it does not correspond to the lowest acoustic, thermal, or embodied carbon performance across the catalogue, which highlights that total thickness could be incorporated as an additional objective in future multi-objective work.

Family 1

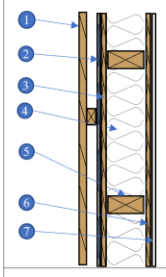


Layer number	Layer distribution	Thickness (mm)
1	Wood cladding	24
2	Wind barrier	-
3	Planking spruce wood	25
4	Mineral wool	200
5	Construction wood stud (e = 625 mm)	200
6	Planking spruce wool	24
7	Mineral wool	40
8	Gypsum board	12.5

Assembly's performance:
Acoustic performance: R_w (Cr; Ctr) = 52 (−3; −10) dB
Thermal performance: U_{value} = 0.15 W/m² K
Total Embodied Carbon: EC = 24.805 kg CO_2 eq/m²
Total thickness: L = 396.5 mm
Surface area: SA = 54.4 Kg/m³

(a)

Family 2

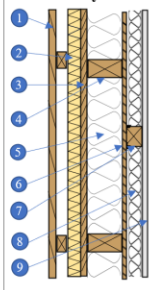


Layer number	Layer distribution	Thickness (mm)
1	Wood cladding	24
2	Wind barrier	-
3	Planking spruce wood	25
4	Mineral wool	200
5	Construction wood stud (e = 625 mm)	200
6	Planking spruce wool	24
7	Gypsum board	12.5

Assembly's performance:
Acoustic performance: R_w (Cr; Ctr) = 49 (−2; −8) dB
Thermal performance: U_{value} = 0.21 W/m² K
Total Embodied Carbon: EC = 20.308 kg CO_2 eq/m²
Total thickness: L = 316.5 mm
Surface area: SA = 47.8 Kg/m³

(b)

Family 3

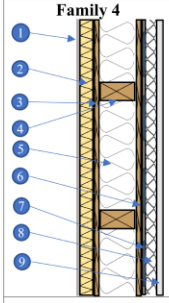


Layer number	Layer distribution	Thickness (mm)
1	Wood cladding	24
2	Wood wool composite boards	50
3	Fiberboard	15
4	Construction wood stud (e = 625 mm)	200
5	Mineral wool	200
6	OSB	15
7	Mineral wool	40
8	Spruce wood battens mounted on resilient clips	40
9	Gypsum board	12.5

Assembly's performance:
Acoustic performance: R_w (Cr; Ctr) = 55 (−3; −9) dB
Thermal performance: U_{value} = 0.15 W/m² K
Total Embodied Carbon: EC = 33.45 kg CO_2 eq/m²
Total thickness: L = 380.5 mm
Surface area: SA = 73.9 Kg/m³

(c)

Family 4

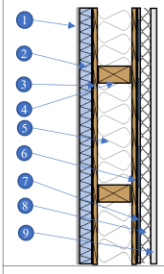


Layer number	Layer distribution	Thickness (mm)
1	Plaster external wall	10
2	Wood wool composite boards	50
3	Planking spruce wood	24
4	Construction wood stud (e = 625 mm)	200
5	Mineral wool	200
6	Planking spruce wool	24
7	Vapor barrier	-
8	Mineral wool	40
9	Gypsum board	12.5

Assembly's performance:
Acoustic performance: R_w (Cr; Ctr) = 53 (−3; −8) dB
Thermal performance: U_{value} = 0.16 W/m² K
Total Embodied Carbon: EC = 28.91 kg CO_2 eq/m²
Total thickness: L = 354.5 mm
Surface area: SA = 73.5 Kg/m³

(d)

Family 5

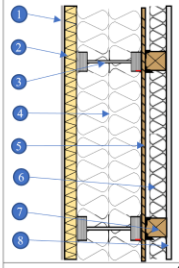


Layer number	Layer distribution	Thickness (mm)
1	Plaster external wall	10
2	Wood wool composite boards	60
3	Planking spruce wood	24
4	Construction wood stud (e = 625 mm)	240
5	Mineral wool	240
6	Planking spruce wool	24
7	Vapor barrier	-
8	Mineral wool	40
9	Gypsum board	12.5

Assembly's performance:
Acoustic performance: R_w (Cr; Ctr) = 54 (−1; −7) dB
Thermal performance: U_{value} = 0.13 W/m² K
Total Embodied Carbon: EC = 37.015 kg CO_2 eq/m²
Total thickness: L = 407.5 mm
Surface area: SA = 81.2 Kg/m³

(e)

Family 6

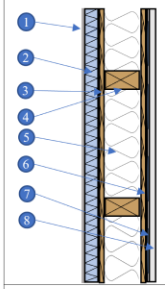


Layer number	Layer distribution	Thickness (mm)
1	Plaster external wall	7
2	Wood fiber insulation board	60
3	Light composite wood-based beam (I-beam) (e = 625 mm)	300
4	Cellulose fiber	300
5	OSB	15
6	Cellulose fiber	80
7	Spruce wood battens mounted on resilient clips	80
8	Gypsum board	15

Assembly's performance:
Acoustic performance: R_w (Cr; Ctr) = 59 (−2; −7) dB
Thermal performance: U_{value} = 0.1 W/m² K
Total Embodied Carbon: EC = 33.944 kg CO_2 eq/m²
Total thickness: L = 477 mm
Surface area: SA = 74.7 Kg/m²

(f)

Family 7



Layer number	Layer distribution	Thickness (mm)
1	Plaster external wall	7
2	Wood fiber insulation board	60
3	Planking spruce wood	24
4	Construction wood stud (e = 625 mm)	240
5	Mineral wool	240
6	Planking spruce wood	24
7	Vapor barrier	-
8	Gypsum board	12.5

Assembly's performance:
Acoustic performance: R_w (Cr; Ctr) = 53 (−3; −9) dB
Thermal performance: U_{value} = 0.15 W/m² K
Total Embodied Carbon: EC = 31.77 kg CO_2 eq/m²
Total thickness: L = 287.5 mm
Surface area: SA = 78.2 Kg/m²

(g)

Figure 17. Representative Pareto-optimal assemblies for each family, selected based on proximity to the ideal point in normalized objective space. (a) Family 1, (b) Family 2, (c) Family 3, (d) Family 4, (e) Family 5, (f) Family 6, (g) Family 7.

CONCLUSIONS

This study presented a multi-objective analysis of timber facade assemblies, evaluating the relationships between airborne sound insulation, thermal transmittance, and embodied carbon through correlation and Pareto analyses. A total of 382 assemblies were collected from literature, and their thermal performance and embodied carbon were calculated. The acoustic dataset was collected from experimentally tested assemblies across different laboratories.

A strong correlation between airborne sound insulation (R_w) and thermal transmittance (U_{value}) was identified across all families, with R^2 values ranging from 0.69 to 0.88, R_w values ranging from 49 to 57 dB, and U_{value} ranging from 0.09 to 0.26 W/m²K. This relationship is attributed to the increase in the total mass of the assembly, where families incorporating denser wood-based sheathing and two insulation layers exhibited higher acoustic-thermal correlation. On the other hand, no correlation was found between acoustic insulation and embodied carbon. Results indicate that acoustic performance can be achieved at different embodied carbon levels depending on material selection and configuration.

Furthermore, the Pareto analysis results in 46 non-dominated assemblies across the seven families. From a design perspective, the strong acoustic-thermal correlation implies that increasing insulation thickness and selecting denser sheathing materials simultaneously improve both sound insulation and thermal resistance. For applications requiring higher acoustic or thermal performance, an increase in total insulation

thickness across two separate insulation layers should be expected, reflecting the trade-off quantified in this study, as each 40 mm increment improves acoustic and thermal performance by 1 dB and 0.02-0.04 W/m²K, respectively, at an embodied carbon cost of 2–3 kg CO_2 eq./m².

Finally, future work would expand the dataset to include broader facade assemblies such as massive wall systems. The LCA boundary should be extended to operational energy stages, and additional design objectives such as structural performance, cost, or durability should be incorporated. Further validation of the Pareto-optimal configurations through in-situ measurements is also recommended.

References

1. Anderson, R.; Dawson, E.; Muszynski, L.; Hildesley, W. *International Mass Timber Report*; Trifecta Collective LLC: Arlington, VA, USA, 2025. Available online: https://masstimberconference.com/report/download/ (accessed on 12 July 2026).
2. Park, S.H.; Lee, P.J.; Jeong, J.H. Effects of noise sensitivity on psychophysiological responses to building noise. *Build. Environ.* **2018**, *136*, 302–311. https://doi.org/10.1016/J.BUILDENV.2018.03.061.
3. Guski, R.; Schreckenberg, D.; Schuemer, R. WHO Environmental Noise Guidelines for the European Region: A Systematic Review on Environmental Noise and Annoyance. *Int. J. Environ. Res. Public Health* **2017**, *14*, 1539. https://doi.org/10.3390/ijerph14121539.
4. *ISO 10140-2:2021*; Acoustics—Laboratory measurement of sound insulation of building elements—Part 2: Measurement of Airborne Sound Insulation. International Organization for Standardization: Geneva, Switzerland, 2021.
5. *ASTM E90*; Standard Test Method for Laboratory Measurement of Airborne Sound Transmission Loss of Building Partitions and Elements. ASTM: West Conshohocken, PA, USA, 2023. https://doi.org/10.1520/E0090-09.
6. *ASTM E413-22*; Classification for Rating Sound Insulation. ASTM International: West Conshohocken, PA, USA, 2022. https://doi.org/10.1520/E0413-22.
7. *ISO 717-1*; Acoustics—Rating of Sound Insulation in Buildings and of Building Elements—Part 1: Airborne Sound Insulation. International Organization for Standardization: Geneva, Switzerland, 2013.

8. Balderrama, A.; Kang, J.; Prieto, A.; Luna-Navarro, A.; Arztmann, D.; Knaack, U. Effects of Façades on Urban Acoustic Environment and Soundscape: A Systematic Review. *Sustainability* **2022**, *14*, 9670. https://doi.org/10.3390/su14159670.

9. Basner, M.; Babisch, W.; Davis, A.; Brink, M.; Clark, C.; Janssen, S. Auditory and non-auditory effects of noise on health. *Lancet* **2014**, *383*, 1325–1332. https://doi.org/10.1016/S0140-6736(13)61613-X.

10. Rindel, J.H. *Sound Insulation in Buildings*; CRC Press: Boca Raton, FL, USA, 2017. https://doi.org/10.1201/9781351228206.

11. Asdrubali, F.; Ferracuti, B.; Lombardi, L.; Guattari, C.; Evangelisti, L.; Grazieschi, G. A review of structural, thermo-physical, acoustical, and environmental properties of wooden materials for building applications. *Build. Environ.* **2017**, *114*, 307–332. https://doi.org/10.1016/j.buildenv.2016.12.033.

12. Frontczak, M.; Wargocki, P. Literature survey on how different factors influence human comfort in indoor environments. *Build. Environ.* **2011**, *46*, 922–937. https://doi.org/10.1016/j.buildenv.2010.10.021.

13. Ürge-Vorsatz, D.; Cabeza, L.F.; Serrano, S.; Barreneche, C.; Petrichenko, K. Heating and cooling energy trends and drivers in buildings. *Renew. Sustain. Energy Rev.* **2015**, *41*, 85–98. https://doi.org/10.1016/J.RSER.2014.08.039.

14. Cabral, M.R.; Blanchet, P. A State of the Art of the Overall Energy Efficiency of Wood Buildings—An Overview and Future Possibilities. *Materials* **2021**, *14*, 1848. https://doi.org/10.3390/ma14081848.

15. Dewsbury, M.; Chandler, T. Massive timber as effective thermal mass in Australian contemporary housing. In *Proceedings of the Living and Learning: Research for a Better Built Environment: 49th International Conference of the Architectural Science Association 2015*; The Architectural Science Association and The University of Melbourne: Melbourne, Australia, 2015; pp. 382–392.

16. Scoczynski Ribeiro, R.; Arnela, M.; Zea, E.; Vila, A.P.; Rodrigues, N.N.A.; Giglio, T.; Zara, R.B.; de Melo Moura, J.D. Acoustic and thermal performance of an innovative façade constructed with Brazilian plantation wood. *J. Build. Eng.* **2025**, *104*, 112348. https://doi.org/10.1016/j.jobe.2025.112348.

17. Bader Eddin, M.; Ménard, S.; Laratte, B.; Wu, T.V. A Design Methodology Incorporating a Sound Insulation Prediction Model, Life Cycle Assessment (LCA), and Thermal Insulation: A Comparative Study of Various Cross-Laminated Timber (CLT) and Ribbed CLT-Based Floor Assemblies. *Acoustics* **2024**, *6*, 1021–1046. https://doi.org/10.3390/acoustics6040056.

18. Leonard, S.J.; Eddin, M.B.; Prichard, M.K.; Broyles, J.M.; Brown, N.C.; Ménard, S. Trade-offs in embodied carbon and acoustic insulation for mass timber floor assemblies. In Proceedings of the *13th World Conference on Timber Engineering*;

WCTE: Brisbane, Australia, 2023; Volume 2, pp. 858–867. https://doi.org/10.52202/069179-0117.

19. Miskinis, K.; Dikavicius, V.; Buska, A.; Banionis, K. Influence of EPS, mineral wool and plaster layers on sound and thermal insulation of a wall: A case study. *Appl. Acoust.* **2018**, *137*, 62–68. https://doi.org/10.1016/j.apacoust.2018.03.001.
20. Caniato, M.; Bettarello, F.; Ferluga, A.; Marsich, L.; Schmid, C.; Fausti, P. Thermal and acoustic performance expectations on timber buildings. *Build. Acoust.* **2017**, *24*, 219–237. https://doi.org/10.1177/1351010X17740477.
21. Caniato, M.; Bettarello, F.; Ferluga, A.; Marsich, L.; Schmid, C.; Fausti, P. Acoustics of lightweight timber buildings: A review. *Renew. Sustain. Energy Rev.* **2017**, *80*, 585–596. https://doi.org/10.1016/j.rser.2017.05.110.
22. Nurzyński, J. Is thermal resistance correlated with sound insulation? *Energy Procedia* **2015**, *78*, 152–157. https://doi.org/10.1016/j.egypro.2015.11.131.
23. Liu, H.; Zhao, X. Thermal conductivity analysis of high porosity structures with open and closed pores. *Int. J. Heat Mass Transf.* **2022**, *183*, 122089. https://doi.org/10.1016/j.ijheatmasstransfer.2021.122089.
24. *ASTM C518-21*; Test Method for Steady-State Thermal Transmission Properties by Means of the Heat Flow Meter Apparatus. ASTM International: West Conshohocken, PA, USA, 2021. https://doi.org/10.1520/C0518-21.
25. Di Bella, A.; Granzotto, N.; Pavarin, C. Comparative analysis of thermal and acoustic performance of building elements. In *Proceedings of the Forum Acusticum, Krakow*; EAA: Madrid, Spain, 2014.
26. Deb, K.; Wang, L. *Multi-Objective Optimization Using Evolutionary Algorithms: An Introduction*; Springer: Berlin/Heidelberg, Germany; London, UK, 2011; pp. 3–34. https://doi.org/10.1007/978-0-85729-652-8_1.
27. Skov, R.; Parigi, D.; Damkilde, L. Multi-objective room acoustics optimization of timber folded plate structure. In *Proceedings of the IASS Annual Symposia*; International Association for Shell and Spatial Structures (IASS): Madrid, Spain, 2017; Volume 2017, pp 1–10.
28. Hammad, A.W.; Akbarnezhad, A.; Oldfield, P. Optimising embodied carbon and U-value in load bearing walls: A mathematical bi-objective mixed integer programming approach. *Energy Build.* **2018**, *174*, 657–671. https://doi.org/10.1016/J.ENBUILD.2018.05.061.
29. Chen, Z.; Hammad, A.W.A.; Kamardeen, I.; Akbarnezhad, A. Optimising Embodied Energy and Thermal Performance of Thermal Insulation in Building Envelopes via an Automated Building Information Modelling (BIM) Tool. *Buildings* **2020**, *10*, 218. https://doi.org/10.3390/BUILDINGS10120218.

30. Bradley, J.; Birta, J. *Laboratory Measurements of the Sound Insulation of Building Façade Elements*; National Research Council of Canada: Ottawa, ON, Canada, 2000. https://doi.org/10.4224/20386467.

31. Polleres, S.; Plößnig, B. *External Wall-dataholz.eu*; Holzforschung Austria—Austrian Forest Products Research Society: Vienna, Austria, 2026. Available online: https://www.dataholz.eu/en/components/external-wall.htm (accessed on 10 March 2026).

32. Boulet, S.; Kouyoumji, J.; Achard, G. Objective and subjective qualification of acoustic and thermal comfort in timber framed houses. In *Proceedings of the INTER-NOISE and NOISE-CON Congress and Conference Proceedings*; Institute of Noise Control Engineering: Reston, VA, USA, 2009; pp. 3666–3674.

33. Höller, C. Review and comparison of ASTM and ISO standards on sound transmission in buildings. In *Proceedings of the INTER-NOISE and NOISE-CON Congress and Conference Proceedings 2018*, *Chicago, IL, USA, 26–29 August 2018*, Institute of Noise Control Engineering: Reston, VA, USA, 2018.

34. Nilsson, E.; Ménard, S.; Bard, D.; Hagberg, K. Effects of building height on the sound transmission in cross-laminated timber buildings—Airborne sound insulation. *Build. Environ.* **2023**, *229*, 109985. https://doi.org/10.1016/J.BUILDENV.2023.109985.

35. Plag, R. UBAKUS—U-Wert Berechnung n.d. Available online: https://www.ubakus.de (accessed on 8 April 2026).

36. *Canadian Commission on Building and Fire Codes. National Building Code of Canada 2020: Volume 1*, 15th ed.; National Research Council of Canada: Ottawa, ON, Canada, 2020.

37. *ISO 6946:2022*; Building Components and Building Elements—Thermal Resistance and Thermal Transmittance—Calculation Methods. International Organization for Standardization: Geneva, Switzerland, 2022.

38. Ciroth, A. ICT for environment in life cycle applications: OpenLCA—A new open source software for Life Cycle Assessment. *Int. J. Life Cycle Assess.* **2007**, *12*, 209–210. https://doi.org/10.1065/lca2007.06.337.

39. Hammond, P.G.; Jones, C.; Lowrie, E.F.; Tse, P. *A BSRIA Guide: Embodied Carbon: The Inventory of Carbon and Energy (ICE)*; BSRIA: Bracknell, UK, 2011.

40. Verband für Dämmsysteme, Putz und Mörtel e.V. (VDPM). Environmental Product Declaration: Plastering Mortar, Normal Plaster/Finishing Plaster, EPD-VDP-20230398-IBO1-DE; Institut Bauen und Umwelt e.V. (IBU): Berlin, Germany, 2024. Available online: https://www.sto.de/cepcom/de/Dokumente/Service-Tools/EPD/EPD-VDP-20230398-IBO3-DE(EN).pdf (accessed on 29 September 2026).

41. Knauf Ceiling Solutions GmbH & Co. KG. *Environmental Product Declaration: Heradesign Acoustic Panels Euroclass A2*, EPD-KNA-20230208-IBI1-EN; Institut

Bauen und Umwelt e.V. (IBU): Berlin, Germany, 2024. Available online: https://epd-online.com (accessed on 29 September 2026).

42. Zerari, S.; Franchino, R.; Pisacane, N. *Cost and Carbon Intensity Analysis of Different Bio-Based Insulation Materials across European Countries*; EDP Sciences: Les Ulis, France, 2024. https://doi.org/10.1051/e3sconf/202458501010.
43. EPD International AB. *Environmental Product Declaration Programme: The International EPD® System Gypsum Board-RG 12.5mm*; EPD International AB: Stockholm, Sweden, 2024.
44. Marler, R.T.; Arora, J.S. Survey of multi-objective optimization methods for engineering. *Struct. Multidiscip. Optim.* **2004**, *26*, 369–395. https://doi.org/10.1007/s00158-003-0368-6.
45. Hafiz, F.; Swain, A.; Mendes, E. Multi-objective evolutionary framework for non-linear system identification: A comprehensive investigation. *Neurocomputing* **2020**, *386*, 257–280. https://doi.org/10.1016/J.NEUCOM.2019.12.095.
46. Schütze, O.; Cuate, O. The Pareto Tracer for the treatment of degenerated multi-objective optimization problems. *Eng. Optim.* **2025**, *57*, 261–286. https://doi.org/10.1080/0305215X.2024.2420726.
47. Jollife, I.T.; Cadima, J. Principal component analysis: A review and recent developments. *Philos. Trans. A Math. Phys. Eng. Sci.* **2016**, *374*, 20150202. https://doi.org/10.1098/RSTA.2015.0202.
48. Petchrompo, S.; Coit, D.W.; Brintrup, A.; Wannakrairot, A.; Parlikad, A.K. A review of Pareto pruning methods for multi-objective optimization. *Comput. Ind. Eng.* **2022**, *167*, 108022. https://doi.org/10.1016/J.CIE.2022.108022.
49. Wang, Z.; Rangaiah, G.P. Application and Analysis of Methods for Selecting an Optimal Solution from the Pareto-Optimal Front obtained by Multiobjective Optimization. *Ind. Eng. Chem. Res.* **2017**, *56*, 560–574. https://doi.org/10.1021/ACS.IECR.6B03453.
50. Nath, B.; Roy, S.; Das, B.; Ehyaei, M.A. Experimental and numerical study of a novel composite building wall U-value. *Therm. Sci. Eng. Prog.* **2024**, *53*, 102751. https://doi.org/10.1016/J.TSEP.2024.102751.
51. Zhen, L.; Li, M.; Cheng, R.; Peng, D.; Yao, X. Multi-objective Test Problems with Degenerate Pareto Fronts. *arXiv* **2018**, arXiv:1806.02706. https://doi.org/https://arxiv.org/abs/1806.02706.
52. Brockhoff, D.; Zitzler, E. Objective Reduction in Evolutionary Multiobjective Optimization: Theory and Applications. *Evol. Comput.* **2009**, *17*, 135–166. https://doi.org/10.1162/EVCO.2009.17.2.135.

3.7 STUDENT CONTRIBUTION

The student's contributions to this article were as follows:

- Conduct of a literature review in the fields of building acoustics, thermal insulation, and embodied carbon in timber construction, in order to define the scientific objectives and structure the research work.
- Collection of wall assembly configurations and their associated airborne sound insulation performance (R_w) from open-access sources.
- Calculation of the thermal transmittance (U_{value}) and embodied carbon (EC) for each assembly based on their material composition.
- Development and implementation of the multi-objective Pareto optimization framework from scratch using Python, including correlation analysis, Pareto front identification, and design catalogue construction.
- Analysis of results and interpretation of the trade-offs between acoustic, thermal, and environmental performance across the seven assembly families.
- Writing of the manuscript according to the recommendations of the supervisory team.
- Creation of all figures and graphics.
- Compilation of references.

CONCLUSION

This research was motivated by the absence of an integrated evaluation framework that simultaneously accounts for acoustic performance, thermal performance, and embodied carbon in timber-based facade assemblies. In conventional design practice, these three dimensions are often treated independently, which can lead to suboptimal solutions when trade-offs are not explicitly quantified.

The methodological framework developed in this work combined experimental data collection, analytical calculations, and numerical assessment tools to build a consistent database of facade assemblies. Acoustic performance was primarily characterized using standardized airborne sound insulation indicators, while thermal behavior was evaluated through steady-state heat transfer calculations using validated simulation tools in accordance with ISO-based methodologies. In parallel, embodied carbon was quantified using life cycle assessment principles focusing on the product stage (A1–A3). This dataset enabled a coherent multi-criteria comparison across a wide range of timber facade configurations.

Based on this dataset, statistical analyses were conducted to investigate the relationships between acoustic insulation, thermal transmittance, and embodied carbon. The results highlighted that these performance indicators are not independent. In particular, correlations were observed between the thermal and acoustic performances in facade configurations, mainly driven by the shared influence of material layers, density distribution, and cavity insulation strategies. However, the relationship with embodied carbon remained more complex, as improvements in performance could be achieved through different material combinations with varying environmental impacts.

The multi-criteria analysis framework, based on Pareto efficiency, allowed the identification of non-dominated facade assemblies that represent optimal trade-offs between competing objectives. Rather than producing a single “best” solution, this approach generated a set of feasible configurations offering different balances between sound insulation, thermal efficiency, and embodied carbon. This type of output is particularly relevant for early-stage design, where decision-making is driven by project-specific priorities rather than a single performance criterion.

From a practical perspective, the results of this research provide a structured decision-support approach for engineers and designers working with timber facades. The proposed database of assemblies and their associated performance indicators can be used as a reference to guide material selection and assembly design. In addition, the study demonstrates that improving acoustic or thermal performance does not necessarily require a proportional increase in embodied carbon, provided that assembly design is optimized in a multi-criteria context.

Despite these contributions, several limitations must be acknowledged. The analysis is based on available published data and standardized calculation methods, which may not fully capture in-situ variability, construction tolerances, or long-term hygrothermal and acoustic behavior. In addition, the embodied carbon assessment is limited to the initial product stage and does not include end-of-life scenarios or operational impacts, which could influence the overall environmental balance in a full life cycle perspective.

Finally, future work could extend this research by integrating dynamic hygrothermal simulations, more detailed acoustic modeling, and expanded life cycle assessment boundaries including modules beyond A1–A3. Further experimental

validation of facade configurations would also strengthen the observed correlations and improve the robustness of the analysis framework. In addition, the integration of cost and constructability constraints could further enhance the practical applicability of the proposed approach.

LIST OF REFERENCES

[1] Roy A, Emily D, Lech M, Will Hildesley. International Mass Timber Report. Trifecta Collective LLC: Arlington, VA, USA; 2024 2025. https://masstimberconference.com/report/download/ (accessed July 12, 2026).

[2] Asdrubali F, Ferracuti B, Lombardi L, Guattari C, Evangelisti L, Grazieschi G. A review of structural, thermo-physical, acoustical, and environmental properties of wooden materials for building applications. Build Environ 2017;114:307–32. https://doi.org/10.1016/j.buildenv.2016.12.033.

[3] Frontczak M, Wargocki P. Literature survey on how different factors influence human comfort in indoor environments. Build Environ 2011;46:922–37. https://doi.org/10.1016/J.BUILDENV.2010.10.021.

[4] Park SH, Lee PJ, Jeong JH. Effects of noise sensitivity on psychophysiological responses to building noise. Build Environ 2018;136:302–11. https://doi.org/10.1016/J.BUILDENV.2018.03.061.

[5] Brown AL, van Kamp I. WHO Environmental Noise Guidelines for the European Region: A Systematic Review of Transport Noise Interventions and Their Impacts on Health. International Journal of Environmental Research and Public Health 2017, Vol 14, Page 873 2017;14:873. https://doi.org/10.3390/IJERPH14080873.

[6] Busch T. The Future Of Acoustical Provisions In The NBCC - Canadian Consulting Engineer. CANADIAN CONSULTANT Engineer 2021. https://www.canadianconsultingengineer.com/features/the-future-of-acoustical-provisions-in-the-nbcc/ (accessed April 27, 2026).

[7] Oghazi NR, Jusselme T, Andersen M. Carbon budgets at the component scale and their impacts on design choices: the façade as a case study. J. Phys. Conf. Ser., vol. 2600, Institute of Physics; 2023. https://doi.org/10.1088/1742-6596/2600/15/152016.

[8] Zapata-Webborn E, Hanmer C, Oreszczyn T, Huebner G, McKenna E, Few J, et al. Winter demand falls as fuel bills rise: Understanding the energy impacts of the cost-of-living crisis on British households. Energy Build 2024;305:113869. https://doi.org/10.1016/J.ENBUILD.2023.113869.

[9] Nurzyński J. Is Thermal Resistance Correlated With Sound Insulation? Energy Procedia 2015;78:152–7. https://doi.org/10.1016/J.EGYPRO.2015.11.131.

[10] Hassan SA. The effect of residential building fa ade design on energy consumption for hot desert climate. IOP Conf. Ser. Mater. Sci. Eng., vol. 928, IOP Publishing Ltd; 2020. https://doi.org/10.1088/1757-899X/928/2/022029.

[11] Medved S. Building Acoustics and Noise Control in Buildings. Springer Tracts in Civil Engineering 2022:331–406. https://doi.org/10.1007/978-3-030-74390-1_5.

[12] Holger Rindel J. Sound insulation in buildings. Sound Insulation in Buildings 2017:1–450. https://doi.org/10.1201/9781351228206/SOUND-INSULATION-BUILDINGS-JENS-HOLGER-RINDEL.

[13] Madaras GS, Heuer AE. Effects of noise flanking paths on ceiling attenuation class (CAC) ratings of ceiling systems and inter-room speech privacy. Canadian Acoustics 2015;43.

[14] Craik RJM. The noise reduction of flanking paths. Applied Acoustics 1987;22:163–75. https://doi.org/10.1016/0003-682X(87)90034-X.

[15] Galbrun L. The prediction of airborne sound transmission between two rooms using first-order flanking paths. Applied Acoustics 2008;69:1332–42. https://doi.org/10.1016/J.APACOUST.2007.08.010.

[16] ISO 10140-2:2021 - Acoustics — Laboratory measurement of sound insulation of building elements — Part 2: Measurement of airborne sound insulation n.d. https://www.iso.org/standard/79487.html (accessed December 18, 2024).

[17] E336 Standard Test Method for Measurement of Airborne Sound Attenuation between Rooms in Buildings n.d. https://www.astm.org/standards/e336 (accessed August 8, 2024).

[18] ISO 10140-2:2021 - Acoustics — Laboratory measurement of sound insulation of building elements — Part 2: Measurement of airborne sound insulation n.d. https://www.iso.org/standard/79487.html (accessed August 8, 2024).

[19] Vigran TE. Building Acoustics 2014. https://doi.org/10.1201/9781482266016.

[20] ISO 10140-1:2021 - Acoustics — Laboratory measurement of sound insulation of building elements — Part 1: Application rules for specific products n.d. https://www.iso.org/standard/73910.html (accessed August 8, 2024).

[21] E492 Standard Test Method for Laboratory Measurement of Impact Sound Transmission Through Floor-Ceiling Assemblies Using the Tapping Machine n.d. https://www.astm.org/e0492-22.html (accessed August 8, 2024).

[22] ISO 10140-5:2021(en), Acoustics — Laboratory measurement of sound insulation of building elements — Part 5: Requirements for test facilities and equipment n.d. https://www.iso.org/obp/ui/en/#iso:std:iso:10140:-5:ed-2:v1:en (accessed December 18, 2024).

[23] Zhao Basc P. IMPACT SOUND INSULATION PERFORMANCE OF FLOATING FLOOR ASSEMBLIES ON MASS TIMBER SLABS. 2022.

[24] ISO 717-1; Acoustics—Rating of Sound Insulation in Buildings and of Building Elements—Part 1: Airborne Sound Insulation. International Organization for Standardization: Geneva, Switzerland: 2013.

[25] Rindel JH. Sound Insulation in Buildings. Boca Raton, FL, USA: CRC Press; 2017. https://doi.org/10.1201/9781351228206.

[26] Oriti D, Sindoni L, Wilson-Ewing E, Cai G, Cao L-M, Hu Y-P, et al. First law of thermodynamics and Friedmann equations ofFriedmann-Robertson-Walker universe. Journal of High Energy Physics 2005;2005:050. https://doi.org/10.1088/1126-6708/2005/02/050.

[27] Berge A, Johansson P. Literature Review of High Performance Thermal Insulation Report in Building Physics. n.d.

[28] ISO 6946:2017 - Building components and building elements — Thermal resistance and thermal transmittance — Calculation methods n.d. https://www.iso.org/standard/65708.html (accessed August 8, 2024).

[29] ASTM International. compass 2019. https://compass.astm.org/content-access?contentCode=ASTM%7CC1363-19%7Cen-US (accessed December 14, 2025).

[30] Liu M, Sun Y, Sun C, Yang X. STUDY ON THERMAL INSULATION AND HEAT TRANSFER PROPERTIES OF WOOD FRAME WALLS. WOOD RESEARCH 2018. https://www.woodresearch.sk/wr/201802/07.pdf (accessed October 23, 2026).

[31] Plag R. UBAKUS - U-Wert Berechnung. n.d. https://www.ubakus.de (accessed April 8, 2026).

[32] Gerlich V, Sulovská K, Zálešák M. COMSOL Multiphysics validation as simulation software for heat transfer calculation in buildings: Building simulation software validation. Measurement 2013;46:2003–12. https://doi.org/10.1016/J.MEASUREMENT.2013.02.020.

[33] Hens HSLC. Building physics -- heat, air and moisture : fundamentals, engineering methods, material properties and exercises 2024:369.

[34] Luikov AV. Analytical Heat Diffusion Theory 2014:703.

[35] Allan D. Pierce. Acoustics: An Introduction to Its Physical Principles and Applications. Third Edition. 1980. https://doi.org/10.1007.

[36] Buildings and Climate Change Summary for Decision Makers Sustainable Buildings & Climate Initiative. n.d.

[37] Pomponi F, Moncaster A. Embodied carbon mitigation and reduction in the built environment – What does the evidence say? J Environ Manage 2016;181:687–700. https://doi.org/10.1016/j.jenvman.2016.08.036.

[38] Trinh TMKH, Hou. An Overview of Building Lifecycle Embodied Carbon Emissions Research. 2017.

[39] Chastas P, Theodosiou T, Bikas D. Embodied energy in residential buildings-towards the nearly zero energy building: A literature review. Build Environ 2016;105:267–82. https://doi.org/10.1016/j.buildenv.2016.05.040.

[40] Ibn-Mohammed T, Greenough R, Taylor S, Ozawa-Meida L, Acquaye A. Operational vs. embodied emissions in buildings - A review of current trends. Energy Build 2013;66:232–45. https://doi.org/10.1016/j.enbuild.2013.07.026.

[41] Matthew Eckelman, Sarah Nunberg. Life Cycle Assessment Explained. Sustainability Tools in Cultural Heritage 2025. https://stich.culturalheritage.org/life-cycle-assessment-explained/#site-header (accessed April 23, 2025).

[42] Van Herzele C. EN 15978:2026 - A Harmonized Method to Assess the Environmental Performance of Buildings - CEN-CENELEC. 2026.

[43] SimaPro - Sustainability insights for informed changemakers n.d. https://simapro.com/ (accessed December 14, 2025).

[44] Cecobois – Centre d'expertise sur la construction commerciale en bois n.d. https://cecobois.com/ (accessed December 14, 2025).

[45] openLCA.org | openLCA is a free, professional Life Cycle Assessment (LCA) and footprint software with a broad range of features and many available databases, created by GreenDelta since 2006 n.d. https://www.openlca.org/ (accessed December 14, 2025).

[46] Athena Sustainable Materials Institute n.d. https://www.athenasmi.org/ (accessed December 14, 2025).

[47] Deb K. Multi-Objective Optimization. Search Methodologies: Introductory Tutorials in Optimization and Decision Support Techniques 2005:273–316. https://doi.org/10.1007/0-387-28356-0_10.

[48] Li R, Shari Z, Ab Kadir MZA. A review on multi-objective optimization of building performance - Insights from bibliometric analysis. Heliyon 2025;11:e42480. https://doi.org/10.1016/J.HELIYON.2025.E42480.

[49] Deb K, Wang L. Multi-objective Optimization Using Evolutionary Algorithms: An Introduction. Springer, Berlin, Germany: Springer, London; 2011, p. 3–34. https://doi.org/10.1007/978-0-85729-652-8_1.

[50] Van Thai M, Galimard P, Elachachi SM, Ménard S. Multi-objective optimization of cross laminated timber-concrete composite floor using NSGA-II. Journal of Building Engineering 2022;52:104285. https://doi.org/10.1016/j.jobe.2022.104285.

[51] Armand-Decker S, Garnesson T, Galimard P, Ndiaye A, Sempey A, ere P, et al. Optimisation multi-objectif de planchers intermédiaires bois tenant compte d'objectifs mécaniques et environnementaux. HAL Archives-Ouvertes 2015. https://doi.org/hal.archives-ouvertes.fr/hal-01167667.

[52] Costa D, Serra J, Quinteiro P, Dias AC. Life cycle assessment of wood-based panels: A review. J Clean Prod 2024;444:140955. https://doi.org/10.1016/J.JCLEPRO.2024.140955.

[53] Vardaxis NG, Bard D, Persson Waye K. Review of acoustic comfort evaluation in dwellings—part I: Associations of acoustic field data to subjective responses from building surveys. Building Acoustics 2018;25:151–70. https://doi.org/10.1177/1351010X18762687.

[54] Ayres RU. Life cycle analysis: A critique. Resour Conserv Recycl 1995;14:199–223. https://doi.org/10.1016/0921-3449(95)00017-D.

[55] Papadopoulos AM. State of the art in thermal insulation materials and aims for future developments. Energy Build 2005;37:77–86. https://doi.org/10.1016/J.ENBUILD.2004.05.006.

[56] Ritter M, Skog K. Science Supporting the Economic and Environmental Benefits of Using Wood and Wood Products in Green Building Construction. Forest Service U S Department of Agriculture 2011. https://doi.org/https://doi.org/10.2737/FPL-GTR-206.

[57] De Araujo V, Aguiar F, Jardim P, Mascarenhas F, Marini L, Aquino V, et al. Is Cross-Laminated Timber (CLT) a Wood Panel, a Building, or a Construction System? A Systematic Review on Its Functions, Characteristics, Performances, and Applications 2023. https://doi.org/10.3390/10.3390/f14020264.

[58] Falk, Robert. Wood as a Sustainable Building Material. Forest Products 2009. https://www.woodworks.org/why-wood/sustainability/ (accessed October 23, 2026).

[59] Bahrami A, Jakobsson J, Söderroos T. Factors Influencing Choice of Wooden Frames for Construction of Multi-Story Buildings in Sweden. Buildings 2023, Vol 13, Page 217 2023;13:217. https://doi.org/10.3390/BUILDINGS13010217.

[60] Unterrainer AW. Wood-A Sustainable Building Material? 2018. https://doi.org/10.5176/2301-394X_ACE18.43.

[61] Milner HR, Woodard AC. Sustainability of engineered wood products. Sustainability of Construction Materials 2016:159–80. https://doi.org/10.1016/B978-0-08-100370-1.00008-1.

[62] Wieruszewski M, Mazela B. Lamelirano drvo (CLT) kao alternativni oblik drva za gradnju. Drvna Industrija 2017;68:359–67. https://doi.org/10.5552/drind.2017.1728.

[63] Erik Serrano. Limnologen-Experiences from an 8-storey timber building. 2009.

[64] Levée V. ORIGINE POINTE-AUX-LIÈVRES ECOCONDOS QUEBEC CITY. Canadian Wood Council 2018. https://cwc.ca/wp-content/uploads/2019/03/Origine-Case-Study.pdf (accessed October 23, 2026).

[65] Gagnon S, Bilek EM (Ted), Podesto L, Crespell P. Chapter 1: CLT Introduction to cross-laminated timber. In: CLT Handbook: Cross-Laminated Timber / Edited by Erol Karacabeyli, Brad Douglas -- U S Ed 2013; Pp 1-45 2013:1–57.

[66] Ivanovic-Sekularac J, Šekularac N. Wood as element of façade cladding in modern architecture. Research Gate 2012. https://www.researchgate.net/publication/294647271_Wood_as_element_of_facade_cladding_in_modern_architecture (accessed October 23, 2026).

[67] González-Retamal M, Forcael E, Saelzer-Fuica G, Vargas-Mosqueda M. From Trees to Skyscrapers: Holistic Review of the Advances and Limitations of Multi-Storey Timber Buildings. Buildings 2022, Vol 12, Page 1263 2022;12:1263. https://doi.org/10.3390/BUILDINGS12081263.

[68] Park SH, Lee PJ, Jeong JH. Effects of noise sensitivity on psychophysiological responses to building noise. Build Environ 2018;136:302–11. https://doi.org/10.1016/J.BUILDENV.2018.03.061.

[69] Asdrubali F, Ferracuti B, Lombardi L, Guattari C, Evangelisti L, Grazieschi G. A review of structural, thermo-physical, acoustical, and environmental properties of wooden materials for building applications. Build Environ 2017;114:307–32. https://doi.org/10.1016/j.buildenv.2016.12.033.

[70] Guski R, Schreckenberg D, Schuemer R. WHO Environmental Noise Guidelines for the European Region: A Systematic Review on Environmental Noise and Annoyance. International Journal of Environmental Research and Public Health, Vol 14, Page 1539 2017;14:1539. https://doi.org/10.3390/IJERPH14121539.

[71] ASTM International. Standard Test Method for Laboratory Measurement of Airborne Sound Transmission Loss of Building Partitions and Elements. West Conshohocken: 2016.

[72] ASTM International. Test Method for Laboratory Measurement of Impact Sound Transmission Through Floor-Ceiling Assemblies Using the Tapping Machine 2022. https://doi.org/10.1520/E0492-22.

[73] Huang X, Zhao W, Huang Z, Wang Y, Du Y, Du L, et al. Study on sound insulation performance of walls in traditional timber dwellings of the Miao ethnic group in Qiandongnan. Sci Rep 2026;16:8690. https://doi.org/10.1038/S41598-026-41450-1.

[74] Bradley JS, Birta JA. Publisher's version / Version de l'éditeur. NRC Publications Archive 2000:1–185. https://doi.org/10.4224/20386112.

[75] Ayres RU. Life cycle analysis: A critique. Resour Conserv Recycl 1995;14:199–223. https://doi.org/10.1016/0921-3449(95)00017-D.

[76] Parsons K. Human Thermal Environments : The Effects of Hot, Moderate, and Cold Environments on Human Health, Comfort and Performance, Second Edition. Human Thermal Environments 2007. https://doi.org/10.1201/9781420025248.

[77] Gratia E, De Herde A. Design of low energy office buildings. Energy Build 2003;35:473–91. https://doi.org/10.1016/S0378-7788(02)00160-3.

[78] Mohammad, Gagnon S, Douglas B. Introduction to cross laminated timber. Wood Des Focus 2012;2. https://doi.org/https://awc.org/wp-content/uploads/2021/12/fdocuments.us_introduction-to-cross-laminated-timber.pdf.

[79] Ürge-Vorsatz D, Cabeza LF, Serrano S, Barreneche C, Petrichenko K. Heating and cooling energy trends and drivers in buildings. Renewable and Sustainable Energy Reviews 2015;41:85–98. https://doi.org/10.1016/J.RSER.2014.08.039.

[80] Abu-Jdayil B, Mourad AH, Hittini W, Hassan M, Hameedi S. Traditional, state-of-the-art and renewable thermal building insulation materials: An overview. Constr Build Mater 2019;214:709–35. https://doi.org/10.1016/J.CONBUILDMAT.2019.04.102.

[81] Berge A, Johansson P. Literature Review of High Performance Thermal Insulation Report in Building Physics. Chalmers 2012.

[82] Balasbaneh AT, Sher W. Comparative sustainability evaluation of two engineered wood-based construction materials: Life cycle analysis of CLT versus GLT. Build Environ 2021;204:108112. https://doi.org/10.1016/J.BUILDENV.2021.108112.

[83] Sandanayake M, Lokuge W, Zhang G, Setunge S, Thushar Q. Greenhouse gas emissions during timber and concrete building construction —A scenario based comparative case study. Sustain Cities Soc 2018;38:91–7. https://doi.org/10.1016/J.SCS.2017.12.017.

[84] Steiger R, Gülzow A. Validity of bending tests on strip-shaped specimens to derive bending strength and stiffness properties of cross-laminated solid timber (CLT) 2009.

[85] Hung Anh LD, Pásztory Z. An overview of factors influencing thermal conductivity of building insulation materials. Journal of Building Engineering 2021;44:102604. https://doi.org/10.1016/J.JOBE.2021.102604.

[86] Srivaro S, Pásztory Z, Le Duong HA, Lim H, Jantawee S, Tomad J. Physical, mechanical and thermal properties of cross laminated timber made with coconut wood. European Journal of Wood and Wood Products 2021;79:1519–29. https://doi.org/10.1007/s00107-021-01741-y.

[87] Song HY, Cheng XX, Chu L. Effect of Density and Ambient Temperature on Coefficient of Thermal Conductivity of Heat-Insulated EPS and PU Materials for Food Packaging. Applied Mechanics and Materials 2014;469:152–5. https://doi.org/10.4028/WWW.SCIENTIFIC.NET/AMM.469.152.

[88] Khordad R, Razi F. Effect of temperature and distribution function of depolarization factor on thermal conductivity of carbon nanotube-based composites. Superlattices Microstruct 2013;64:439–50. https://doi.org/10.1016/J.SPMI.2013.09.044.

[89] Lakatos Á. Moisture induced changes in the building physics parameters of insulation materials. Sci Technol Built Environ 2016;22:252–60. https://doi.org/10.1080/23744731.2016.1131567.

[90] Jerman M, Černý R. Effect of moisture content on heat and moisture transport and storage properties of thermal insulation materials. Energy Build 2012;53:39–46. https://doi.org/10.1016/J.ENBUILD.2012.07.002.

[91] Berardi U. The impact of temperature dependency of the building insulation thermal conductivity in the Canadian climate. Energy Procedia 2017;132:237–42. https://doi.org/10.1016/J.EGYPRO.2017.09.684.

[92] Janssen H, Van De Walle W. The impact of pore structure parameters on the thermal conductivity of porous building blocks. Constr Build Mater 2022;324:126681. https://doi.org/10.1016/J.CONBUILDMAT.2022.126681.

[93] Liu H, Zhao X. Thermal conductivity analysis of high porosity structures with open and closed pores. Int J Heat Mass Transf 2022;183:122089. https://doi.org/10.1016/j.ijheatmasstransfer.2021.122089.

[94] The Engineering ToolBox (2003). Solids, Liquids and Gases - Thermal Conductivities 2003.

[95] Dewsbury M, Chandler T. Massive timber as effective thermal mass in Australian contemporary housing. Living and Learning: Research for a Better Built Environment: 49th International Conference of the Architectural Science Association 2015:382–92.

[96] Kang Y, Jo HH, Kim S. Enhancing indoor comfort and building energy efficiency with cross-laminated timber (CLT) in hygrothermal environments. Journal of Building Engineering 2024;84. https://doi.org/10.1016/j.jobe.2024.108582.

[97] Scoczynski Ribeiro R, Arnela M, Zea E, Vila AP, Rodrigues NNA, Giglio T, et al. Acoustic and thermal performance of an innovative façade constructed with Brazilian plantation wood. Journal of Building Engineering 2025;104:112348. https://doi.org/10.1016/j.jobe.2025.112348.

[98] Zapata-Webborn E, Hanmer C, Oreszczyn T, Huebner G, McKenna E, Few J, et al. Winter demand falls as fuel bills rise: Understanding the energy impacts of the cost-of-living crisis on British households. Energy Build 2024;305. https://doi.org/10.1016/j.enbuild.2023.113869.

[99] Schabowicz K, Zawiślak Ł. Numerical Comparison of Thermal Behaviour between Ventilated Facades. Studia Geotechnica et Mechanica 2021;42:297–305. https://doi.org/10.2478/sgem-2019-0044.

[100] Alhawari A, Mukhopadhyaya P. Thermal bridges in building envelopes – An overview of impacts and solutions. International Review of Applied Sciences and Engineering 2018;9:31–40. https://doi.org/10.1556/1848.2018.9.1.5.

[101] Karagiozis A. Analysis of the Hygrothermal Behavior of residential high-rise building components. Canada Mortgage and Housing Corporation 1997.

[102] Ye Q, Gong Y, Ren H, Peng L, Zhang H. Theoretical, numerical and experimental studies on thermal insulation performance of different cross laminated timber walls. Journal of Building Engineering 2023;72. https://doi.org/10.1016/j.jobe.2023.106640.

[103] Miskinis K, Dikavicius V, Buska A, Banionis K. Influence of EPS, mineral wool and plaster layers on sound and thermal insulation of a wall: a case study. Applied Acoustics 2018;137:62–8. https://doi.org/10.1016/j.apacoust.2018.03.001.

[104] Georgescu SV, Șova D, Campean M, Coșereanu C. A Sustainable Approach to Build Insulated External Timber Frame Walls for Passive Houses Using Natural and Waste Materials. Forests 2022;13. https://doi.org/10.3390/f13040522.

[105] Al Rim K, Ledhem A, Douzane O, Dheilly RM, Queneudec M. Influence of the proportion of wood on the thermal and mechanical performances of clay-cement-wood composites. Cem Concr Compos 1999;21:269–76. https://doi.org/10.1016/S0958-9465(99)00008-6.

[106] Miskinis K, Dikavicius V, Buska A, Banionis K. Influence of EPS, mineral wool and plaster layers on sound and thermal insulation of a wall: a case study. Applied Acoustics 2018;137:62–8. https://doi.org/10.1016/j.apacoust.2018.03.001.

[107] Caniato M, Bettarello F, Ferluga A, Marsich L, Schmid C, Fausti P. Thermal and acoustic performance expectations on timber buildings. Building Acoustics 2017;24:219–37. https://doi.org/10.1177/1351010X17740477.

[108] Caniato M, Marzi A, Monteiro da Silva S, Gasparella A. A review of the thermal and acoustic properties of materials for timber building construction. Journal of Building Engineering 2021;43:103066. https://doi.org/10.1016/J.JOBE.2021.103066.

[109] Nurzyński J. Is thermal resistance correlated with sound insulation? Energy Procedia, vol. 78, 2015, p. 152–7. https://doi.org/10.1016/j.egypro.2015.11.131.

[110] Di Bella A, Granzotto N, Pavarin C. Comparative analysis of thermal and acoustic performance of building elements. Forum Acusticum, Krakow 2014.

[111] Santos P, Sousa L, Godinho L, Correia JR, Dias AMPG. Acoustic and thermal behaviour of cross-insulated timber panels. Journal of Building Engineering 2021;44:103309. https://doi.org/10.1016/J.JOBE.2021.103309.

[112] Bader Eddin M, Ménard S, Laratte B, Wu TV. A Design Methodology Incorporating a Sound Insulation Prediction Model, Life Cycle Assessment (LCA), and Thermal Insulation: A Comparative Study of Various Cross-Laminated Timber (CLT) and Ribbed CLT-Based Floor Assemblies. Acoustics 2024;6:1021–46. https://doi.org/10.3390/acoustics6040056.

[113] Kouyoumji J-L, Achard G, Professor -Design). New energy efficient lightweight building technologies, acoustic and thermal interactions. n.d.

[114] Birol F, La Camera F. The Breakthrough Agenda Report “Accelerating Sector Transitions Through Stronger International Collaboration.” 2023.

[115] Shirazi A, Baabak A. EMBODIED LIFE CYCLE ASSESSMENT COMPARISON OF SINGLE FAMILY RESIDENTIAL HOUSES CONSIDERING THE 1970s TRANSITION IN CONSTRUCTION INDUSTRY: ATLANTA CASE STUDY. 2018.

[116] Kumar V, Lo Ricco M, Bergman RD, Nepal P, Poudyal NC. Environmental impact assessment of mass timber, structural steel, and reinforced concrete buildings based on the 2021 international building code provisions. Build Environ 2024;251. https://doi.org/10.1016/j.buildenv.2024.111195.

[117] Leonard SJ, Eddin MB, Prichard MK, Broyles JM, Brown NC, Ménard S. Trade-offs in embodied carbon and acoustic insulation for mass timber floor assemblies. 13th World Conference on Timber Engineering, WCTE 2023, vol. 2, 2023, p. 858–67. https://doi.org/10.52202/069179-0117.

[118] Bligh J. Quantifying and Reducing Embodied Carbon in the Acoustic Design of Mass Timber Buildings. InterNoise 2022. https://www.proceedings.com/content/069/069179-0556open.pdf (accessed October 23, 2026).

[119] Murphy KR, Broyles JM. A primer on low-carbon design in architectural acoustics using a case study of residential floorsa). JASA Express Lett 2025;5. https://doi.org/10.1121/10.0034783.

[120] Arslan D, Mohammadpourkarbasi H, Sharples S. Sensitivity analysis of the impact of environmental product declaration values on whole life carbon assessment: A case study using expanded polystyrene insulation for the retrofit of a building in Turkiye. Building Services Engineering Research and Technology 2024;45:101–21. https://doi.org/10.1177/01436244231221396.

[121] Grazieschi G, Asdrubali F, Thomas G. Embodied energy and carbon of building insulating materials: A critical review. Cleaner Environmental Systems 2021;2. https://doi.org/10.1016/j.cesys.2021.100032.

[122] Lewis M, Waldman B, Lambert M. EPD 101 Embodied Carbon Accounting for Materials 2024:1–4. https://carbonleadershipforum.org/environmental-product-declarations-epd-101/ (accessed October 23, 2026).

[123] Anderson R, Dawson E, Muszynski L. Modular mass timber units are being installed for workforce housing in big sky, Montana. United State of America: 2024. https://doi.org/10.1061.

[124] Guski R, Schreckenberg D, Schuemer R. WHO Environmental Noise Guidelines for the European Region: A Systematic Review on Environmental Noise and Annoyance. Int J Environ Res Public Health 2017;14. https://doi.org/10.3390/ijerph14121539.

[125] ISO 10140-2:2021 - Acoustics — Laboratory measurement of sound insulation of building elements — Part 2: Measurement of airborne sound insulation. International Organization for Standardization: Geneva, Switzerland: 2021.

[126] ASTM E90; Standard Test Method for Laboratory Measurement of Airborne Sound Transmission Loss of Building Partitions and Elements: West Conshohocken, PA, USA; 2023. https://doi.org/10.1520/E0090-09.

[127] ASTM E413-22; Classification for Rating Sound Insulation. ASTM International: West Conshohocken, PA, USA: 2022. https://doi.org/10.1520/E0413-22.

[128] Balderrama A, Kang J, Prieto A, Luna-Navarro A, Arztmann D, Knaack U. Effects of Façades on Urban Acoustic Environment and Soundscape: A Systematic Review. Sustainability (Switzerland) 2022;14:9670. https://doi.org/10.3390/su14159670.

[129] Basner M, Babisch W, Davis A, Brink M, Clark C, Janssen S, et al. Auditory and non-auditory effects of noise on health. The Lancet 2014;383:1325–32. https://doi.org/10.1016/S0140-6736(13)61613-X.

[130] Frontczak M, Wargocki P. Literature survey on how different factors influence human comfort in indoor environments. Build Environ 2011;46:922–37. https://doi.org/10.1016/j.buildenv.2010.10.021.

[131] Cabral MR, Blanchet P. A State of the Art of the Overall Energy Efficiency of Wood Buildings—An Overview and Future Possibilities. Materials;14(8):1848 2021. https://doi.org/10.3390/ma14081848.

[132] Bader Eddin M, Ménard S, Laratte B, Wu TV. A Design Methodology Incorporating a Sound Insulation Prediction Model, Life Cycle Assessment (LCA), and Thermal Insulation: A Comparative Study of Various Cross-Laminated Timber (CLT) and Ribbed CLT-Based Floor Assemblies. Acoustics 2024;6:1021–46. https://doi.org/10.3390/acoustics6040056.

[133] Caniato M, Bettarello F, Ferluga A, Marsich L, Schmid C, Fausti P. Acoustics of lightweight timber buildings: A review. Renewable and Sustainable Energy Reviews 2017;80:585–96. https://doi.org/10.1016/j.rser.2017.05.110.

[134] ASTM C518-21; Standard Test Method for Steady-State Thermal Transmission Properties by Means of the Heat Flow Meter Apparatus. ASTM International, West Conshohocken, PA, USA; 2021. https://doi.org/10.1520/C0518-21.

[135] Skov R, Parigi D, Damkilde L. Multi-objective room acoustics optimization of timber folded plate structure. InProceedings of IASS Annual Symposia 2017 Sep 28 (Vol 2017, No 5, Pp 1-10) International Association for Shell and Spatial Structures (IASS) n.d.

[136] Hammad AW, Akbarnezhad A, Oldfield P. Optimising embodied carbon and U-value in load bearing walls: A mathematical bi-objective mixed integer programming approach. Energy Build 2018;174:657–71. https://doi.org/10.1016/J.ENBUILD.2018.05.061.

[137] Chen Z, Hammad AWA, Kamardeen I, Akbarnezhad A. Optimising Embodied Energy and Thermal Performance of Thermal Insulation in Building Envelopes via an Automated Building Information Modelling (BIM) Tool. Buildings 2020, Vol 10, Page 218 2020;10:218. https://doi.org/10.3390/BUILDINGS10120218.

[138] Bradley J, Birta J. Laboratory measurements of the sound insulation of building façade elements. National Research Council of Canada. Ottawa, Canada. 2000. https://doi.org/10.4224/20386467.

[139] Polleres S, Plößnig B. External wall-dataholz.eu. Holzforschung Austria – Austrian Forest Products Research Society: Vienna, Austria, n.d. https://www.dataholz.eu/en/components/external-wall.htm (accessed March 10, 2026).

[140] Boulet S, Kouyoumji J, Achard G. Objective and subjective qualification of acoustic and thermal comfort in timber framed houses. Proceedings of INTER-NOISE and NOISE-CON Congress and Conference Proceedings, Institute of Noise Control Engineering 2009;2009. No. 3:3666–74.

[141] Höller C. Review and comparison of ASTM and ISO standards on sound transmission in buildings. INTER-NOISE 2018, Chicago, Illinois: 2018.

[142] Nilsson E, Ménard S, Bard D, Hagberg K. Effects of building height on the sound transmission in cross-laminated timber buildings – Airborne sound insulation. Build Environ 2023;229:109985. https://doi.org/10.1016/J.BUILDENV.2023.109985.

[143] Plag R. UBAKUS—U-Wert Berechnung n.d. https://www.ubakus.de (accessed April 8, 2026).

[144] National Building Code of Canada 2020: Volume 1. 15th Edition. Ottawa, Canada: National Research Council of Canada; 2020.

[145] ISO 6946:2022, Building Components and Building Elements—Thermal Resistance and Thermal Transmittance—Calculation Methods. International Organization for Standardization: Geneva, Switzerland: 2022.

[146] Ciroth A. ICT for environment in life cycle applications: openLCA—A new open source software for Life Cycle Assessment. International Journal of Life Cycle Assessment 2007;12:209–10. https://doi.org/10.1065/lca2007.06.337.

[147] Hammond PG, Jones C, Lowrie EF, Tse P. A BSRIA Guide: Embodied Carbon: The Inventory of Carbon and Energy (ICE). Bracknell, UK: 2011.

[148] Knauf Ceiling Solutions GmbH & Co. KG. ENVIRONMENTAL PRODUCT DECLARATION. 2024. https://doi.org/10.01.2029.

[149] Zerari S, Franchino R, Pisacane N. Cost and Carbon Intensity Analysis of Different Bio-based Insulation Materials across European Countries n.d. https://doi.org/10.1051/e3sconf/202458501010.

[150] knauf LLC. Gypsum board – RG 12.5 mm [Environmental product declaration]. 2024. https://doi.org/https://www.environdec.com/library/epd12093.

[151] Marler RT, Arora JS. Survey of multi-objective optimization methods for engineering. Structural and Multidisciplinary Optimization 2004;26:369–95. https://doi.org/10.1007/s00158-003-0368-6.

[152] Hafiz F, Swain A, Mendes E. Multi-objective evolutionary framework for non-linear system identification: A comprehensive investigation. Neurocomputing 2020;386:257–80. https://doi.org/10.1016/J.NEUCOM.2019.12.095.

[153] Schütze O, Cuate O. The Pareto Tracer for the treatment of degenerated multi-objective optimization problems. Engineering Optimization 2025;57:1:261–86. https://doi.org/10.1080/0305215X.2024.2420726.

[154] Jollife IT, Cadima J. Principal component analysis: a review and recent developments. Philos Trans A Math Phys Eng Sci 2016;374:20150202. https://doi.org/10.1098/RSTA.2015.0202.

[155] Petchrompo S, Coit DW, Brintrup A, Wannakrairot A, Parlikad AK. A review of Pareto pruning methods for multi-objective optimization. Comput Ind Eng 2022;167:108022. https://doi.org/10.1016/J.CIE.2022.108022.

[156] Ovchinnikova E, Kozhubaev Y, Sitzhanova E, Potekhin V, Kim I, Chentsov V. Multi-Criteria Optimization of Production Processes of Mining Companies. Processes 2026, Vol 14, Page 1239 2026;14:1239. https://doi.org/10.3390/PR14081239.

[157] Wang Z, Rangaiah GP. Application and Analysis of Methods for Selecting an Optimal Solution from the Pareto-Optimal Front obtained by Multiobjective Optimization. Ind Eng Chem Res 2017;56:560–74. https://doi.org/10.1021/ACS.IECR.6B03453.

[158] Wang Z, Rangaiah GP. Application and Analysis of Methods for Selecting an Optimal Solution from the Pareto-Optimal Front obtained by Multiobjective Optimization. Ind Eng Chem Res 2017;56:560–74. https://doi.org/10.1021/ACS.IECR.6B03453.

[159] Nath B, Roy S, Das B, Ehyaei MA. Experimental and numerical study of a novel composite building wall U-value. Thermal Science and Engineering Progress 2024;53:102751. https://doi.org/10.1016/J.TSEP.2024.102751.

[160] Zhen L, Li M, Cheng R, Peng D, Yao X. Multi-objective Test Problems with Degenerate Pareto Fronts. Arxiv 2018 2018. https://doi.org/https://arxiv.org/abs/1806.02706.

[161] Brockhoff D, Zitzler E. Objective Reduction in Evolutionary Multiobjective Optimization: Theory and Applications. Evol Comput 2009;17:135–66. https://doi.org/10.1162/EVCO.2009.17.2.135.